A BIOGEOCHEMICAL STUDY OF GROUNDWATER ARSENIC CONTAMINATION IN THE SOUTHERN WILLAMETTE BASIN, OREGON, USA

by

SCOTT CHARLES MAGUFFIN

A DISSERTATION

Presented to the Department of Geological Sciences
and the Graduate School of the University of Oregon
in partial fulfillment of the requirements
for the degree of
Doctor of Philosophy

September 2016

DISSERTATION APPROVAL PAGE

Student: Scott Charles Maguffin

Title: A Biogeochemical Study of Groundwater Arsenic Contamination in the Southern Willamette Basin, Oregon, USA

This dissertation has been accepted and approved in partial fulfillment of the requirements for the Doctor of Philosophy degree in the Department of Geological Sciences by:

Qusheng Jin	Chairperson
Mark H. Reed	Core Member
James Watkins	Core Member
Scott Bridgham	Institutional Representative

and

Scott L. Pratt	Dean of the Graduate School

Original approval signatures are on file with the University of Oregon Graduate School.

Degree awarded September 2016

DISSERTATION ABSTRACT

Scott Charles Maguffin

Doctor of Philosophy

Department of Geological Sciences

September 2016

Title: A Biogeochemical Study of Groundwater Arsenic Contamination in the Southern Willamette Basin, Oregon, USA

The mobilization and transformation of arsenic within the critical zone is a major cause of human suffering worldwide. Microorganisms, as they grow and utilize organic matter, accelerate redox processes that can transform and mobilize arsenic within aquifers on a large scale. As such, naturally occurring groundwater arsenic is a particularly hazardous problem that is chronically poisoning over 100 million people annually. Historically, groundwater arsenic research has been focused on the two principal inorganic arsenic species: arsenate [As(V)] and arsenite [As(III)]. Recently, organic arsenic species have garnered more attention due to their mobility, toxicity, and contemporary recognition of the ephemeral yet significant role they have in the global arsenic cycle. Here, I discuss laboratory and in situ experiments focused on exploring how microorganisms transform, mobilize, and sequester arsenic within a biogeochemically complex aquifer system. In my laboratory experiments, I collected aquifer sediments from a naturally contaminated bedrock aquifer and incubated a series of laboratory microcosms. Our results show that simultaneously robust iron and sulfate reduction temporarily mitigated arsenic contamination but then directed arsenic to an unstable adsorbed phase were it was later mobilized. Second, I discuss two aquifer injection experiments designed to examine in situ

microbial redox processes and the further explore the potential to stimulate arsenic sequestration through arsenic-sulfide precipitation. Our results show that in situ stimulation of microbial metabolisms accelerated the reduction of arsenic bearing iron (oxy)hydroxides as well as sulfate and arsenic reduction. Within 3 weeks of these contemporaneously occurring redox reactions, 90% of the dissolved inorganic arsenic was removed (~2000 ppb) and an effective long-term, anaerobically stable, sequestration of arsenic was observed by way of a significant increase of arsenic-sulfide precipitate. Finally, using both the laboratory and field experiments, I explore the potential of organic arsenic production rates under stimulated conditions. We report new methylation rates that are consequential to the potential efficacy of enhanced, biologically-driven arsenic remediation and the reconsidered significance of biomethylation pathways in aquifers. These results expand our current understanding of the metabolic reach aquifer microorganisms potentially have over the fate of arsenic.

This dissertation includes unpublished material.

CURRICULUM VITAE

NAME OF AUTHOR: Scott Charles Maguffin

GRADUATE AND UNDERGRADUATE SCHOOLS ATTENDED:

University of Oregon, Eugene
Illinois State University
State University of New York - College at Geneseo

DEGREES AWARDED:

Doctor of Philosophy, Geological Sciences, 2016, University of Oregon
Master of Science, Hydrogeology, 2007, Illinois State University
Bachelor of Arts, Geology, 2004, State University of New York - College at Geneseo

AREAS OF SPECIAL INTEREST:

Groundwater biogeochemistry, arsenic, biomethylation

PROFESSIONAL EXPERIENCE:

Graduate Teaching & Research Fellow, Department of Geological Sciences
University of Oregon, 2010-2016

Hydrogeologist/Case Manager, Kleinfelder, Cambridge, MA
2007 – 2010

Geologist, Environmental Partners Group, Quincy, MA
University of Oregon, 2006-2007

GRANTS, AWARDS, AND HONORS:

General University Scholarship, University of Oregon, 2015

Baldwin Scholarship for outstanding scholastic achievement, University of Oregon, 2015
Marthe E. Smith Memorial Science Scholarship, University of Oregon, 2014

Baldwin Scholarship for outstanding scholastic achievement, University of Oregon, 2014

Thayer Scholarship for outstanding scholastic achievement, University of Oregon, 2013

Johnston Scholarship for outstanding scholastic achievement, University of Oregon, 2012

Thayer Fellowship, University of Oregon, 2010

PUBLICATIONS:

Maguffin, S.C.; Kirk, M.F.; Daigle, A.R.; Hinkle, S.R.; Jin, Q. Nature Geoscience. 2015, *8*, 2–5. Substantial contribution of biomethylation to aquifer arsenic cycling

ACKNOWLEDGMENTS

I would like to thank Qusheng Jin for being a supportive and dedicated advisor and for his help with this manuscript. His dedication to good science, high standards, honesty, and kind insight has helped me to become a better researcher. I would also like to thank the rest of my dissertation committee – James Watkins, Mark Reed, and Scott Bridgham – for their guidance and support these past years. Scott Bridgham has been especially gracious with his time and laboratory resources – thank you. I am also grateful to everyone at the University of Oregon that have been an important part of my life here in Eugene, academic and otherwise. In particular, I have been very fortunate to have had such wonderful officemates and friends here in the department: Al Handwerger, Kristin Sweeney, Kristina Walowski, Randy Krogstad, Rob Skarback, Dan Sulak, Stanley Mordensky, Kelley Rabjohns, Shannon McKernan, Ben Shapiro, and Marisa Acosta.

I am very grateful for the friends and family who have been part of my life and have supported me throughout this journey. I owe a debt of thanks and an acknowledgment of my sincerest appreciation to the following people: To my parents Dan, Diane, Bill, and Patty, who encouraged my appreciation for nature and inquiry and supported my educational efforts. To my sister Jennifer, who has always been there for me as a my most trusted friend and confidant. To Robby Spirelli, Garrett Risberg, Kristin Riis, and Sean Padden for being a positive influence on my life and for letting me be part of yours. To Corina, who has been an enormously important part of my life and who continually inspired me to be a better scientist and person. Thank you to the Campers – Chris Mulhall, Bryan Mulhall, John Rosa, JP Mulhall, James Weigel, Brandon McDonald, and Brian Weigel, and the rest of the Narrowsburg crew – for keeping home close. Lastly, thank you

to the New York Metropolitans for reminding me that trivial moments can seem important, and vice versa.

This research would not have been possible without the work done by Ashely Daigle, Jordan Mohrhardt, Chris Bristow, and Kyle Ohnstadt. Thank you to the NSF for funding my research – without which these contributions would not be possible (Grant 0810190).

Live the remainder.

TABLE OF CONTENTS

Chapter Page

Chapter Page

LIST OF FIGURES

Figure Page

Chapter II

Chapter III

LIST OF FIGURES

LIST OF TABLES

LIST OF TABLES

CHAPTER I

INTRODUCTION

Arsenic is a ubiquitous and toxic contaminant in the critical zone, and is linked to cancers of the skin, bladder, and kidneys. Arsenic is also one of the highest priority pollutant on the National Priorities List ("Superfund sites") in the United States.[1] The most severe cases of human exposure to arsenic have occurred in South and Southeast Asia, where naturally-occurring arsenic in groundwater regularly exceeds the World Health Organization (WHO) standard of 10 ppb[2]. An estimated 100 million people have been exposed to elevated levels of arsenic in drinking water, in what has been labeled "the largest mass poisoning of a population in history".[3–5] Exposure to arsenic through consumption of contaminated groundwater is also a problem in the United States, particularly in Oregon, Maine, New Jersey, and Florida [6–8]. Groundwater arsenic contamination can also be affected by indigenous aquifer microorganisms that influence groundwater chemistry by way of consuming organic compound; these reduction-oxidation processes can incorporate arsenic species and change arsenic's solubility.

In surface and subsurface aquatic systems, arsenic is typically present as the inorganic oxyanions arsenate (As(V)) and arsenite (As(III)) but also occur as methylated species.[9] Understanding the biogeochemical controls on the distribution of these species is critical because arsenic species have different toxicities, mobility, and fates in the environment. Due to inorganic arsenic's proclivity to adsorb onto some aquifer media, such as clays and iron oxides, a common process attributed as a source of groundwater arsenic contamination is the reduction of arsenic-bearing ferric iron (oxy)hydroxide minerals. This contaminating process is strongly dependent on the microbial activity and

the geochemistry of the aquifer, particularly pH, dissolved concentrations of arsenic and other adsorbing species, and the mineral composition of aquifer itself.[10,11] On the other hand, recent studies point to the reduction of groundwater sulfate as a mechanism for limiting groundwater arsenic through the precipitation of arsenic and iron-sulfide minerals.[12,13] The efficacy of these processes as a remediation strategy is not well understood, especially in the context of more complicated biogeochemical networks within arsenic contaminated aquifer systems.

In Chapter II, in preparation for publication in *Environmental Science & Technology*, I discuss a series of incubated laboratory experiments that explore several aquifer-biogeochemical systems. These experiments examine the role of indigenous microorganisms in sulfate and iron reducing environments with respect to dissolved inorganic arsenic contamination and the additional effect of ethanol-stimulated microbial activity.

In Chapter III, in preparation for publication in *Environmental Science & Technology*, I discuss the results of two aquifer push-pull injection tests into an arsenic-contaminated aquifer. The first push-pull experiment explored in situ biogeochemical reactions and the natural, unstimulated microbial community's ability to mobilize arsenate in a controlled geochemical regime. The second experiment examined the aquifer's geochemical response alongside ethanol-stimulated microbial activity.

In addition to microorganisms cycling arsenic between inorganic arsenic species, many microorganisms also possess the *arsM* gene, which confers the ability to methylate arsenic via the arsenite S-adenosylmethionine methyltransferase enzyme (ArsM). This gene allows microorganisms to transform or 'methylate' inorganic arsenic to pentavalent methylated forms[14]. Arsenic methylation remains poorly understood relative to other

microbial arsenic transformations but the ability to methylate is widespread in natural systems and is present in diverse eukaryotic and prokaryotic genomes[15] with some cultures of *arsM*-bearing microbes capable of quick arsenic methylation[16]. Despite these findings, the concentrations of methylated arsenic in many aquatic environments remain low[17,18], and it is currently not known if this is due to limitations to arsenic methylation rates or to processes like sorption or arsenic demethylation which prevent the accumulation of methylated arsenic in aquatic systems.

Attention to arsenic contamination has typically focused on inorganic As(III) and As(V). However, recent focus on pathways of arsenic into food[19] and within groundwater systems[18] has brought new attention to the importance of methylated arsenic. Several methylated arsenic species are volatile and significantly more mobile than their inorganic counterparts; therefore, arsenic's transport potential within and out of groundwater increases with methylation.[20] The mass transfer of volatile arsenic species from the saturated zone to the vadose zone may create a concentration gradient that drives diffusive transport of volatile arsenic species out of groundwater. In particular, biological (e.g. microbial) arsenic methylation, in both groundwater and the shallow subsurface, is a potentially significant pathway relative to other global fluxes of arsenic [18,21–23] and may result in arsenic moving from groundwater to shallow subsurface environments.

In Chapter IV, in preparation for publication in *Environmental Science & Technology*, I discuss observed organic arsenic chemistry in the laboratory and field experiments from Chapters II and III. I also identify new methylating capabilities of indigenous aquifer microbial communities under ethanol-stimulated conditions.

In this dissertation, by coupling laboratory and field geochemical experiments and utilizing the stimulation of naturally occurring aquifer microorganisms, I have been able

to identify the importance of competing biogeochemical reactions relating to arsenic mobility and quantify rates of important organic arsenic reactions.

CHAPTER II

CONTROL OF REDOX CHEMISTRY ON THE EFFICIENCY OF ARSENIC BIOREMEDIATION

In preparation for submission to *Environmental Science & Technology*.

Scott C. Maguffin and Qusheng Jin designed the project. The manuscript was written by S.C.M with input from Q.J. Q.J. and S.C.M. conducted laboratory experiments. Samples were collected and analyzed by S.C.M. Jing Sun and Benjamin C. Bostick carried out synchrotron analyses.

1. Introduction

Groundwater arsenic contamination is a significant global health problem that impacts tens of millions of people worldwide.[1–3] As a groundwater species, arsenic mainly occurs as pentavalent arsenate [As(V)] and trivalent arsenite [As(III)]. A key process controlling the occurrence and concentration of groundwater arsenic is its adsorption onto surfaces of ferric minerals and clays.[4–6] In most groundwater environments, As(V) has a stronger affinity for adsorption than As(III)[7]. In addition to its adsorption properties, arsenic mobilization is controlled by microbial redox processes. For example, microbially driven ferric iron reduction by iron reducing bacteria (FeRB) can dissolve arsenic-bearing ferric minerals, releasing arsenic into groundwater.[8–14] Microbes can also oxidize arsenite or reduce arsenate, controlling groundwater arsenic levels by determining arsenic speciation and its corresponding sorption properties.

Sulfate reducing bacteria (SRB) can also be a significant control on groundwater arsenic mobilization; arsenic does not typically exceed World Health Organization (WHO) contamination limits in groundwater where sulfate is abundant.[15–18] One explanation for this is that sulfate reduction can sequester arsenic by promoting the

precipitation of iron and arsenic sulfide minerals, a process that removes dissolved arsenic by either incorporating it into the mineral structure or providing additional sorbing locations.

These biogeochemical processes are typically intertwined with each other. Therefore, an important question is how simultaneous biogeochemical processes drive the mobilization, transport, and fate of arsenic in aquifers. Furthermore, can arsenic be bioremediated through the stimulation of microbial metabolisms? Here, we explore the role of sulfate, iron, arsenic, and indigenous microorganisms under natural and stimulated conditions by using three biologically active batch reactor experiments. We used sediments and indigenous microorganisms from a naturally contaminated bedrock aquifer to construct laboratory microcosm incubation experiments. With a specific focus on arsenic transformation, we examined how microorganisms respond to variations in groundwater chemistry and available energy under simulated bedrock aquifer conditions and the resulting efficacy of arsenic bioremedation.

2. Study Area and Experimental Setup

Laboratory experiments were constructed using extracted aquifer sediments from the saturated, anaerobic, and arsenic contaminated volcaniclastic sandstone unit within the Fisher Formation located southern Willamette Basin, Oregon, USA. The aquifer consists of units of late Eocene to Oligocene andesitic lapilli tuffs and volcaniclastic sandstone as well as basalt and andesitic lava flows.[20,21] We constructed the experiments to simulate three different conditions: 1) in situ (Reactor N); 2) ethanol stimulated (Reactor E); 3) ethanol and sulfate stimulated (Reactor ES). A batch-reactor identical to Reactor N was prepared and then autoclaved as the biological control (Reactor A). Each experiment contained a slurry mixture of aquifer material collected from the field site

combined with a synthetic groundwater. Aquifer material was homogenized for in an anaerobic chamber before combining with the synthetic groundwater. Biologically active reactors N, E, and ES were prepared in quadruplicate (Reactor A in triplicate) in 1-liter airtight glass containers by mixing 150 g of crushed bedrock sediments and 600 mL of synthetic groundwater. The aqueous medium was fashioned to reflect the Na-Cl type groundwater of this part of the Willamette Basin; chemical analyses of in situ groundwater conditions were used as a reference for the synthetic groundwater (Table B1, Appendix B). All glassware, rubber stoppers, and equipment were acid washed and autoclaved before use. All reactors were incubated at 15°C in the dark.

All microcosms experiments were incubated in the dark at 20°C for the duration of the experiment. The microcosms were initially run for a period of 28 days without any amendment. The purpose of this "mobilization phase" was to follow the natural release of arsenic and other geogenic chemicals. Any microbial activity during this initial mobilization phase relied on endogenous substrates present naturally.[19]

Aqueous and gas phase samples were collected every 4-7 days. Experiments were gently shaken before sampling to homogenize the solution and release trapped gases into the headspace. Approximately 8 mL of solution was anaerobically extracted from each reactor. Extracted solutions were either used immediately to measure pH, ferrous iron, and sulfide or centrifuged, filtered (0.22 μM), and frozen at -20 °C for future arsenic and anion analyses. Gaseous samples were anaerobically extracted from the headspace using a gas-tight needle and syringe. We measured methane and CO_2 by gas chromatography using a flame ionization detector equipped with a methanizer (SRI Instruments, Torrance, CA, USA).

We analyzed pH using standard electrodes. Sulfide and ferrous iron were analyzed using Hach method 2244500 and 103769 with a DU Series 500 Spectrophotometer (Appendix A). Frozen samples were shipped overnight to the Illinois Sustainable Technology Center for arsenic speciation and total arsenic analyses (see methods, Appendix A). Total arsenic analyses were completed using a VG Elemental PQ Excel ICP-MS with a yttrium internal standard that was calibrated daily. We used ion chromatography and high performance liquid chromatography (HPLC) to analyze for anion chemistry. Anion results were normalized to chloride concentrations to account for analytical drift.

Solid phase samples from before and after the incubation were preserved at -70C until solid phase sequential extraction analyses were conducted. Acid volatile sulfide and chromium reducible sulfur methods followed methods outlined in Kirk et al. (2010).[22] Samples collected on days 3 and 50 were also analyzed using x-ray absorption near-edge structure (XANES) and micro-focused synchrotron X-ray fluorescence (μSXRF) mapping for arsenic and iron.

3. Results

In Reactor E and ES, ethanol decreased to below detection limits within 24 days while acetate accumulated to concentrations similar to that of initial ethanol concentrations (Fig. 1). The onset of ethanol depletion was accompanied by a drop in pH from 8.0±0.1 to 6.0±0.1 at day 12 of the experiment. Concurrent with the pH decrease were increases in dissolved arsenite, arsenate, sulfide, Fe(II), and H_2 (g). Reactors A and N varied little in pH throughout the incubation ($\overline{pH}$: 7.8±0.25) (Fig. 1). We did not detect any ethanol, acetate, ferrous iron, sulfide, methane, or H_2 in Reactor A at any time.

In stimulated experiments, dissolved ferrous iron was detected after 3 days into the experiment and continued increasing until about day 20 when it began to steadily decrease (Fig. 1). Within our sampling window, maximum dissolved iron concentrations were contemporaneous with the depletion of ethanol in both Reactors E and ES.

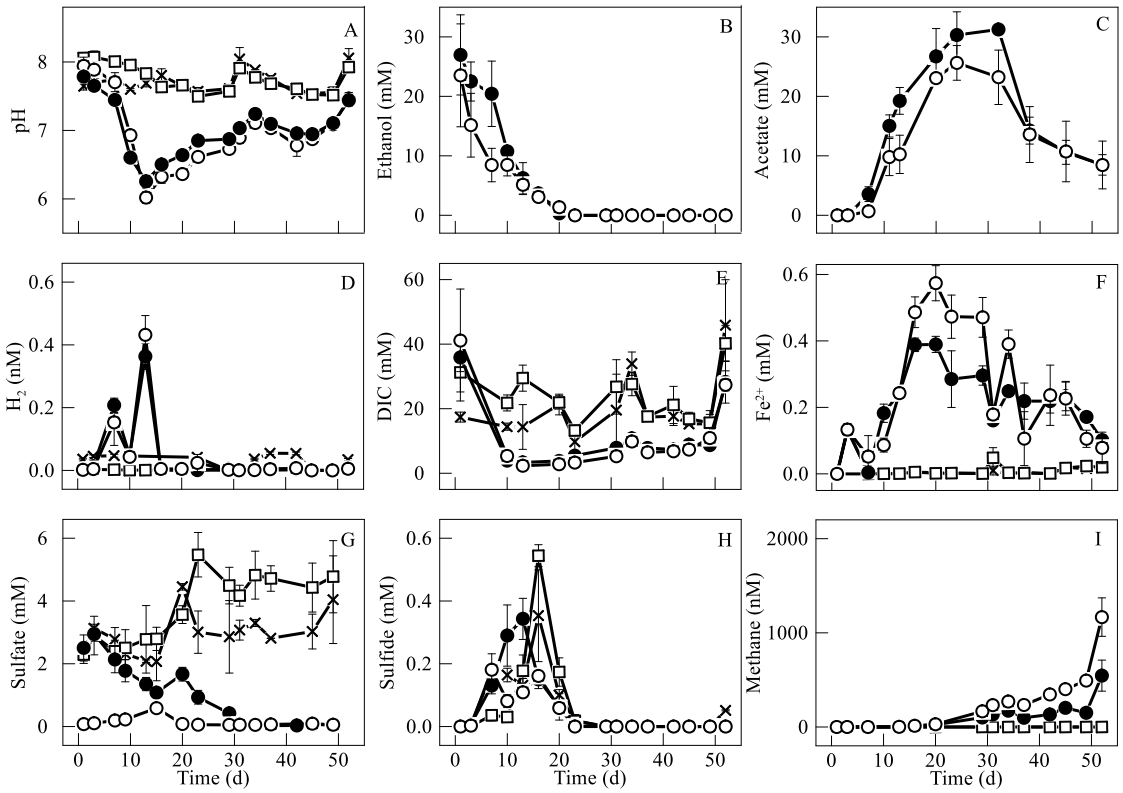

Figure 1. Variations with time in pH and concentrations of ethanol, acetate, dihydrogen (H_2), dissolved inorganic carbon (DIC), ferrous iron, sulfate, sulfide, and methane (CH_4) in Reactor A (×), N (□), E (○), and ES (●). Data points represent the mean of the measurement and error bars are the standard deviation.

In Reactors A and N, about 2.5 mM of sulfate were added, and dissolved sulfate accumulated over time to about 4 and 5 mM, respectively. Although no sulfate was added to Reactor E experiments, sulfate was detected at low concentrations (approximately 0.3 mM) at the beginning of the experiments. In Reactor ES, 2.5 mM sulfate was also added at the beginning of the experiment. In ethanol stimulated experiments, we observed minimum dissolved sulfate concentrations of 0.055 $\pm$ 0.011 mM and 0.54 $\pm$ 0.011 mM

for Reactors E and ES, respectively. Sulfide was produced in all biologically active experiments with maximum concentrations ranging from 0.2 mM (Reactor E) to 0.58 (Reactor N). All stimulated experiments showed peak H_2 concentrations (approximately 500 μmoles/L) after thirteen days; however, after 16 days all H_2 was depleted and not detected thereafter. See Appendix B for complete aqueous results from laboratory experiments.

Fluoride concentrations in non-stimulated experiments maintained a relatively stable background concentration with the exception of a sharp increase and decrease between day 7 and 20 (Fig 2). This fluctuation was nearly identical in both Reactor A and N. In stimulated experiments fluoride concentration began to increase after day 3 and continued to do so until about days 14-17. Comparatively, chloride concentrations are stable throughout the experiment for all experimental reactors.

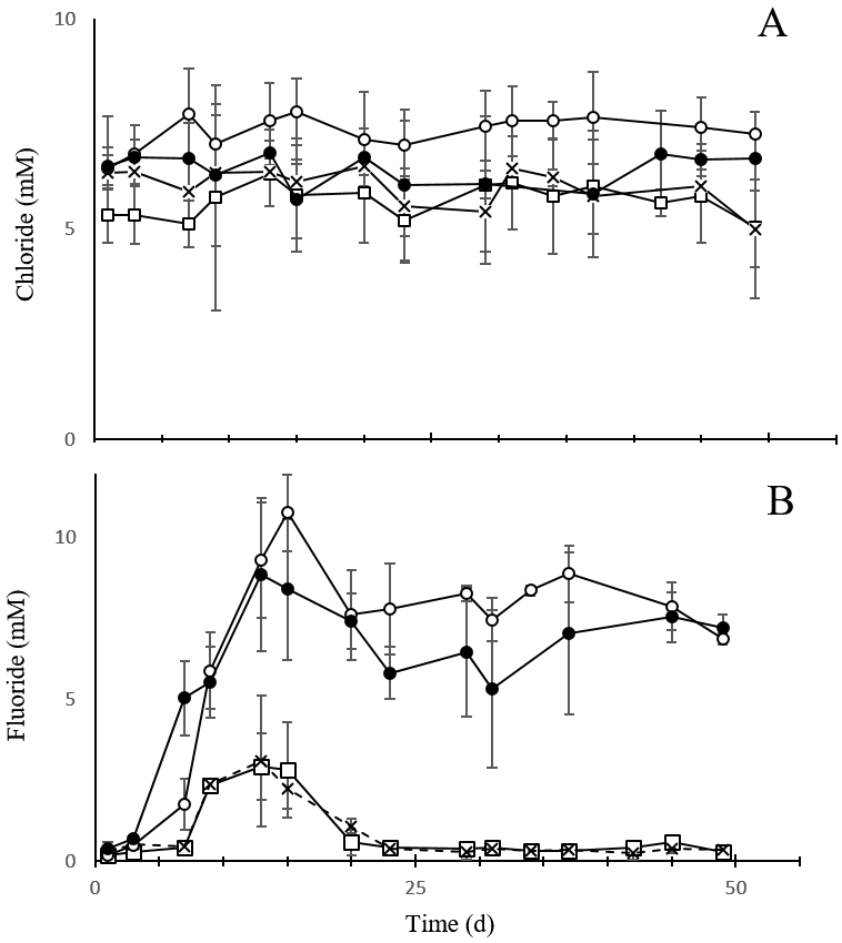

Figure 2. Variations with time in concentrations of chloride and fluoride in Reactor A (×), N (□), E (○), and ES (●). Data points represent the mean of measurement and error bars are the standard deviation.

Although the synthetic groundwater included 2.5 mM of dissolved arsenate, initial dissolved arsenate concentrations did not exceed 0.6±0.1 mM (Fig. 3). In Reactor N, arsenate gradually increased throughout the experiment, reaching concentrations as high as 1.0±0.3 mM. Among stimulated experiments, dissolved arsenic species exhibited unique concentrations. In Reactor E, we observed significantly higher arsenate concentrations throughout weeks 2 and 3; during this time Reactor ES arsenate concentrations remained close to background levels. Arsenite concentrations in both stimulated experiments increased to approximately 1100 ppb after 7 days; however, in Reactor ES arsenite quickly decreased to below initial concentrations (approximately 200 ppb) before gradually increasing and exceeding 2000 ppb after about 35 days. Conversely, the initial spike of arsenite in Reactor E was followed by a steady increase that never exceeded 2000 ppb. After 35 days, Reactor ES exceeded Reactor E in arsenate, arsenite, and total arsenic concentrations.

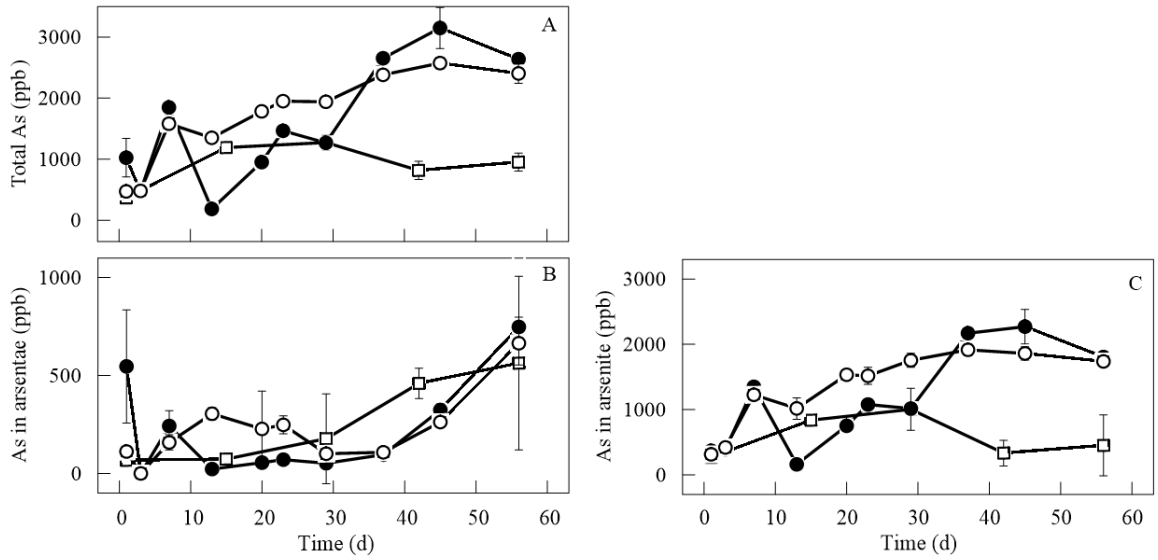

Figure 3. Variations with time in the concentrations of total arsenic, and arsenic in arsenate and arsenite in Reactor N (□), E (○), and ES (●). Data points represent the mean of measurement and error bars are the standard deviation. Reactor A did not exhibit any changes in arsenic concentrations over time and is not shown.

Methane was detected in all ethanol-stimulated experiments and first observed at low concentrations (approximately 0.2 mmol*L^{-1}) after day 16. Reactor ES exhibited a lower rate of methanogenesis than Reactor E. In all ethanol-amended experiments, the rate of methanogenesis increased significantly, after ethanol was completely depleted (day 27).

Synchrotron analyses of solid material show the sloughed, pre-experimental aquifer media to be 66%±12% ferrihydrite (Table 1). In stimulated experiments, final concentrations of ferrihydrite decreased to 49%±7% and 52%±12% for Reactors E and ES, respectively. Hematite increased from 6+2% (bedrock) to 12±11% (Reactor N), 19±2% (Reactor E), and 10±2% (Reactor ES). Siderite was detected in Reactor ES only.

Table 1. Synchrotron analyses of solid phase samples.

	Ferrihydrite $Fe(OH)_3$	FeOOH Goethite	Fe_2O_3 Hematite	magnetite Fe_3O_4	Hornblende ($Fe^{2+/3+}$ silicate)	Siderite $FeCO_3$
Bedrock	66±12%	1±5%	6±2%	0±3%	27±4%	0±4%
Reactor N	19±54%	30±23%	12±11%	0±15%	38±19%	0±16%
Reactor E	49±7%	5±3%	19±2%	0±2%	28±3%	0±2%
Reactor ES	52±12%	9±5%	10±2%	0±3%	22±4%	6±4%

Sequential extraction analyses show solid phase ferrous iron increasing from 14.7±7.5 mmol·(kg water)$^{-1}$ (before incubation) to 18.0±5.0, 40.8±15.9, and 54.2±9.0 mmol·(kg water)$^{-1}$ for Reactors N, E, and ES, respectively (Table 2). Analyses also revealed an increase in sulfide minerals from 0.054±0.020 mmol·(kg water)$^{-1}$ (before incubation) to 0.110±0.03, 0.122±0.012, and 6.8±3.2 mmol·(kg water)$^{-1}$ in Reactors N, E, and ES, respectively.

Table 2. Acid volatile sulfide (AVS), chromium-reducible sulfur (CRS), and ferrous iron (Fe^{2+}) before and after incubation in Reactor N, E, and ES.

Reactors	AVS [mmol·(kg water) −1]	CRS [mmol·(kg water) −1]	Fe^{2+} [mmol·(kg water) −1]
Before incubation	0.054±0.020	0.043±0.016	14.7±7.5
Reactor N	0.110±0.033	0.118±0.069	18.0±5.0
Reactor E	0.122±0.115	0.044±0.008	40.8±15.9
Reactor ES	6.800±3.193	0.076±0.026	54.2±9.0

Solid phase analyses show decreases of arsenic in arsenic-bearing amorphous ferric iron oxyhydroxides in Reactors N, E, and ES as well as increases in arsenic-sulfide precipitates in Reactors E and ES (Table 3). The largest increase of arsenic co-precipitated with acid volatile sulfide (AVS) was observed in Reactor E, however a modest increase was observed in Reactor ES as well. Reactor ES showed the greatest

accumulation of adsorbed arsenic throughout the incubation while both Reactors N and E exhibited similar amounts as pre-incubation sediments.

Table 3. Amount of arsenic A) ionically bound; B) strongly adsorbed; C) co-precipitated with AVS, carbonate, Mn oxides, and very amorphous iron oxyhydroxides; D) co-precipitated with amorphous iron oxyhydroxides; E) co-precipitated with crystalline iron oxyhydroxides; and F) co-precipitated with pyrite and amorphous As_2S_3 before and after incubation in Reactor N, E, and ES.

Reactors	A [μmol·(kg water) −1]	B [μmol·(kg water) −1]	C [μmol·(kg water) −1]	D [μmol·(kg water) −1]	E [μmol·(kg water) −1]	F [μmol·(kg water) −1]]
Before incubation	26.8±13.0	135.6±0.6	68.3±4.5	418.1±164.5	50.7±17.4	6.3±0.0
Reactor N	14.5±1.5	129.3±16.6	59.6±7.9	254.1±108.1	58.8±9.8	1.8±1.8
Reactor E	56.3±4.4	138.7±3.9	105.2±11.3	122.0±89.8	47.0±33.3	0.0±0.0
Reactor ES	68.1±24.8	202.6±35.1	77.8±12.2	272.8±93.1	37.8±10.6	0.0±0.0

Synchrotron analyses of solid phase arsenic (Table 4) show that Reactor N yielded the lowest percentage of arsenite but the highest percentage of As_2S_3. Among stimulated experiments Reactor E had less arsenite and more arsenate and As_2S_3 than Reactor ES.

Table 4. Synchrotron analyses of final solid phase arsenic samples.

	As(III)	As(V)	As_2S_3
Reactor N	69.3±0.3%	13.6±0.2%	15.9±0.4%
Reactor E	73.2±0.3%	15.2±0.2%	11.8±0.4%
Reactor ES	79.1±0.3%	11.1±0.2%	9.7±0.4%

4. Discussion

The primary goal of this study was to assess biostimulation as a strategy for *in situ* arsenic remediation.[17,22] We stimulated microbial metabolisms with ethanol in two experiments (Reactor E and ES); the enhanced metabolic activity had a significant effect on the

concentrations and speciation of dissolved arsenic as well as how effectively dissolved arsenic was sequestered. Microorganisms in the unstimulated experiment (Reactor N) also exhibited the ability to transform and mobilize arsenic species into the dissolved phase. However, our results show that ethanol stimulated experiments yielded significantly higher dissolved arsenic concentrations than those under natural conditions, and that the addition of sulfate made no statistically significant difference in arsenic sequestration.

In Reactors E and ES, the ethanol amendment stimulated methanogenesis as well as microbial reduction of iron, arsenate, and sulfate. We see evidence that ferric iron reduction was strongly coupled to syntrophic ethanol oxidation. Syntrophic ethanol oxidation yields acetate, H_2, and H^+; as a result, we observed a significant decrease in pH through day 12 and a corresponding accumulation of acetate. Very low H_2 concentrations were maintained through H_2-driven prokaryote redox processes which prolonged the thermodynamic favorability of syntrophic ethanol oxidation.[23] Acetate production maintained a 1:1 ratio with ethanol consumption during the first 21 days of the experiment; we surmise that negligible acetate oxidation occurred before day 21 and that H_2 was the primary electron donor for most redox processes before day 21. Furthermore, hydrogenotrophic ferric iron reduction, sulfate reduction, and methanogenesis consume protons (2, 1, and 1 H^+ per molecule FeOOH, $SO_4^{=}$, HCO_3^-, respectively)[24], which explains the increase in pH after day 12.

Based on changes (or lack thereof) in fluoride and chloride concentrations, we can deduce the timing and duration of ferric iron reduction. Ferrihydrite is the main ferric mineral among other significant ferric minerals including goethite and hematite in the aquifer (synchrotron results). Microbial reduction of ferric minerals results in the dissolution of the minerals and the release of sorbed chemical species, such as fluoride

and arsenic, into groundwater. At circumneutral pH, fluoride has a high adsorption potential on ferrihydrite and strongly interferes with the sorption of other species onto ferric iron minerals.[25] On the other hand, chloride does not sorb significantly and thus can be taken as a conservative tracer. In other words, we can identify the onset and cessation of microbial iron reduction on the basis of the difference between fluoride and chloride dynamics in the experiments. In Reactor E, dissolved ferrous iron (Fig 1) and fluoride (Fig 2) concentrations increased through the first 17 days of the incubation. Around this time ferrous iron reached peak concentrations and fluoride concentrations stabilized. Compared to Reactor ES, Reactor E exhibited higher ferrous iron and fluoride concentrations, both of which are strong indications that iron reduction was more significant.

Solid phase analyses also point towards more ferric iron reduction in Reactor E than ES. Iron sequential extraction procedures indicate about 0.6 moles of ferric iron were initially present in all reactors (not shown). Synchrotron based x-ray microspectroscopy of solid phase mineralogy show decreases in ferrihydrite from 66±12% to 49±7% and 52±12% in Reactors E and ES, respectively.

Although Reactor E was not amended with sulfate, notable amounts of sulfide were produced between 10 and 20 days. Based on the increase of sulfate in Reactor A and N, the source of additional sulfate for microbial sulfate reduction was likely from the dissolution of sulfate minerals in the aquifer sediments. Sulfide production occurred simultaneously with iron reduction, which yielded iron-sulfide precipitate (Table 3). Sulfide was produced in all biologically active experiments and at least 3 mM of sulfate was reduced to sulfide in Reactor ES; however, we never detected more dissolved sulfide in Reactor ES than in Reactor E or N. We attribute this to the robust iron reduction

occurring throughout this part of the experiment which produced dissolved ferrous iron and scavenged the sulfide before it could be detected. Solid phase analyses of sulfide mineralogy support this hypothesis.

In Reactor E, arsenate reduction began within a few days and continued throughout at least day 45. Although approximately 2.5 ppm of arsenate was included in the artificial groundwater solution, less than half was observed in initial dissolved phase concentrations in all experiments (Fig 3). We attribute this to the significant sorption of arsenate onto ferric minerals, especially at lower pH.[25]

In both Reactors E and ES, iron reduction quickly began and arsenate desorbed from dissolving hydrous ferric oxide (HFO) minerals; this is evidenced by the increase in fluoride and the quick increase of dissolved arsenite (>1000 ppb) by way of arsenate reduction. We attribute very similar arsenite concentrations in Reactor E and ES through day 8 to similar initial iron reduction rates and efficient reduction of arsenate by AsRB. However, due to the greater amount of ferric iron reduction in Reactor E than ES, significantly more total dissolved arsenate (most of which was quickly reduced to arsenite) existed in the dissolved phase of Reactor E between 8 and 30 days.

In Reactor ES, we observed approximately 30% less dissolved ferrous iron as well as lower and earlier peak fluoride concentrations than in Reactor E. This further indicates that less robust ferric iron reduction occurred in Reactor ES. We conclude that the presence of dissolved sulfate caused SRB to effectively compete with FeRB for H_2 enough to significantly lessen the amount of ferric iron reduction in Reactor ES.

We see further evidence of the importance of iron reduction and its role in the fate of arsenic in each experiment's solid phase data. As previously discussed, iron reduction is a key driver of arsenic mobilization. Arsenic sequential extraction analyses showed

that most pre-experiment, arsenic-bearing aquifer minerals occurred as co-precipitated with amorphous iron oxyhydroxide. Although Reactors N, E, and ES showed reduction in the amounts of arsenic that was co-precipitated with amorphous iron minerals, the reduction in Reactor E was most significant, which in turn, released the largest amount of arsenic. Furthermore, Reactor ES yielded significantly more adsorbed arsenic than all other reactors; this is likely a result from additional adsorbing locations provided by iron-sulfide precipitates. We measured 68±22% more adsorbed arsenic (day 55) in Reactor ES than Reactor E. These data account for part of the mid-experiment lull in total dissolved arsenic in Reactor ES, much of which went on to desorb later in the experiment due to a change in pH.

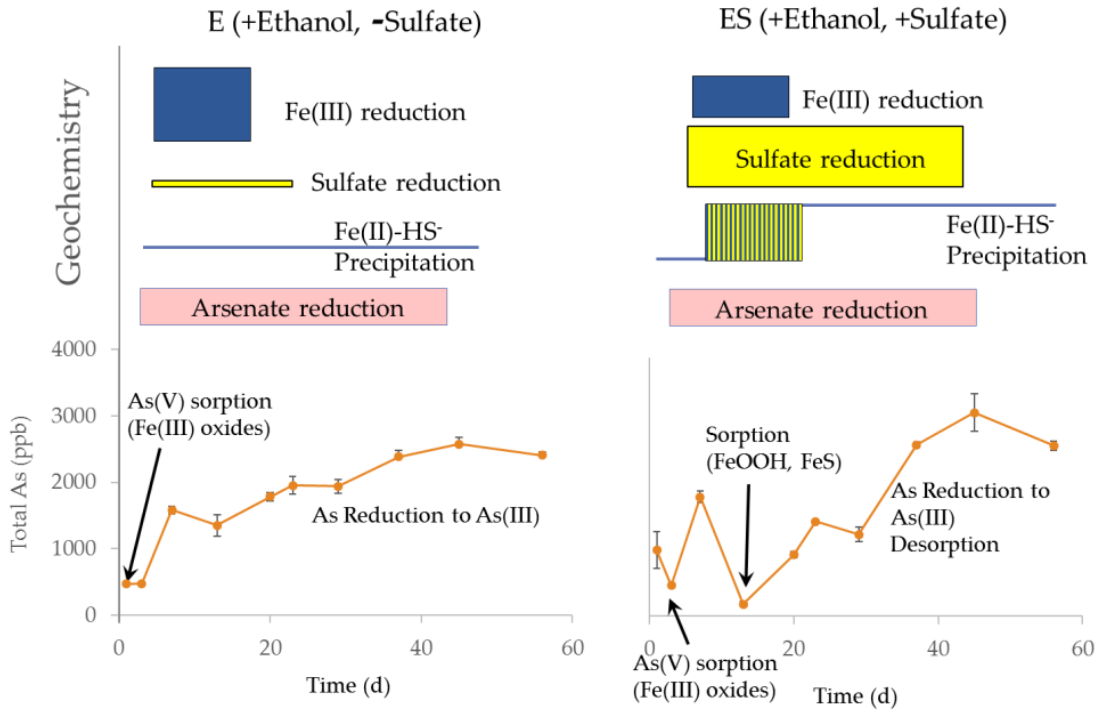

Figure 4. Illustration of redox processes and total arsenic concentrations over time in Reactors E and ES. The dashed line represents projected total arsenic concentrations based on groundwater mixing only; the solid line represents measured total arsenic concentrations.

Based on previous work by Kirk et al. (2012), we expected that dissolved arsenic in Reactor ES would be drawn out of solution as an impurity within an iron-sulfide precipitate. Although iron reduction and the resulting dissolution of ferrihydrite catalyzed the desorption of arsenic species and resulted in initial increases in dissolved arsenic in Reactors E and ES, the dynamics of pH in in these reactors played an important role. A graphical representation of important redox processes is shown in Figure 4. Arsenate sorption onto ferrihydrite decreases with increasing pH and previous studies have also shown that arsenate sorption kinetics are more greatly affected by pH than arsenite.[26–29] In fact, Raven at al. (1998) observed little difference in arsenite sorption (at similar concentrations) onto ferrihydrite between pH 4.6 and 9.2. However, although the pH changes in Reactors E and ES were nearly identical, the retardation of iron reduction in Reactor ES proved significant; it provided more sorbing locations for arsenic due to the preservation of adsorption sites. Furthermore, precipitating iron sulfide minerals also provided sorption sites that were not originally present. Reactor ES therefore yielded significantly lower dissolved arsenic concentrations (between days 12 and 30) but only temporarily as the previously noted gradual increase in pHs increased overall arsenic solubility throughout the experiment. This is reflected in the gradual rise of dissolved arsenic concomitant with the increase in pH in Reactor ES and final arsenic concentrations nearly identical to those observed in Reactor E.

7. Conclusion

Solid phase analyses of acid volatile sulfide reveal that very little arsenic was incorporated into the sulfide precipitate. We surmise that the temporarily muted (days 12 through 30) concentrations of dissolved arsenic in Reactor ES are due to decreased

amounts of iron and arsenic reduction due to SRB, FeRB, and AsRB competition for H_2; this resulted in less ferrihydrite dissolution and therefore less arsenic desorption. Also, iron sulfide minerals provided additional sorbing locations for dissolved arsenic. This, combined with pH-sorption dynamics influenced largely by syntrophic ethanol oxidation, kept arsenic out of the dissolved phase during the time of peak iron and sulfate reduction and resulted in very little arsenic being sequestered as an impurity within iron sulfides or as an arsenic sulfide. The retained adsorbed arsenate species in Reactor ES maintained their sorbed locations due to low pH but eventually entered the dissolved phase.

The results of these experiments suggest that biostimulation was effective at temporarily lowering dissolved arsenic concentrations but may not be means for arsenic remediation, especially regarding the efficacy of sequestering arsenic as part of the mineral structure in iron and arsenic sulfides. Instead, biostimulation of ferric iron and sulfate reduction may create a dual effect of iron-sulfide precipitation without first mobilizing adsorbed arsenic to be incorporated into the mineral. This may be avoidable with efforts to 1) control pH and therefore arsenic adsorption and 2) delay sulfate reduction until arsenic is sufficiently mobilized – perhaps with a delayed injection of sulfate into the system.

6. Bridge I

In this chapter (Chapter II), I collected aquifer sediments from a naturally contaminated bedrock aquifer ($[As^{III}] \geq 3000$ ppb), constructed laboratory microcosm by adding sulfate and ethanol, and incubated for 2 months. Ethanol-sulfate experiments initially yielded significant iron-sulfide precipitates and lowered arsenic contamination to ~200 ppb; however, arsenic levels later increased to ~3600 ppb; with 31% (~202

μmol×(kg water)$^{-1}$) and 12% (~78 μmol×(kg water)$^{-1}$) of solid phase arsenic apportioned as adsorbed and arsenic-sulfide, respectively. Ethanol-only experiments yielded higher initial arsenic contamination (~1500 ppb), however 22% (~105 μmol×(kg water)$^{-1}$) of solid phase arsenic was sulfide-sequestered. Our results show that robust, simultaneous iron and sulfate reduction can temporarily mitigate arsenic contamination, but may marginalize sulfide's ability to scavenge arsenic and instead direct it to the less stable adsorbed phase. This research highlights the complications of arsenic remediation via biostimulation with respect to competing redox reactions, microbial activity, and secondary controls on the fate of arsenic such as pH changes as a result of ethanol oxidation. In the following chapter (Chapter III), for comparison, I explore similar biogeochemical reactions through a series of *in situ* aquifer push-pull tests.

CHAPTER III

ATTENUATION OF GROUNDWATER ARSENIC THROUGH STIMULATION OF AQUIFER MICROORGANISMS

In preparation for submission to *Environmental Science & Technology*

The manuscript was written by Scott C. Maguffin with input from Qusheng Jin. Q.J. and Ashley Daigle. designed the project. Samples were collected and analyzed by S.C.M, Q.J. and A.D. Q.J., A.D., and S.C.M. conducted analyses. Jing Sun and Benjamin C. Bostick carried out synchrotron analyses.

1. Introduction

Arsenic cycling within the critical zone threatens the health and well-being of an estimated 100 million people around the world.[1] Although it is widely distributed within the critical zone, exposure is especially hazardous by way of groundwater. Either through use as drinking water through or irrigation and bioaccumulation in food, arsenic poisoning by this pathway can lead to skin lesions, neuropathy, diabetes, cardiovascular disease, and cancer.[2,3] Arsenicosis is a major problem in South and Southeast Asia as well as in the United States.[4–6]

In groundwater systems, arsenic is typically present as the inorganic oxyanions arsenate [As(V)] and arsenite [As(III)][7,8]. The properties of these arsenic species are subject to biological and geochemical controls and exhibit different toxicities and mobilities in the environment. Biological processes mediate transformations between these different arsenic species, and the genetic basis for some of these microbial processes is increasingly well understood. Recent attention has been directed towards biogeochemical processes that cause and could mitigate arsenic contamination through enhanced attenuation of natural chemical and biological regimes.[9–11]

Reduction of ferric (oxy)hydroxide minerals is considered a common source of groundwater arsenic contamination.[12–16] The presence of arsenic as an impurity within ferric iron minerals is consequential in iron reducing environments and its release through the dissolution of its host structure may increase As(V) concentrations in the dissolved or adsorbed phase. In common groundwater environments, As(V) is competitive for adsorbing locations, however, desorption by competing molecules such as phosphate or organic compounds can desorb As(V) and increase dissolved phase arsenic concentrations.[17–19] Microorganisms capable of utilizing As(V) as an electron acceptor and reducing it to As(III) complicate the biogeochemical network of aquifer microorganism reactions and can further increase dissolved arsenic concentrations.

Recent studies have focused on the presence of groundwater sulfate and its effect on arsenic contamination.[11,20–24] Typically, in aquifers where sulfate reduction is an active process, dissolved groundwater arsenic is low.[4,11,24–26] Laboratory experiments have shown that the reduction of sulfate and subsequent production of dissolved sulfide can be an effective mechanism for removing dissolved arsenic, either by precipitating it with iron-sulfide or in an arsenic-sulfide mineral[27].

Here, we use two aquifer push-pull tests to investigate biogeochemical redox processes controlling the naturally occurring arsenic contamination in a bedrock aquifer. We explore the natural proclivities for electron acceptors of *in situ* microorganisms and examine the potential use of their metabolisms to mitigate dissolved arsenic contamination. Through stimulated simultaneous redox reactions, we show that promoted sulfate reduction in the presence of arsenic-contaminated groundwater can effectively sequester arsenic in anaerobically-stable solid phase minerals.

2. Methods

2.1 Study Area

Push-pull tests were conducted within the bedrock aquifer in the southern Willamette Basin, Oregon, USA (Fig. 1). The bedrock aquifer, locally known as the Fisher Formation, ranges up to 2,100 meter-thick and consists of volcaniclastic arkosic sandstone, mudflows deposits, and andesitic lapilli tuffs and breccias[4,28,29]. Hydrologically, the Fisher Formation has relatively low permeability and is considered part of the basement confining unit within the western Cascade Range.[29] A survey of local wells (n = 23) indicates the Fisher Formation is oligotrophic, anaerobic, and variably contaminated with both As(III) and dimethylarsinic acid DMAs(V) (769±1051 and 6.1±4.8 ppb, respectively); the Na-Cl type groundwater exhibits low dissolved organic carbon (DOC) (4.7±3.6 ppm), alkalinity 5.9±3.1 $meq_{*}L^{-1}$, and a pH of 7.7±0.5. See Appendix C for groundwater composition of the bedrock aquifer.

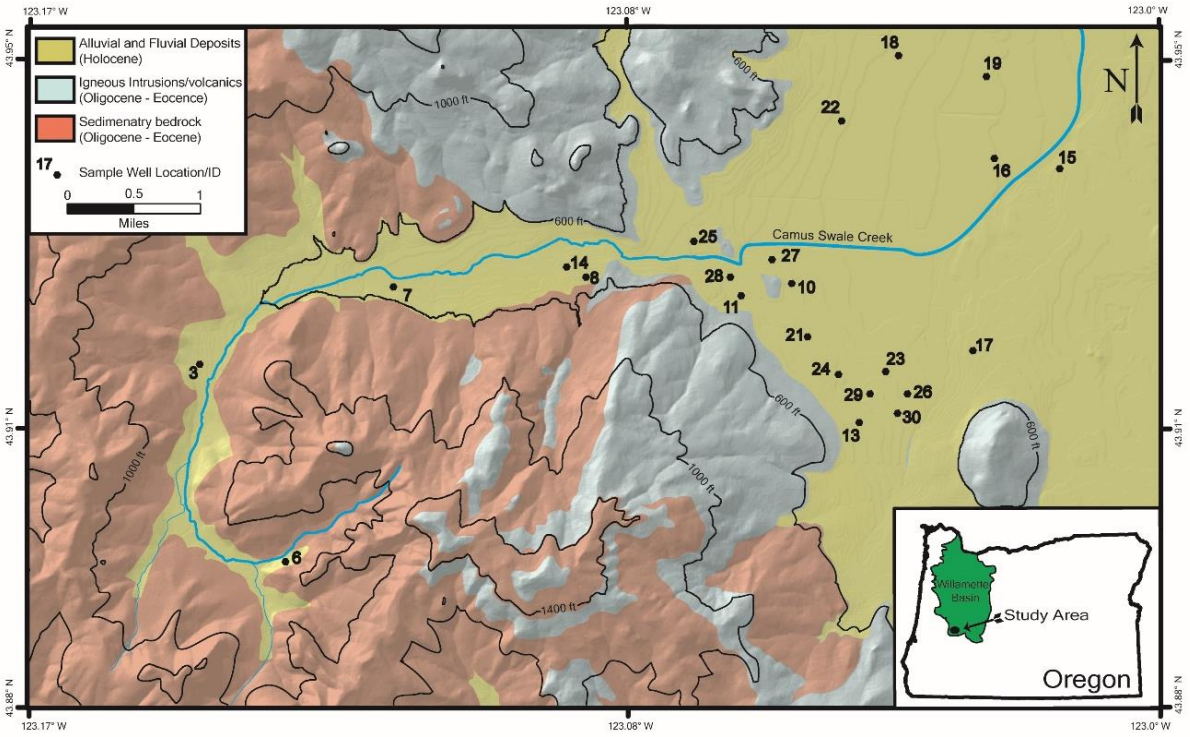

Figure 1. Geologic map of field site and well locations the Eugene-Springfield area of Oregon, USA. Well 13 was used for control injection test and stimulated injection test field experiments. Figure reproduced from Maguffin et al. (2015) with permission.

To conduct aquifer push-pull tests, we drilled a borehole 38 meters into an arsenic-contaminated part of the bedrock aquifer. Groundwater samples were analyzed for background chemistry. Aquifer transmissivity was characterized by slug-tests every 1.5 m between 26 and 38 m depth to determine the most effective location for experimental solution injection. We installed stainless steel packers at 29 m and 32 m depth to isolate a 3 m section of the aquifer for push-pull test injections. A PVC pipe connected the packer-isolated borehole column to the ground surface where it was connected to a peristaltic pump; the pump was used for injections of experimental solutions and the subsequent sampling of groundwater.

2.2 Push-pull experiments

The first push-pull test was a controlled injection test. In order to create the necessary 40-gallon control solution, we extracted groundwater from a nearby well and adjusted it to the desired parameters (Table 1). In order to track mixing and dilution between the control solution and nearby groundwater, we designed the control solution to have a relatively low chloride concentration and monitored the rate at which chloride increased to background concentrations. Solution preparation included the purging of dissolved oxygen (DO) with a gas mixture of N_2 and CO_2 (95% and 5%, respectively). Solution anaerobicity was confirmed through continuous monitoring with a DO meter. The anaerobic control solution was pumped into the packer-isolated borehole column at a rate of 2 gallons/minute to begin the control injection test. Daily samples were collected throughout the first week and subsequent samples were collected every 2-4 days. A second test was conducted by injecting an ethanol amended solution (EAS) and will hereby be referred to as the stimulated inject test. With the exceptions of volume and minor differences in solution chemistry (Table 1), the EAS was prepared for injection by employing control solution methods outlined above. The EAS was amended with 100 ppm bromide to establish mixing rates.

Table 1. Experimental chemistry

		Pretest	Control	Ethanol
Volume	(gal)	n.a.	40	100
T	(^{o}C)	15.6	19.2	16.3
pH		7.6	7.0	7.3
Conductivity	(μS)	2090	1233	1960
Alkalinity	(mM)	12.4	11.8	20.7
Ethanol	(mM)	0	0	40
Bromide	(mM)	0.00	0.00	1.25
Chloride	(mM)	17.4	2.84	0.67
Ferrous Iron	(mM)	0.02	0.01	0.00
Sulfate	(mM)	2.54	1.38	0.51
As(III)	(ppb)	2300	28	8.8
As(V)	(ppb)	130	1900	2000

To prepare solid phase control samples, we collected unweathered bedrock from nearby exposed Fisher Formation. Bedrock samples were crushed to reduce particle size diameters to 100 - 700 μm. The granular bedrock mixture was mixed for homogeneity and allotted into a series of mesh-screen containment units. We prepared 7 of these bedrock sample units and began incubating them within the packer-isolated borehole three months prior to the field experiments.

2.3 Sample Collection

Daily, post-injection aqueous samples were collected throughout the first week after each push-pull injection; subsequent sampling occurred every 2-4 days. Groundwater samples were filtered (0.45 micron) and preserved appropriately for laboratory analyses and arsenic speciation (Appendix A). *In situ* field measurements included temperature pH, conductance, [Fe^{2+}], and [HS^-]. Incubating solid phase samples were extracted from *in situ*, temporarily housed in a chilled, anaerobic containment unit and frozen at -80^o C for future analytical work. We collected and analyzed for methane

and CO_2 using a flexible tedlar bag technique intended for gas chromatography (EPA Method 3C).

2.4 Analytical Techniques

Field analyses of ferrous iron and sulfide were conducted using the Hach method 103769 and 2244500, respectively (Appendix A). We analyzed the alkalinity of groundwater samples using burette titration methods (EPA Method 310.1). We used ion chromatography, HPLC, and ICP-MS for groundwater speciation of arsenic and anion chemistry. Low molecular weight organic acids were analyzed using a NPH derivatization protocol based on Albert and Martens (1997)[30]. Solid phase analyses were conducted for ferrous and ferric iron, sulfide, and arsenic. Microfocused synchrotron X-ray fluorescence (μSXRF) maps for arsenic and iron were conducted on solid phase samples collected on days 3 and 50. (see Appendix A for analytical methods)

3. Results

3.1 Push-pull Experiments

During the control injection test, neither ethanol nor acetate was detected (data not shown). Only small fluctuations in sulfate and ferrous iron were observed in the first three weeks of the experiment, after which subtle increases in both species occurred. Ferrous iron reached a maximum concentration of 0.04 mM on day 42 (Fig. 1) and sulfate concentrations were relatively constant through day 23 (1.46±0.057 mM), and steadily increased to 2.4 mM after 54 days into the experiment. Dissolved sulfide showed little variation in concentration until day 42, after which sulfide concentrations remained low throughout the experiment (Fig. 3).

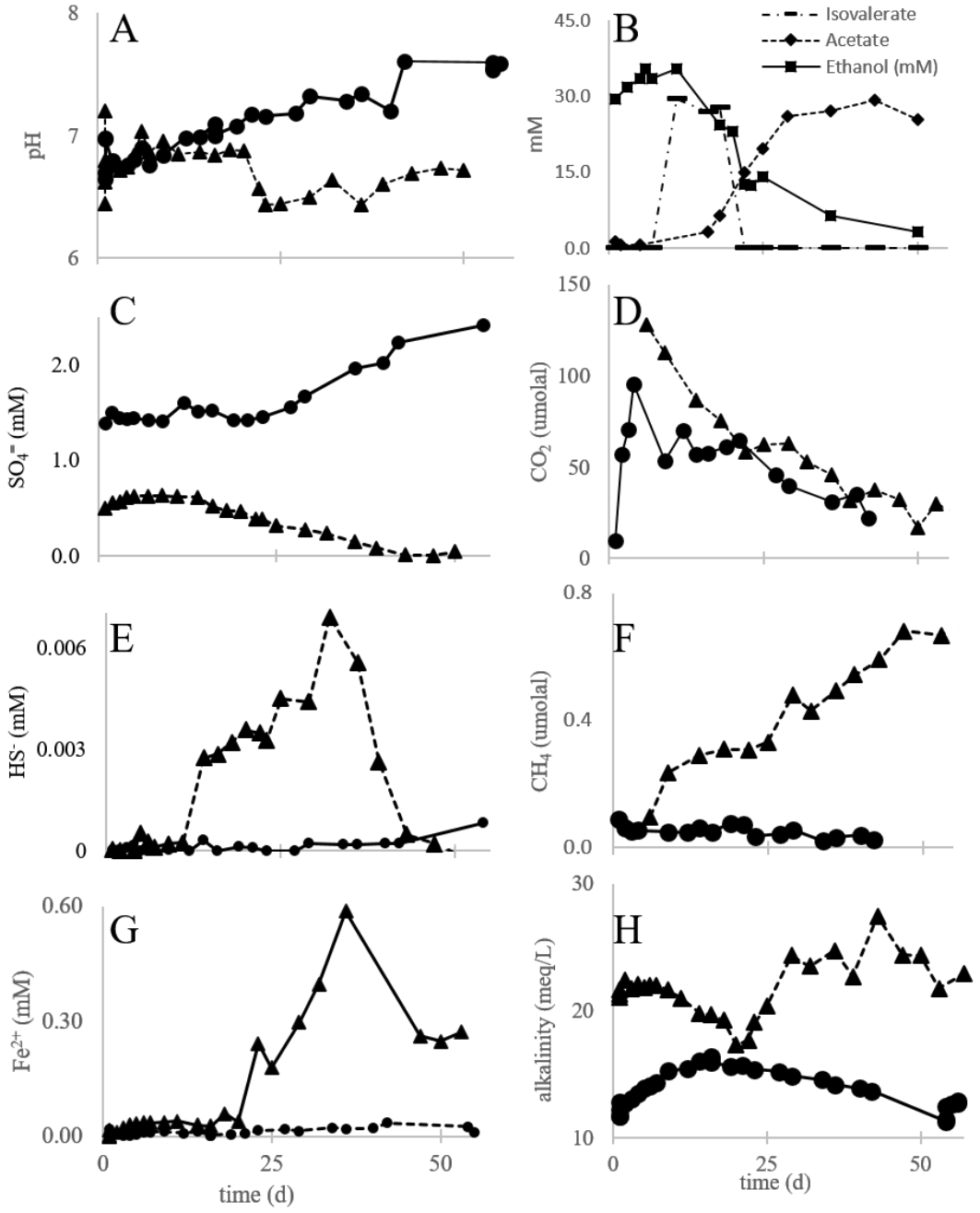

Figure 2. Variations with time in pH (A), organic matter (B), sulfate (C), CO_2 gas (D), sulfide (E), CH_4 gas (F), ferrous iron (G), and alkalinity (H) in the control injection test (•) and stimulated injection test (▲). Panel B only pertains to the stimulated injection test.

At the beginning of the control injection test, arsenate and arsenite exhibited concentrations of 1900 and 7 ppb, respectively. Within two days, arsenate concentration

decreased to 840 ppb and arsenite concentration increased to 1100 ppb. Afterwards, arsenate increased with time, and reached its maximum concentration of 3500 ppb arsenic at day 14. Arsenate then quickly decreased to 350 ppb at day 16. On the other hand, arsenite first increased to 1100 ppb on day two and decreased to 12 ppb of arsenic on day 14 before quickly increasing to 2900 ppb on day 21.

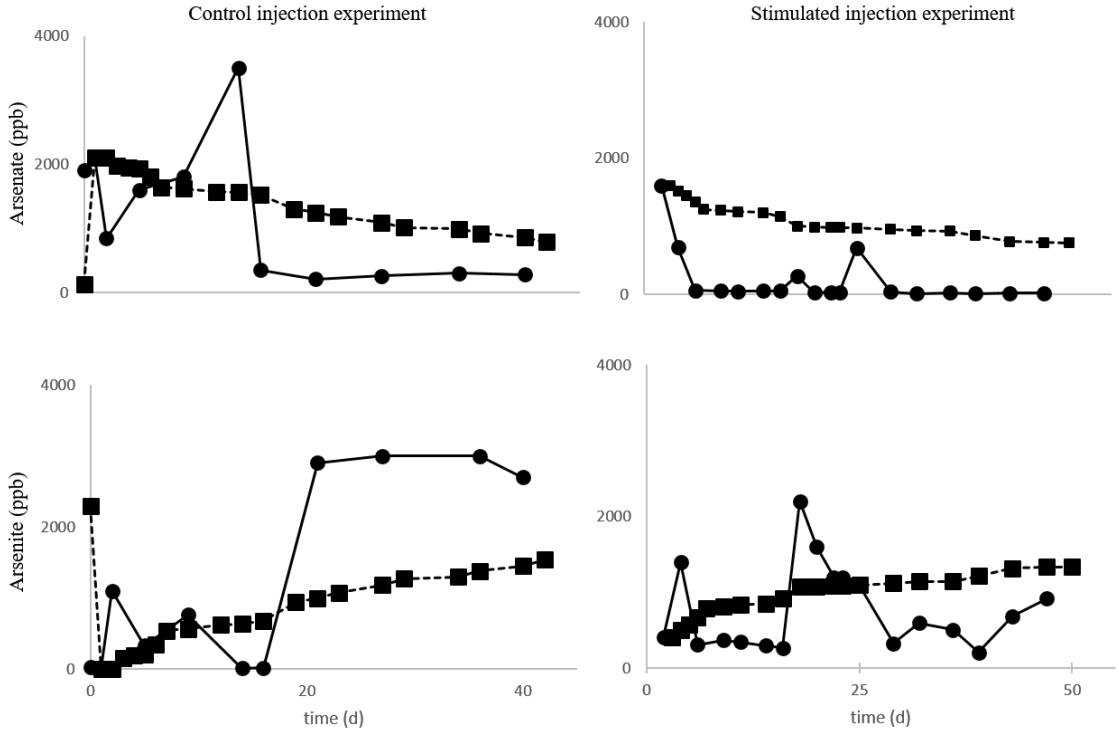

Figure 3. Dissolved arsenic concentrations in groundwater throughout the control injection test (left) and stimulated injection test (right). The dashed lines show the hypothetical concentrations of each species based on groundwater mixing calculations.

Variations in chemical concentrations in the push-pull tests result from both the mixing of the test solution with the groundwater and the production or consumption of chemical compounds around the well borehole. The production and consumption of chemical compounds can be computed based on the extent of the mixing and variations in

chemical conditions. As shown in figure 3, the control injection test exhibited volatile arsenic concentrations before day 20 and a maximum accumulation rate of arsenite of approximately 450 ppb/day. The stimulated injection test exhibited similar volatility in arsenic concentrations but arsenite continued fluctuation after day 20 – though, notably at significantly lower concentrations that in the control injection test. We observed a maximum accumulation rate of arsenite of approximately 600 ppb/day between days 16 and 20.

3.2 Biostimulation

Figure 2 shows how primary groundwater constituents change throughout the biostimulation experiment. In the first few days of the biostimulation experiment, ethanol concentrations increased from 30 to 35 mM. Between days 11 and 50, ethanol decreased at two distinctly different rates: between days 11 and 22 ethanol decreased at rate of 2 mM/day whereas between days 22 and 50 ethanol decreased at a rate of 0.3 mM/day. Concurrent with the decrease in ethanol was the accumulation of acetate. Like ethanol, acetate exhibited multiple phases of accumulation. Between days 1 and 16 and days 43 and 50 acetate increases at a rate of 0.2 mM/day. However, between days 29 and 43 acetate increases at a rate of 1.6 mM/day. We observed a brief but significant spike in isovalerate between days 11 and 18 ranging between 26 and 30 mM. We also detected low concentrations (0.0 - 0.7 mM) of formate, propionate, and valerate throughout the stimulated injection test (see Table A1 in Appendix).

Throughout the control injection test we detected no significant amount of ferrous iron or HS^- and observed an accumulation of sulfate from approximately 1.5 mM to 2.5 mM. However, the stimulated injection test shows robust accumulation of both HS- and ferrous iron between days 11 and 36. Ferrous iron accumulated between day 20 and 36 at

a rate of 0.034 mM/day and decreased between days 36 and 50 at a rate of 0.024 mM/day. Dissolved sulfate in the stimulated injection test briefly accumulated but then steadily decreased at a rate of 0.016 mM/day to <0.01 mM by day 43. Stimulated injection test sulfate concentrations did not begin decreasing until day 9 but continued a steady decline until day 47 when background concentrations were reached.

During the biostimulation experiment, arsenate quickly decreased from an initial concentration of 1600 ppb on day 3 to 61 ppb on day 6. The relatively low (9-60 ppb) groundwater As(V) concentrations persisted throughout the experiment with the exception of two sampling events. As(V) was measured at 270 and 680 ppb on day 18 and 25, respectively. Arsenite concentration exhibited two significant spikes throughout the experiment; a brief, initial spike (410, 1400, and 310 ppb on days 2, 4, and 6, respectively) and then between days 16 and 18 As(III) increased from 270 to 2200 ppb, after which As(III) concentrations gradually decreased to 330 by day 29. Subsequent As(III) concentrations remained between 330 and 690 ppb.

3.3 Solid phase

Chemical extraction of solid phase arsenic show that ionically bound and strongly adsorbed arsenic decreased with time in the experiment (Table 2). There was no significant change in the amounts of arsenic that precipitated with amorphous iron oxyhydroxides. However, there was a notable decrease in arsenic co-precipitated with crystalline iron oxyhydroxides. Arsenic co-precipitated with pyrite and amorphous As_2S_3 increased towards the end of the experiment.

Table 2. Solid phase arsenic analyses.

stimulated injection test (days)	Ionically bound (ug/g)	Strongly adsorbed (ug/g)	Precipitated with AVS (ug/g)	Precipitated with amorphous Fe oxyhydroxides (ug/g)	Precipitated with crystalline Fe oxyhydroxides (ug/g)	Precipitated with pyrite & amorphous As_2S_3 (ug/g)
3	9.38	46.91	4.77	4.61	2.47	2.11
9	5.94	54.65	6.34	4.28	2.85	1.65
16	8.02	63.59	5.90	2.58	3.04	2.36
22	3.06	55.56	7.22	4.07	2.19	4.81
29	5.56	43.90	5.66	3.51	3.51	8.20
36	3.69	39.73	6.62	4.54	1.76	6.05
50	4.76	39.22	7.10	5.04	1.54	4.86

Acid volatile sulfide (AVS) and chromium reducible sulfide (CRS) were only detected in the last two solid phase sampling days during the stimulated injection test (Table 3). Samples collected on day 36 and 50 show AVS concentrations to be 6.6±4.8 and 6.6±9.2 and CRS concentrations of 11.4±7.3 and 10.5±9.0, respectively (Table 2). Iron analyses of solid phase samples from the stimulated injection test show an increasing trend of ferrous iron concentrations and high analytical variability in amorphous and crystalline ferric iron (Table 4).

Table 3. Formation of acid volatile sulfides (AVS) and chromium reducible sulfides (CRS) during the biostimulation experiment. Sample analysis was carried out in triplicate, and the results are reported as average ± standard deviation in S per dry weight of sample.

Time (days)	AVS (mg/g)	CRS (mg/g)
3	0±0.0	0±0.0
9	0±0.0	0±0.0
16	0±0.0	0±0.0
22	0±0.0	0±0.0
36	6.6±4.8	11.4±7.3
50	6.6±9.2	10.5±9.0

Table 4. Iron speciation in solid phase mineralogy

stimulated injection test (days)	Fe^{2+} (mg/g)	Fe total (mg/g)	Fe^{3+} (amorphous) (mg/g)	Fe^{3+} (crystalline) (mg/g)
3	8.3 ± 0	15.3 ± 0	7 ± 0	87.4 ± 0
9	11.3 ± 1.2	19.6 ± 5.3	8.3 ± 5.1	76.6 ± 73.1
16	14.2 ± 0	19.7 ± 0	5.5 ± 0	-
22	14.1 ± 4	23.8 ± 5.4	9.7 ± 5.6	50.0 ± 59.0
29	9.2 ± 0	15.7 ± 0	6.5 ± 0	-
36	16.2 ± 1.9	14.3 ± 5.8	8.1 ± 5.9	18.5 ± 18.4
50	13.74 ± 0	21 ± 0	7.3 ± 0	73 ± 0.0

Synchrotron XANES analyses of solid phase samples revealed differences in iron and arsenic between days 3 and 50 (Table 5). Notable changes to iron mineralogy included decreases in goethite and ferrihydrite and increase in magnetite. Arsenic results include an observed decrease in As(III) and a significant increase in As_2S_3.

Table 5. Synchrotron results for arsenic and iron.

	Day 3	Day 50
As(III)	80.3%±0.26%	66.3%±0.26%
As(V)	19.2%±0.18%	28.8%±0.18%
As_2S_3	0.252%±0.32%	4.79%±0.36%
Siderite $FeCO_3$	0.0%±2.9%	0.0%±3.3%
FeOOH Goethite	11.5%±4%	0.24%±4.7%
Fe_2O_3 Hematite	0.003%±1.9%	0.9%±2.2%
magnetite Fe_3O_4	1.2%±2.6%	8.9%±3%
Biotite (Fe^{2+} silicate)	1.1%±3.1%	0.19%±3.5%
Hornblende ($Fe^{2+/3+}$ silicate)	12.8%±3.4%	28.1%±3.9%
Ferrihydrite $Fe(OH)_3$	73.3%±9.5%	61.6%±11%

4. Discussion

We explored the feasibility of biostimulation as a strategy for *in situ* arsenic bioremediation by carrying out two push-pull experiments in the bedrock aquifer of Southern Willamette Basin, Oregon. We analyzed in situ rates of biogeochemical processes under both natural and biostimulation conditions. This introduction of ample electron donating compounds in the form of ethanol and its decompositional products stimulated microbial metabolisms. The decomposition of ethanol, as well as the production and decomposition of acetate had significant effects on arsenic contamination and sequestration. Previous laboratory experiments that used bedrock aquifer media have shown that indigenous microorganisms are capable of utilizing common aquifer species such as sulfate, ferric iron, and the problematic As(V) to oxidize these organic compounds.[11,27] We see similar trends in these *in situ* experiments. Furthermore, here we report for the first time *in situ* sequestration of groundwater arsenic into arsenic sulfide minerals through the stimulation of microbial metabolisms.

4.1 Push-pull experiment redox processes

Microbial utilization of ethanol began approximately 6 days after the EAS injection. We observed a modest increase in acetate and a significant but short-lived accumulation of isovalerate between days 6 and 14. The presence of both acetate and isovalerate appeared to have a significant effect on sulfate, iron, and As(V) reduction, as well as methanogenesis. Less concentrated organic acids such as formate, propionate and valerate were detected but do not appear to have played a significant role in primary redox chemistry.

Given that the chemistry of the control solution closely simulated *in situ* conditions, our expectations were that only background levels of dissolved ferrous iron (<

0.04 mM) would be observed. We expected the stimulated injection test to simulate multiple redox metabolisms and yield insight into microbial use of electron acceptors and corresponding interactions between redox products. We observed little accumulation of ferrous iron (< 0.04 mM) throughout the control injection test. Likewise, between days 1 and 20 of the stimulated injection test, we observed similar background ferrous iron concentrations (c. 0.04 mM); however, dissolved ferrous iron quickly accumulated from day 16 through day 36 to 0.59 mM at a rate of 0.03 mM/day.

Ethanol depletion exhibited a moderate correlation with ferrous iron production (R^2 = 0.78, n=10) but was likely not directly involved in the ferric iron redox reaction. Acetate, a product of ethanol decomposition, increased between days 16 and 32; its concentrations strongly correlated with ferrous iron accumulation (R^2 = 0.98, n=5) indicating that microorganisms likely oxidized acetate by reducing ferric iron. We hypothesize that fermentation was the primary decomposing mechanism for ethanol and yielded increases in acetate, H_2, and H^+ concentrations.

Although 1.5 mM of dissolved sulfate were available at the beginning of the control injection test, sulfate steadily accumulated over time due to the influx of in situ groundwater. We detected little HS^- throughout the control injection test and surmise that only a minimal sulfate reduction occurred. The increase in background sulfate after day 50 correlated with an increase in sulfate reduction (R^2 = 0.83, n=4) and is demonstrated by small increases in dissolved HS^-.

Although we observed low levels of dissolved HS^- throughout the first 11 days of the stimulated injection test, we detected only minimal changes in sulfate. Significant stimulated injection test sulfate reduction began around day 11; this is evidenced by the decrease in sulfate concentrations and the accumulation of HS^-. The significant rate of

HS^- production between days 11 and 32 show sustained, prolific sulfate reduction occurring alongside both ferric iron reduction, As(V) reduction, and methanogenesis.

4.2 Arsenic redox processes

The dissolved control injection test As(V) concentrations exhibited volatility in the first 14 days; this was likely a manifestation of ongoing adsorption exchanges. However, between days 14 and 16, As(V) decreased from 3500 to 350 ppb and between days 16 and 21 we observed an increase in As(III) from 15 to 2900 ppb. Based on comparisons to As(V) and As(III) mixing calculations, it is clear that significant As(V) reduction occurs between days 14 and 21. After 21 days, As(V) concentrations stabilized and maintained background, pre-experiment levels, whereas As(III) began to trend towards background levels after day 40. Given that there was little iron reduction occurring throughout the control injection test, the decreasing trend of As(III) after 36 days was probably a result of either the uptick in sulfate reduction or the adsorption of As(III) – or a combination of both.

The initial sharp decrease in As(V) and subsequent increased As(III) concentrations in the stimulated injection test indicate that As(V) was either quickly adsorbed or reduced within the first 4 days. Between days 6 and 18 both As(V) and As(III) remained low and significantly less than what is predicted by mixing calculations. However, at day 18, there is a spike in dissolved As(V) (270 ppb) and a significant amount of dissolved As(III) (2200 ppb). This coincides with the onset of robust iron reduction. Acetate, and possibly isovalerate, stimulated microbial iron reduction and dissolved ferric iron minerals releasing arsenic from its mineral structure and adsorbed locations. Active arsenic reducing bacteria quickly reduced As(V) to As(III), as seen in the nearly non-detectable concentrations of As(V) during this time.

4.3 Solid phase arsenic, iron, and sulfide

The accumulation of dissolved ferrous iron, As(III), and HS^- resulted in the precipitation of iron-sulfide and arsenic-sulfide minerals. We observed evidence of iron and arsenic-sulfide precipitation in the precipitous decrease of HS^- beginning on day 32 and the significant increase of AVS and CRS minerals detected on days 36 and 50 (Table 2). These data correspond to the 0.024 mM/day decrease in dissolved ferrous iron between days 36 and 50. Furthermore, synchrotron analyses show a 20-fold increase in As_2S_3 mineralogy between days 3 and 50; correspondingly, all dissolved HS- and sulfate were removed by day 50. In the absence of sulfate reduction, continued iron reduction by acetate oxidation after 50 days resulted in a new period of dissolved ferrous iron accumulation

Although no solid-phase samples were collected during the control injection test, solid-phase samples were incubated *in situ* during the control experiment; therefore, the first sample of the stimulated injection test is a representative sample of post-control injection test mineralogy. Neither CRS nor AVS minerals precipitated during the control injection test. This is consistent with aqueous data; we observed no significant sulfate reduction nor any dissolved ferrous iron or substantial HS^- accumulation throughout the control experiment.

Control injection test redox reactions showed no proclivity for removing removed dissolved As(III) or sequestering arsenic in reduced solid phase minerals. However, under stimulated conditions provided in the stimulated injection test, we observed simultaneous increases in CRS minerals, solid phase ferrous iron, and arsenic that was co-precipitated with AVS, pyrite, and amorphous As_2S_3, all of which manifested in the last 20 days of the experiment. Furthermore, we observed an overall decrease in arsenic-

bearing amorphous and crystalline ferric iron oxyhydroxides. Significant increases followed by decreases in As(V) and As(III) between days 18 and 30 document the transition of arsenic from arsenic-bearing iron minerals to dissolved arsenic and finally to an arsenic bearing iron-sulfide precipitate (Figure 4). These data provide in situ confirmation of previous work noting the effectiveness of sulfate and iron reduction in removing dissolved arsenic [11,27,31,32].

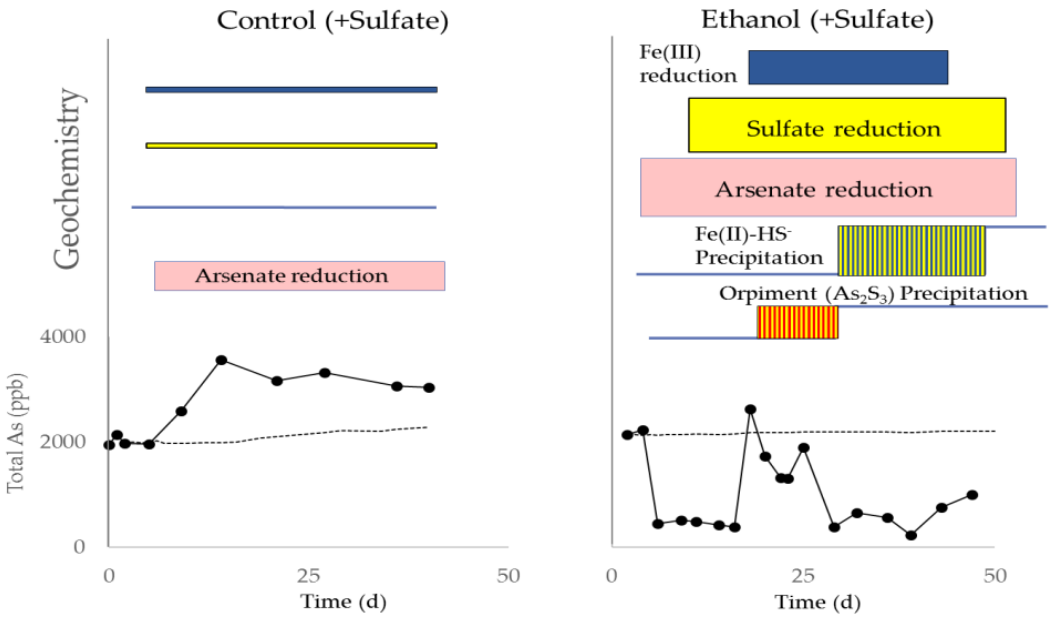

Figure 4. Illustration of redox processes and total arsenic concentrations over time in the control and ethanol stimulated *in situ* experiments. The dashed line represents projected total arsenic concentrations based on groundwater mixing only; the solid line represents measured total arsenic.

4.4 Arsenic mobilization and sequestration

Pretest chemical analyses of bedrock pore water show very low dissolved ferrous iron (~0.02 mM) and HS^- (0.04 mM) while maintaining dangerously high levels of As(III) (~2300 ppb) (Table 1). These data, as well as high background sulfate concentrations and an iron (oxy)hydroxide rich bedrock media, led us to hypothesize that

although the aquifer was anoxic and reducing, arsenic may be a preferred electron acceptor over sulfate or iron (oxy)hydroxides minerals. The control injection test confirmed this hypothesis; we observed no significant iron or sulfate reduction, however, the simulated eutrophic chemical regime of the control injection test resulted in approximately 3000 ppb As(V) being reduced to As(III) at a rate of ~500 ppb/day. Based on mixing calculations, this rate exceeds the influx rate of background As(III) by more than 3 fold.

Although the control injection test mobilized dissolved arsenic only slightly faster than the stimulated injection test during peak arsenic reduction (500 ppb/day versus 480 ppb/day, respectively), the effects of microbial stimulation yielded drastically different final results. Based on the results of the control injection test, namely the exclusively significant redox reactions of arsenic mobilization, the stimulated injection test allowed us to parse the specific compounding effects of sulfate and ferric iron reduction. Sulfate and iron reduction continued concomitantly between 18 and 40 days in the stimulated injection test. Based only on groundwater mixing calculations, we estimate that 2100 ppb total dissolved arsenic would have been available after 40 days; however, only 210 ppb total arsenic was detected in water. This indicates a dissolved arsenic removal rate of 90% when both ferric iron and sulfate reduction occur alongside arsenic reduction. This highly effective rate of arsenic removal can be followed to the solid phase where we observed significant increases in AVS, CRS, and synchrotron-analyzed As_2S_3 that occurred during the stimulated injection test. Compared to the control injection test, we calculated 2300 ppb total dissolved arsenic should have been available after 40 days, instead 2980 ppb total dissolved arsenic was detected; this represents an addition of 29%.

5. Conclusions

Control injection test results show that *in situ* conditions do not require additional electron donors to reduce and mobilize arsenic. However, despite ample sulfate and ferric iron electron accepting resources, arsenic reduction was the only significant redox process observed. Dissolved arsenic accumulation in the control injection test exceeded that of surrounding groundwater flux and maintained levels of approximately 3000 ppb. stimulated injection test results accelerated arsenic reduction while catalyzing ferric iron and sulfate reduction for a period of approximately 22 days. Although As(V) was nearly completely reduced during this time, and As(III) quickly accumulated in the dissolved phase, ferric iron and sulfate reduction effectively removed total dissolved arsenic at a rate of 90%. We tracked the migration of arsenic species from the injected ES and bedrock media to being sequestered in sulfide mineral precipitates. These data reinforce previous laboratory observations that identify iron sulfide precipitation as an effective means of removing arsenic from the dissolved phase in groundwater. For the first time we show effective *in situ* mitigation of arsenic contamination is possible by exploiting natural consortia of microorganisms under partially engineered chemical regime.

6. Bridge II

In this chapter (Chapter III), we conducted two aquifer injection experiments to examine *in situ* microbial redox processes and the potential to stimulate arsenic sequestration through arsenic sulfide precipitation. Our results show that *in situ* stimulation of microbial metabolisms accelerated the reduction of arsenic bearing iron (oxy)hydroxides as well as sulfate and arsenic reduction. Within 3 weeks of these contemporaneously occurring redox reactions, 90% of the dissolved arsenic was removed (~2000 ppb) and an effective long-term, anaerobically stable, sequestration of arsenic was

observed in a 20-fold increase of arsenic-sulfide precipitate. In the following chapter (Chapter IV), I examine organic arsenic reactions from the laboratory and *in situ* experiments discussed in Chapters II and III. I discuss organic arsenic dynamics and rates of arsenic methylation under stimulated conditions.

CHAPTER IV

RAPID GROUNDWATER ARSENIC BIOMETHYLATION THROUGH ETHANOL AMENDMENT

In preparation for submission to *Environmental Science & Technology*.

Scott C. Maguffin, Qusheng Jin, and Ashley Daigle designed the projects. The manuscript was written by S.C.M with input from Q.J. Q.J., A.D., and S.C.M. conducted experiments. Samples were collected and analyzed by S.C.M, Q.J. and A.D.

1. Introduction

Arsenic is a ubiquitous, toxic element that has an insidious knack for enduring as bioavailable species in critical zone environments. The toxicity and mobility of arsenic are particularly hazardous in groundwater systems where contamination is as much a function of the local geology as it is of aquifer microorganisms and groundwater chemistry. Together, these factors can create dangerous levels of dissolved arsenic and can lead to the poisoning of entire communities that depend on local groundwater as a potable resource. Although recent research efforts have focused on the efficacy of enhanced, biologically-driven arsenic sequestration and the significance of biological methylation (biomethylation) pathways in aquifers, the effect of the former on the latter has yet to be studied. Here, we investigate the potential impact of arsenic cycling through biomethylation pathways under a stimulated *in situ* chemical regime similar to those that may effectively sequester arsenic in the solid phase.

A well-established mechanism of arsenic mobilization is the microbial respiration of dissolved organic compounds through the reduction of ferric iron minerals[1–5]. In geologic environments where ferric (oxy)hydroxides minerals bear significant arsenic

content, iron reduction can mobilize mineral-bound arsenic into an adsorbed or dissolved phase. Likewise, dissimilatory arsenate (As(V)) reduction will yield arsenite (As(III)), often a more mobile arsenic species in common groundwater environments.[6] On the other hand, reduction-oxidation (redox) processes can effectively remove dissolved arsenic from groundwater; specifically, the production of sulfide via sulfate reduction has been shown to remove dissolved arsenic through arsenic-sulfide mineral precipitation[7] (Maguffin, 2016 *in prep*). These processes can result in dynamic changes of groundwater arsenic and can cause arsenic concentrations to exceed current drinking water standards. In addition, microorganisms possess the ability to detoxify their local environment, either by transforming arsenic back to arsenite – a less toxic oxidation state - or through biomethylation.

Attention to arsenic contamination has typically focused on inorganic arsenite and arsenate. However, recent focus on pathways of arsenic into food[8] and within groundwater systems[9] has brought new attention to the importance of biomethylated arsenic. Biomethylation of arsenic was first proposed in 1945 when Frederick Challenger outlined a process where methyl groups were successively added onto a metalloid species through alternating oxidative-methylation and reduction reactions[10]. Currently, the volatility and toxicity of methylarsenicals are not widely agreed upon. However, some consensus exists; for example, trivalent monomethylarsonous acid (MMAs(III)) and dimethyarsinous acid (DMAs(III)) are generally considered to be more toxic than inorganic arsenic, whereas pentavalent monomethylarsonic acid (MMAs(V)) and dimethylarsinic acid (DMAs(V)) are considered less toxic than inorganic arsenic[11]. Even less certainty exists for trimethylarsine (TMAs). Despite the lack of clarity regarding the relative toxicity and mobility of all arsenic species, the danger of either inorganic or

methylated arsenic to humans cannot be ignored, particularly since methylated arsenic can be readily converted back to inorganic forms[12,13]. Several methylated arsenic species are volatile and significantly more mobile than their inorganic counterparts; therefore, arsenic's mobility within groundwater increases with methylation[14]. In particular, biological (e.g. microbial) arsenic methylation, in groundwater and the shallow subsurface, are significant pathways relative to global fluxes of arsenic[9,15–17] and results in arsenic moving between reservoirs from soils to the atmosphere or groundwater to shallow subsurface.

Groundwater arsenic methylation has traditionally been viewed as a secondary process relative to redox transformations between arsenate and arsenite. However, recent studies raise concerns regarding the toxicity of groundwater methylarsenicals and their role in the arsenic cycle.[11,12,18] Increased attention has also led to a greater focus on characterizing all groundwater arsenic species. Despite methylarsenicals typically existing at concentrations 1-2 orders of magnitude lower than total dissolved arsenic,[19–25] microorganisms within an oligotrophic aquifer have been shown to produce DMAs(V) at a rate of 0.1% of the total dissolved arsenic per day.[9] This is a current and promising avenue of research in arsenic cycling and may provide insight into future arsenic mitigation techniques. However, the role of biomethylation of arsenic for remediation purposes has not been fully explored. Here, we discuss the results of several arsenic biomethylation experiments and report new rates of enhanced, *in situ* organic arsenic production; these data expand the potential role aquifer microorganisms in arsenic cycling.

2. Study Area and methods

We conducted laboratory incubation experiments and two aquifer injection tests at our study site located in the southern Willamette Basin, Oregon. Using aquifer material, we built 3 laboratory experiments in quadruplicate: N, E, and ES. Experiment N simulated the natural chemistry of the bedrock aquifer with no additional electron donating amendment. Experiments E and ES were both amended with ethanol and ES received an additional supplement of dissolved sulfate (2.5 mM). Experiments were incubated with 600 mL of synthetic groundwater in 1 L bottles at 16ºC in the dark.

We also conducted two aquifer pump tests: a control injection test and a stimulated injection test. The control injection test mimicked in situ groundwater chemistry with no electron donating amendment whereas the stimulated injection test contained c. 30 mM ethanol. We used conservative tracers to track the mixing fraction between the test solution and in situ groundwater throughout the experiments.

Importantly, no laboratory or field test solutions contained organic arsenic. Both laboratory and *in situ* water samples were analyzed for arsenic species and results are reported as 'arsenic as As(V)', As(III), MMAs(V), or DMAs(V)'. Henceforth, we dispense with the preceding clarification and will report concentrations using only the speciation identifier (e.g. As(V)). We were not able to collect or analyze for TMAs(V). Further details of the methods, experimental set up, and site description are available in Maguffin et al. (2015, 2016a, and 2016b)[9,26,27]. We analyzed solid phase samples for iron, sulfide, and arsenic (Supplemental Information). Some laboratory and field data has been reproduced with the permission of copyright owner.

3. Results

In the stimulated injection test, ethanol maintained its largest concentrations (35 mM) between 6 and 11 days. Between 11 and 22 days, ethanol decreased at a rate of 2 mM/day and between days 22 and 50 ethanol decreased at a rate of 0.33 mM/day. In the laboratory experiments, ethanol concentrations began to decrease within the first week. In both laboratory and field experiments, acetate concentrations steadily increased, reaching maximum values on day 24, 32, and 43 in experiments E, ES, and stimulated injection test, respectively (Fig. 1).

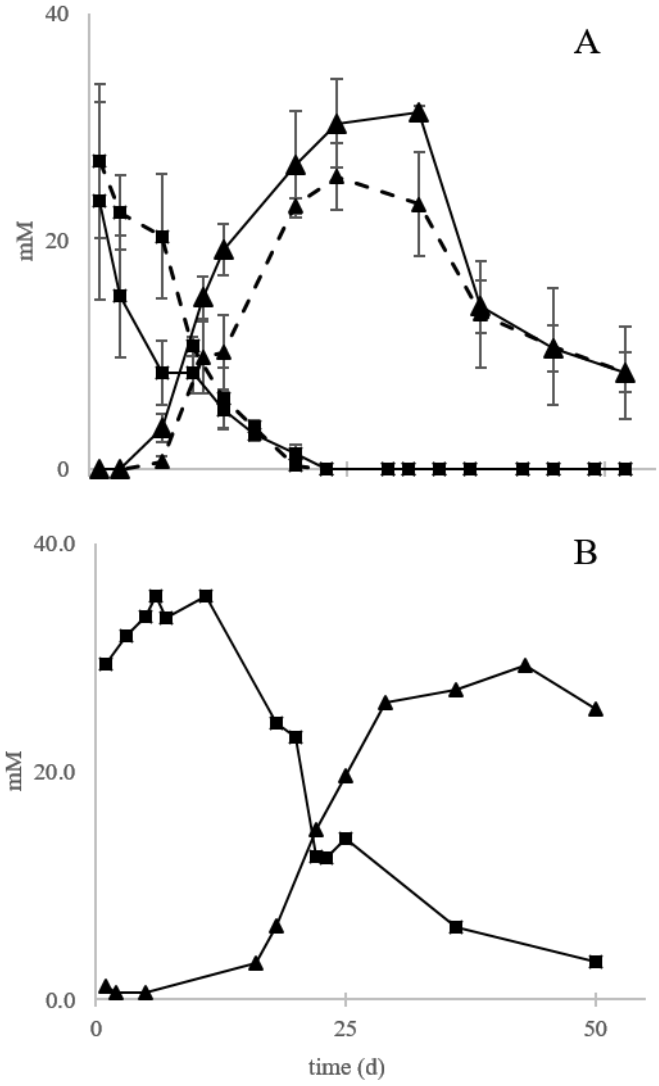

Figure 1. Ethanol (■), acetate (▲) over time in the laboratory experiments (A) and stimulated injection test (B). A solid line indicates that sulfate was added in the experiment. Experiment N is not shows as no organic matter was detected.

In unstimulated experiment N (Fig. 2), MMAs(V) and DMAs(V) accumulated with time, reaching maximum concentrations of 37 and 44 ppb, respectively. Throughout N, the ratios in MMAs(V) to arsenate concentrations remained relatively constant at 2.5±1.1%, with a linear regression coefficient of 0.95 (n=8) (Table 1). In the unstimulated control injection test field experiment, there were two distinct phases of organic arsenic accumulation (Fig. 3). In the first phase, arsenate and MMAs(V) approached their

maximum concentrations after 14 days (3500 and 59 ppb, respectively). The second phase occurred after day 26; arsenite and DMAs(V) reached their maximum concentrations of 3000 and 38 ppb, respectively.

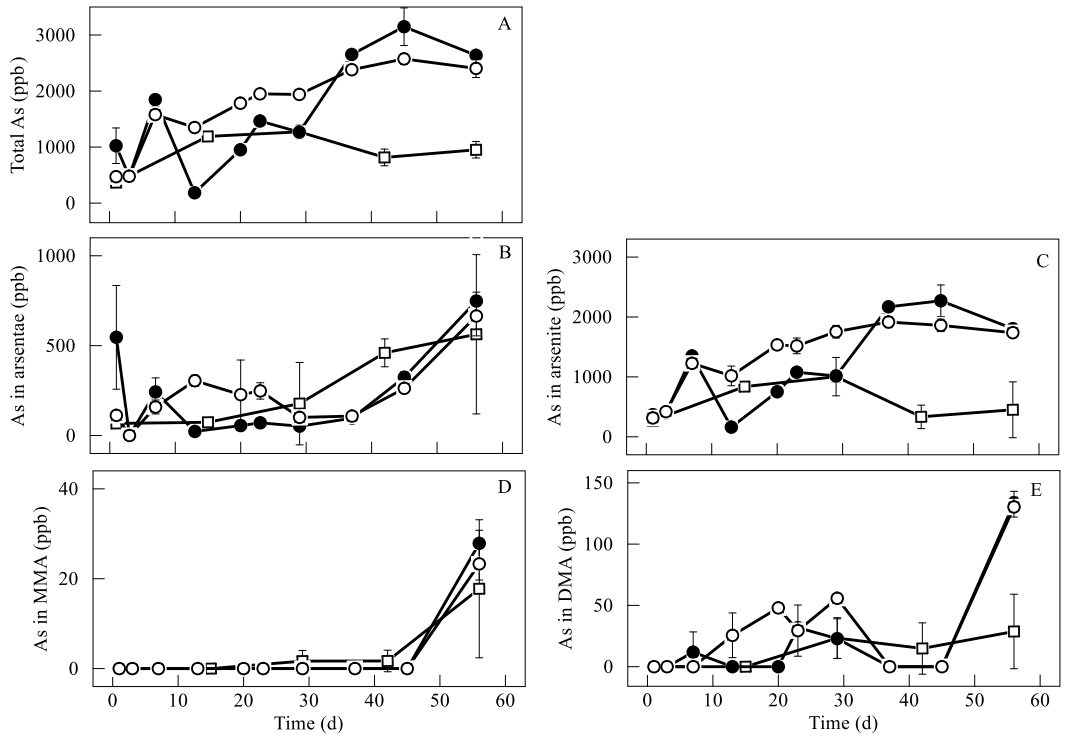

Figure 2. Variations of arsenic species with time in laboratory experiments. Data points represent the mean of measurement and error bars are the standard deviation. Symbols represent Reactor N (□), E (○), and ES (●). Panels A, B, and C are borrowed from Chapter II and included in this figure for context.

In stimulated laboratory experiment E, DMA(V) was first detected after 13 days. In ES, DMA(V) appeared after 27 days. We observed the largest laboratory DMA(V) concentration in Group E (approximately 140 ppb, day 55) (Fig. 2). On the other hand, MMAs(V) was not observed until after day 40. No MMA(V) or DMA(V) was detected in laboratory control experiments (not shown).

Inorganic arsenic in the control injection test exhibited a short-lived peak of As(V) above 3000 ppb (day 14) followed by sustained, elevated As(III) concentrations

approximately 3000 ppb (days 20-40) (Fig. 3). In the stimulated injection test, two significant peaks of elevated As(V) concentrations (Fig. 4). The first peak occurred on day 3 (1600 ppb) of the experiment before concentrations decreased to background concentrations; the second peak occurred on day 25 (1600 ppb). A similar pattern was observed for As(III) in the stimulated injection test. Two significant peaks of As(III) concentrations occurred on day 4 (1400 ppb) and day 18 (2200 ppb).

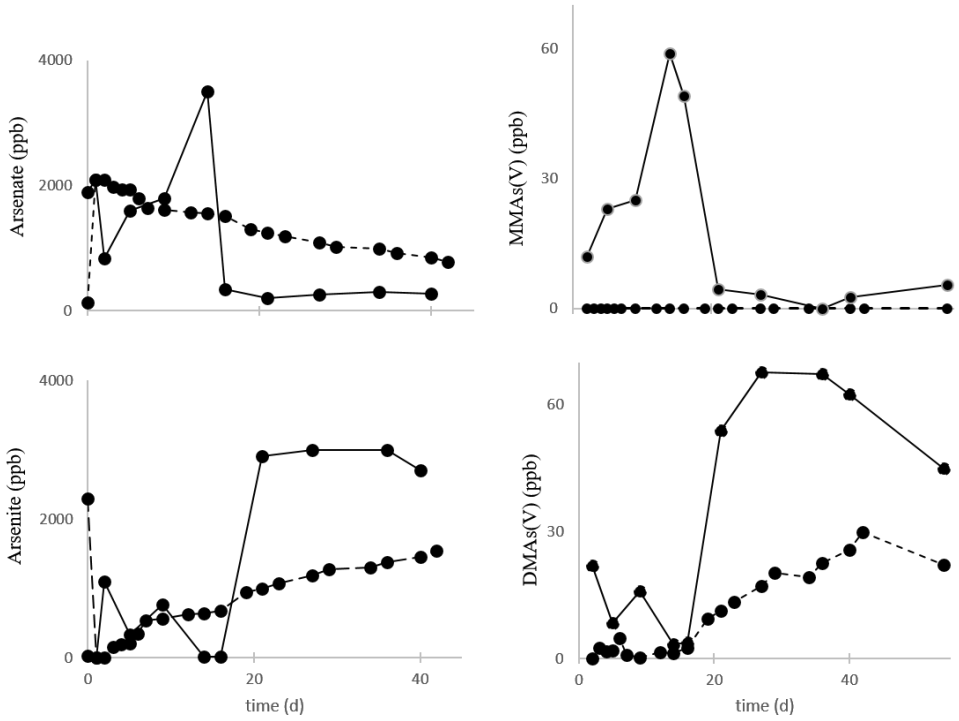

Figure 3. Variations of arsenic species with time in the control injection test. The dashed lines represent the projection of a species concentration based on groundwater mixing. The solid lines are measured concentrations. Inorganic arsenic data from Chapter III is included for context.

In the stimulated injection test (Fig. 4), DMAs(V) concentration quickly increased and reached a maximum concentration of 68 ppb at day 9. MMAs(V) was only briefly detected at the beginning of the experiment and on day 25.

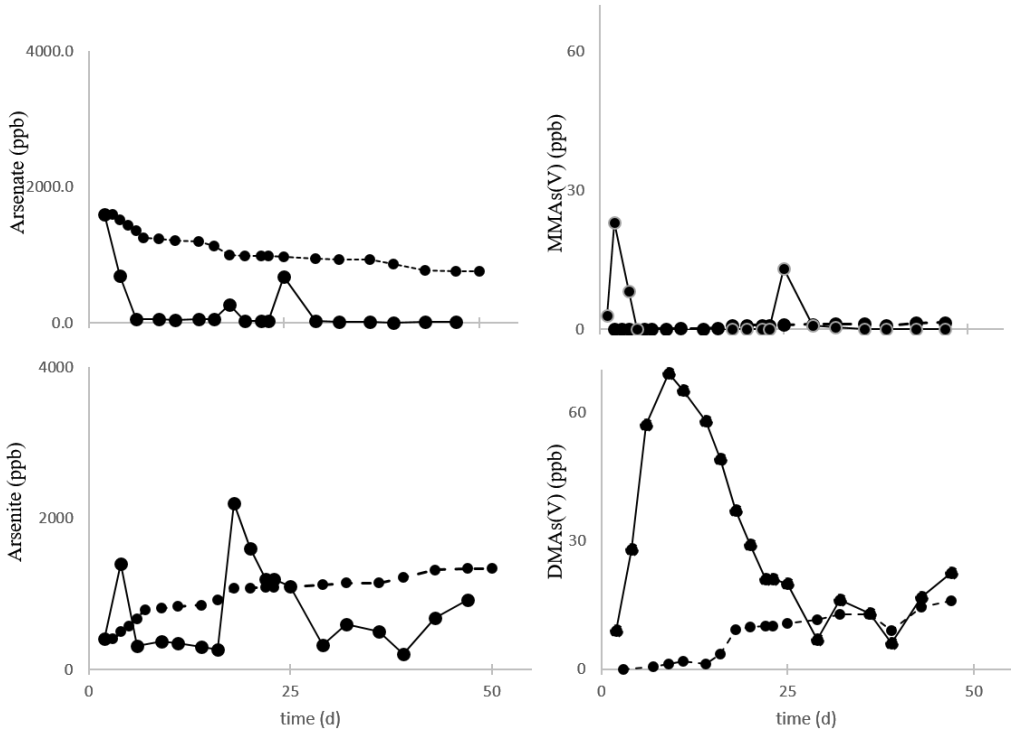

Figure 4. Variations of arsenic species with time in the stimulated injection test. The dashed lines represent the projection of a species concentration based on groundwater mixing. The solid lines are measured concentrations. Inorganic arsenic data from Chapter III is included for context.

There are statistically significant correlations between MMAs(V) and As(V) as well as between DMAs(V) and As(III) (table 1). The accumulation rate varied between sampling events; unstimulated experiments showed smaller average rates of MMAs(V) and DMAs(V) accumulation than the stimulated experiments (table 2). The maximum observed organic arsenic accumulation rate occurred in the stimulated injection test between day 1 and 9; DMAs(V) accumulated at a rate of 7.5 ppb/day. Furthermore, under ethanol oxidizing conditions the field experiment DMAs(V)/As(III) ratio was approximately 4 times the average DMAs(V)/As(III) ratio among all other stimulated laboratory and field experiments.

Table 1. Analysis of arsenic as MMAs(V)/As(V) and DMAs(V)/As(III) relationships in laboratory and field experiments. R^2 represents the linear correlation value between two arsenic species. Column "n" represents the number of data used to calculate each value. Control group (sterilized) laboratory data are not shown as no organic arsenic was produced.

		MMAs(V)/As(V)			DMAs(V)/As(III)			% Organic arsenic of total Inorganic As
		R^2	% MMAs(V)	n	R^2	% DMAs(V)	n	
Unstimulated	Group N (lab)	0.95	2.5±1.1%	8	0.66	4.89±1.6%	9	2.26±2.1%
	Control injection test (*in situ*) [†]	0.99	1.23±0.7%	14	0.90	2.54±1.6%	12	2.04±4.7%
					0.95	27.97±1.8%	5	
Stimulated	Group E (lab)	0.66	1.00±0.9%	28	0.84	4.15±1.9%	10	1.29±1.7%
	Group ES (lab)	0.98	3.12±1.1%	4	0.94	4.46±2.1%	9	1.29±2.0%
	Stimulated injection test (*in situ*) [††]	0.97	2.08±1.3%	7	0.92	3.12±3.8%	17	2.10±0.5%
					0.97	18.6±0.4%	5	15.92±0.6%

[†] *DMAs(V)/As(III) ratio for the in situ experiments exhibited strong bimodal correlations. The five samples from which the high stimulated injection test DMAs(V)/As(III) ratio was calculated were collected between days 6 and 16 (inclusive); the 17 samples that yielded a lower DMAs(V)/As(III) ratio were collected before and after days 6 and 16, respectively. Unlike the stimulated injection test, the high DMAs(V) fractions observed in the control injection test occurred sporadically throughout the experiment.*

Table 2. A comparison of organic arsenic accumulation rates variability and maximum observed throughout each experiment.

		MMAs(V) (ppb/day)		DMAs(V) (ppb/day)	
		Accumulation rate between sampling events	Maximum rate	Accumulation rate between sampling events	Maximum rate
Unstimulated	Group N (lab)	0.89±0.78	2.3	1.47±1.49	5.1
	Control injection test (*in situ*)	4.26±4.02	12.0	3.96±3.08	8.3
Stimulated	Group E (lab)	2.03±0.32	2.5	6.38±4.06	12.7
	Group ES (lab)	2.44±0.27	2.8	8.50±4.48	12.7
	Stimulated injection test (*in situ*)	11.83±11.17	23.0	9.09±3.85	14.5

stimulated injection test analysis of aquifer media show that adsorbed arsenic decreased from an average 55.1±6.8 ug/g throughout the first 16 days to 39.5±0.3 ug/g at the end of the experiment (days 36-50) (table 3), a 28±18% decrease. Analyses also show that acid volatile sulfide (AVS) and chromium reducible sulfide (CRS) were present only after day 36 of the stimulated injection test (table 4).

Table 3. Allocation of solid phase arsenic during the stimulated injection test

stimulated injection test (days)	Ionically bound (ug/g)	Strongly adsorbed (ug/g)	Precipitated with AVS (ug/g)	Precipitated with amorphous Fe oxyhydroxides (ug/g)	Precipitated with crystalline Fe oxyhydroxides (ug/g)	Precipitated with pyrite & amorphous As_2S_3 (ug/g)
3	9.38	46.91	4.77	4.61	2.47	2.11
9	5.94	54.65	6.34	4.28	2.85	1.65
16	8.02	63.59	5.90	2.58	3.04	2.36
22	3.06	55.56	7.22	4.07	2.19	4.81
29	5.56	43.90	5.66	3.51	3.51	8.20
36	3.69	39.73	6.62	4.54	1.76	6.05
50	4.76	39.22	7.10	5.04	1.54	4.86

Table 4. Formation of acid volatile sulfides (AVS) and chromium reducible sulfides (CRS) during the biostimulation experiment. Sample analysis was carried out in triplicate, and the results are reported as average ± standard deviation in S per dry weight of sample.

Time (days)	AVS (mg/g)	CRS (mg/g)
3	0±0.0	0±0.0
9	0±0.0	0±0.0
16	0±0.0	0±0.0
22	0±0.0	0±0.0
36	6.6±4.8	11.4±7.3
50	6.6±9.2	10.5±9.0

4. Discussion

In complex biogeochemical systems such as the one we are studying, demethylation competes, with varying degrees of effectiveness, with methylation and

thus acts as a "cryptic" process that acts to suppress the accumulation and volatilization of methylarsenic in the environment. However, quantifying the amount of methylation (As(III) → MMAs(V) → DMAs(V)) versus demethylation (DMAs(V) → MMAs(V) → As(III)) is not and cannot be apparent from these chemical measurements alone. Therefore, given the complexity of identifying true *in situ* methylation and demethylation rates, we have focused on net accumulation rates through all experiments. The following data represent net changes in organic arsenic irrespective of demethylating/methylating dynamics.

Accumulation rates of MMAs(V) and DMAs(V) in all laboratory experiments were lower than both stimulated and unstimulated field experiments. We attribute this to the difference in biomass concentrations between laboratory experiments and natural aquifers. Nevertheless, we see a consistent increase in MMAs(V) and DMAs(V) average accumulation rates from unstimulated to stimulated experiments in the both lab and field. Maximum observed accumulation rates are also consistently larger among ethanol stimulated experiments. This is not entirely unexpected but it is noteworthy; our results show that arsenic methylation processes are as affected by ethanol stimulation as other inorganic metabolic redox processes, and perhaps more so.

Based on previously reported concentrations, naturally occurring groundwater MMAs(V) and DMAs(V) is known to exist at concentrations between 0.1-10% of total dissolved arsenic[28,9,19–25,29]. Here, we report organic arsenic concentrations that exceeded previously observed levels by a significant amount (Table 1). Furthermore, we show that a robust, ethanol-driven production of organic arsenic effectively removed inorganic arsenic from both the aqueous and solid phases of the experiment’s sampling zone.

In all ethanol-stimulated experiments and the control injection test, the ratio of DMAs(V) to As(III) concentrations strongly correlate; however, in both the stimulated injection test and control injection test the correlations are bimodal (table 1). The bimodal correlations represent two distinct rates of methylating metabolic activity of aquifer microorganisms. Although we observed this pattern in the control injection test, the high DMAs(V) to As(III) ratio was not chronologically consistent, rather, we observed intermittent sampling events where this ratio existed. We interpret this temporal inconsistency as an unpredictable, rapid methylation of available As(III) and hypothesize the intermittency is driven by 1) the availability of a reliable energy source for methylating microorganisms, 2) the triggering of arsenic methylation by toxic levels of As(III), or 3) a combination of these two mechanisms.

The bimodal correlation between DMAs(V) and As(III) in the ethanol-stimulated field experiment was temporally distinct. During an eleven-day period of peak ethanol concentration (days 6-16), organic arsenic was rapidly produced at an average rate of 9.03±3.85 ppb/day with a maximum observed methylation rate of 14.5 ppb/day. During this period of enhanced arsenic methylation, MMAs(V) and DMAs(V) accounted for 15.92±0.6% of all arsenic; this sustained ratio is approximately eight times larger than any other methylating phase in any of the experiments we conducted. Contemporaneous with this remarkably high arsenic methylating event was a significant drop in inorganic arsenic species; As(V) maintained very low concentrations (approximately 50 ppb) and As(III) decreased to concentrations well below expected values (based on either groundwater mixing or potential arsenate reduction). Enhanced organic arsenic production rates ceased on day 16, after which As(III) concentrations rebounded at a rate of approximately 650 ppb/day.

We considered the possibility that the significant decrease of dissolved As(III) during the enhanced methylated phase was, in part, a result of adsorption on to aquifer media. However, solid phase analyses show that only a modest amount of arsenic adsorbed after day three; this coincided with the precipitous decrease in dissolved As(V) and is consistent with previously observed As(V) adsorbing tendencies[30–32]. Furthermore, analysis for iron and arsenic sulfide precipitation allow us to rule out arsenic sequestration through mineral precipitation.

Within the first 16 days of the stimulated injection test, we observed a chemical signature consistent with arsenic reducing and methylating conditions. In fact, the detection of MMAs(V) and DMAs(V) on day 2 (23 and 9 ppb, respectively) indicate that both As(V) reduction and As(III) methylation were underway less than 48 hours after injection. These data show that a rapid progression through the reductive and oxidative-methylation process of arsenic species began quickly and resulted in low dissolved inorganic arsenic concentrations. We observed a second, less speedy series of arsenic speciation transformations between days 20 and 40. Beginning with the observed desorption between solid phase sampling on days 16 and 22, we subsequently observed elevated concentrations in As(V) (days 18 and 22), As(III) (days 18-27), MMAs(V) (day 25), and DMAs(V) (days 32-47). Although this second phase of arsenic transformations was similar to the first phase in how it manifested chemically, we did not observe the same magnitude in methylation rates. However, we did observe another phase of significantly lowered As(III) concentrations between days 29 and 43.

5. Conclusion

These data show that the native consortia of microorganisms are capable of rapidly reducing, mobilizing, and eventually methylating adsorbed arsenate and further

highlights the capability of native microorganisms to methylate arsenic species at significant rates under natural and stimulated conditions. Here, we report new net rates of MMAs(V) and DMAs(V) production under natural and ethanol-amended conditions in both laboratory and aquifer experiments. Although MMAs(V) and DMAs(V) are intermediate methylated species, their accumulation rates shed light on an unintended, yet potentially important by-product of stimulated microbial metabolisms in arsenic contaminated areas. Our results demonstrate that 1) ethanol enhanced As-related metabolic activity can increase biomethylation rates by an order of magnitude or more, and 2) increased microbial activity can produce enough organic arsenic to account for at least 15% of all dissolved arsenic. The ability for aquifer microorganisms to rapidly transform dissolved arsenic into more volatile species could be an effective method of arsenic remediation. Several groundwater remediation studies currently propose the use of accelerated microbial metabolisms[14,33]; in the case of groundwater arsenic, because of the toxicity of methylated arsenic, future assessments of efficacy and impact should consider the production and fate of methylated arsenic. Given the inherent mobility of methylated As[34], these data are a noteworthy reminder that the organic arsenic pathway may be more significant in the transport and fate of groundwater arsenic than is currently recognized.

CHAPTER V

SUMMARY

In this dissertation I explore the biogeochemical role of aquifer microorganisms in contributing to groundwater arsenic contamination. By implementing a variety of laboratory and field experiments as well as analytical and procedural methods, I have contributed to a better understanding of the complex biogeochemical network of reactions responsible for the mobilization and fate of groundwater arsenic.

In Chapter II, I investigate simultaneous biogeochemical redox reactions of aquifer microcosm laboratory experiments. We collected aquifer sediments from a naturally contaminated bedrock aquifer ($[As^{III}] \geq 3000$ ppb), constructed laboratory microcosm by adding sulfate and ethanol, and incubated for two months. Ethanol-sulfate experiments initially yielded significant iron-sulfide precipitates and lowered arsenic contamination to ~200 ppb; however, arsenic levels later increased to ~3600 ppb; with 31% (~202 μmol×(kg water)$^{-1}$) and 12% (~78 μmol×(kg water)$^{-1}$) of solid phase arsenic apportioned as adsorbed and arsenic-sulfide, respectively. Ethanol-only experiments yielded higher initial arsenic contamination (~1500 ppb), however 22% (~105 μmol×(kg water)$^{-1}$) of solid phase arsenic was sulfide-sequestered. Results show that robust, simultaneous iron and sulfate reduction can temporarily mitigate arsenic contamination, but may marginalize sulfide's ability to scavenge arsenic and instead direct it to the less stable adsorbed phase. Therefore, the most effective arsenic-sulfide sequestration may occur when sulfate reduction follows significant iron reduction and its corresponding release of dissolved arsenic.

In Chapter III, I examine the geochemical results of two aquifer injection experiments to examine in situ microbial redox processes and the potential to stimulate arsenic sequestration through arsenic sulfide precipitation. Our results show that in situ stimulation of microbial metabolisms accelerated the reduction of arsenic bearing iron (oxy)hydroxides as well as sulfate and arsenic reduction. Within three weeks of these contemporaneously occurring redox reactions, 90% of the dissolved arsenic was removed (~2000 ppb) and an effective long-term, anaerobically stable, sequestration of arsenic was observed in a 20-fold increase of arsenic-sulfide precipitate.

In Chapter IV, I report new methylation rates that are consequential to the potential efficacy of enhanced, biologically-driven arsenic remediation and the reconsidered significance of biomethylation pathways in aquifers. These results expand our current understanding of the metabolic reach aquifer microorganisms have over the fate of arsenic in the critical zone.

APPENDICES

APPENDIX A

ANALYTICAL PROCEDURES

Total Arsenic Analysis: Total arsenic analysis was performed with a VG Elemental PQ Excel ICP-MS. Yttrium was utilized as an internal standard and the instrument was calibrated daily with reference materials procured from SPEX Certiprep. Verification of instrument calibration was achieved with preparations and analysis of two independent reference materials from the same vendor, but with different lot numbers. These check standards were analyzed post calibration and post sample analysis. Each ICP-MS measurement was conducted in triplicate and a sample duplicate and an analytical sample spike was performed during each assay.

Arsenic Speciation Analysis: Arsenic speciation was achieved with a liquid chromatography system interfaced to the ICP-MS instrument operated in a transient acquisition mode. Separation of the arsenic compounds was achieved with a Phenomenex Luna C18 100A column (250 x 4.40 x 5μ) with a isocratic mobile phase of 2.5 mM oxalic acid, 10mM 1-heptanesulfonic acid (ion-pairing agent) and 0.1% methanol adjusted to a pH of 4 with ammonium hydroxide. The mobile phase flow rate was set at 1.0 ml/min and an injection volume of 30 μl was used. Yttrium prepared at a concentration of 150 ng/ml in mobile phase was employed as an internal standard. Injection of 10 μl of the internal standard was performed post-column and is necessary since mobile phase and sample salts dampen the signal intensity over the course of the assay. Calibration of the instrument was conducted with reference materials obtained from SPEX Certiprep, Sigma, and Chem Service. Verification of instrument calibration was achieved with preparations of reference materials by another chemist other than the one who prepared the calibration standards. Check standards were analyzed post calibration and post sample analysis.

Arsenic Sequential Extraction Procedure

Materials

50mL polypropylene centrifuge tubes, Teflon tip syringes for decanting, 200nm polycarbonate filters, Büchner Funnel, Aluminum Foil, Mortar and pestle, Shaker Plate, Centrifuge, Watch Glass, hot plate, timer, and centrifuges for 1.5 ml and 50 ml tubes.

Chemicals and Reagents

1. Titanium (III) Chloride ($TiCl_3$, M.W. 154.26); 20% in 3% hydrochloric acid; Fisher AA3974330.

2. Water used to prepare the solution is milli-Q water (18.2 mΩ).

3. Acids (HCl and HNO_3) are at trace-metal grade; all other chemicals are at ACS grade.

4. All solutions (except $NaHCO_3$ solution) are degassed for 10 minutes with pure N_2 and stored inside the anaerobic chamber.

Solutions

Solution 1: 1M $MgCl_2$, pH 8

$MgCl_2 \cdot 6H_20$ M.W. 203.30g·mol^{-1}, 1Mx1Lx203.30g·mol^{-1} = 203.30g·L^{-1}

1. Add 203.30g $MgCl_2$ into 1L volumetric flask, fill with about 600 ml Milli-Q water;

2. Place a pH meter in solution along with a stir bar, and adjust pH to 8;

3. Bring the total volume to 1 liter.

Solution 2: 1M NaH_2PO_4, pH 5

$NaH_2PO_4 \cdot H_20$ F.W. 137.99g·mol^{-1}, 1Mx1Lx137.99g·mol^{-1} = 137.99g·L^{-1}

1. Add 137.99g NaH_2PO_4 into 1L volumetric flask, fill with about 600 ml Milli-Q water.

2. Place a pH meter in solution along with a stir bar, and adjust pH to 5;

3. Bring the total volume to 1 liter.

Solution 3: 0.2M Ammonium Oxalate/oxalic acid, pH 3

$(NH_4)_2C_2O_4{\cdot}H_20$ F.W. 142.11$g{\cdot}mol^{-1}$

0.2Mx1Lx142.11$g{\cdot}mol^{-1}$ = 28.42$g{\cdot}L^{-1}$

Oxalic Acid M.W. 134.0$g{\cdot}mol^{-1}$

0.2Mx1Lx134.0 $g{\cdot}mol^{-1}$ = 26.8 $g{\cdot}L^{-1}$

1. And 28.42g Ammonium Oxalate into 1 L volumetric flask,

2. Fill the flask ¾ of the volume with Milli-Q water. *Always add acid to water*

3. Add 28.6 g oxalic acid

4. Place a pH meter in solution along with a stir bar, and adjust pH to 3;

5. Bring the total volume to 1 liter.

Solution 4: 1N HCl

trace metal grade HCl: 35% F.W. 36.46

Density of Conc. HCl = 1.175g/cm^3 at 35%,

((35/100)(1000mL)(1.175g/mL))/36.46$g{\cdot}mol^{-1}$ =11.28M

11.28x=1(1), X = 1/11.28, X = 0.08.86 L, 88.6mL HCl per liter

1. Fill 1L volumetric flask ¾ of the volume with Milli-Q water. *Always add acid to water*

3. Pour about 90 ml trace-metal grade HCl into an acid washed beaker. Transfer 88.6mL HCl into the flask. Do not pipette directly from the acid bottle!!!

3. Cap the flask and invert three time to mix.

4. Fill to 1 L with Milli-Q water

Solution 5: Ti(III)-citrate-EDTA & Bicarbonate solutions:

Ti(III)-citrate-EDTA solution (1 liter) contains 0.05 M $TiCl_3$, 0.05 M Na_2-EDTA, and 0.05 M Na-citrate.

0.05M $TiCl_3$

F.W. 154.26 $g{\cdot}mol^{-1}$, 0.05M x 1L = 0.05x1x154.26= 7.713 $g{\cdot}L^{-1}$

0.05M Na_2-EDTA

$C_{10}H_{14}N_2Na_2O_8{\cdot}2H_2O$ F.W. 372.24 $g{\cdot}mol^{-1}$, 0.05M x 1L = 0.05x1x372.24= 18.612 $g{\cdot}L^{-1}$

0.05M sodium citrate

F.W. 294.10 $g{\cdot}mol^{-1}$, 0.05M x 1L = 0.05x1x294.10= 14.705 $g{\cdot}L^{-1}$

Fill 1L volumetric flask ¾ of the way full with Milli-Q water. *Always add acid to water*

Add 7.713g $TiCl_3$ + 20.81g Na_4-EDTA +14.705g sodium citrate to 1L volumetric flask.

Place a pH meter in solution along with a stir bar.

The solution is degassed with N_2 and pH is adjusted to 7.

Fill to 1L with Milli-Q water.

Solution 6 : $NaHCO_3$ solution

Bicarbonate solution (100 ml) contains 1.0M $NaHCO_3$.

F.W. 84.01$g \cdot mol^{-1}$, 1Mx100mL = 1x0.1x84.01 = 8.401 $g \cdot L^{-1}$

8.401g of $NaHCO_3$ is weighed and moved to the anaerobic chamber.

Prepare the solution inside the anaerobic chamber using N_2-degassed milli-Q water.

Solution 5 and 6 are added together in 10:1 volume ratio (e.g., 40 ml Ti(III)-citrate-EDTA and 4 ml $NaHCO_3$ solution).

Field Sampling

1. Immediately after retrieving sediment packs from the well, place the pack into an anaerobic jar, and purge the jar with N_2 for three minutes.

2. Store the jar at 4^{o}C until returned to lab.

3. Back to the lab, move the jar into the anaerobic chamber. Please open the jar when transporting the jar through the airlock. The vacuum can break a closed jar.

4. Inside the chamber, transfer 0.4 g into a sterile Eppendorf tube and the rest to other Eppendorf tubes. Record exact amount of the sediments.

5. Inside the anaerobic chamber, centrifuge at 11,000g for 25 minutes, remove water from sample using pipetting/decanting. Please balance the rotor before centrifuging.

6. Inside anaerobic chamber, transfer Eppendorf tubes into a labeled Ziploc bags. Store the bags in -80^{o}C freezer until analysis.

Analysis

1. Magnesium Step – Targeting ionically bound arsenic

1. 0.4g of sediment is homogenized inside anaerobic chamber with mortar and pestle until near uniform consistency (<125 microns).

2. Add the sediment into 50mL centrifuge tube (Polypropylene).

3. Add 40mL of 1M $MgCl_2$ at pH 8. Note: sediment-to-extractant ratios of 1:1000 (0.4g to 40mL) are used for each step

4. Tumble-shake sample for 2 hours.

5. Centrifuge for 25 minutes at 11,000g, decant supernatant using a syringe; filter the supernant inside the syringe using 0.2 μm polycarbonate filter into a sampling vial of 150 ml.

6. Repeat step 3 to 5; add the filtrate to the same sampling vial.

7. Repeat step 3 to 5 using Milli-Q water; add the filtrate to the same sampling vial.

8. Acidify the filtrate in the sampling vials with trace metal grade HCl (final concentration 24 mM).

2. PO_4 Step – Targeting strongly adsorbed arsenic

1. Inside the anaerobic chamber, add 40mL of 1M NaH_2PO_4 at pH 5, to the remaining residue.

2. Tumble-shake suspension for 16 hours.

3. Centrifuge for 25 minutes at 11,000g, decant supernatant using a syringe; filter the supernant inside the syringe using 0.2 μm polycarbonate filter into a sampling vial.

4. Repeat step 1 to 3, but shake the suspension for 24 hours.

5. Repeat step 1 to 3 using Milli-Q water and shake the suspension for 30 min.

6. Acidify the filtrate in the sampling vials with trace metal grade HCl (final concentration 24 mM).

3. HCl Step – targeting As coprecipitated with AVS (acid volatile sulfide), carbonates, Mn oxides, and very amorphous Fe oxyhydroxides

1. Inside the anaerobic chamber, add 40mL of 1N HCl to remaining residue

2. Tumble-shake suspension for 1 hour.

3. Centrifuge for 25 minutes at 11,000g, decant supernatant using a syringe; filter the supernant inside the syringe using 0.2 μm polycarbonate filter into a sampling vial.

4. Repeat step 1 to 3 using Milli-Q water.

5. Acidify the filtrate in the sampling vials with trace metal grade HCl (final concentration 24 mM).

4. Ox Step – targeting As coprecipitated with amorphous Fe oxyhydroxides

1. Inside the anaerobic chamber, add 40mL of 0.2M ammonium oxalate/oxalic acid at pH 3, to remaining residue.

2. Cover tube with aluminum foil, tumble shake suspension for two hours.

3. Centrifuge for 25 minutes at 11,000g, decant supernatant using a syringe; filter the supernant inside the syringe using 0.2 μm polycarbonate filter into a sampling vial.

4. Repeat step 1 to 3 using Milli-Q water.

5. Acidify the filtrate in the sampling vials with trace metal grade HCl (final concentration 24 mM).

5. Ti(III)/Citrate/EDTA/bicarbonate extraction – targeting As coprecipitated with crystalline Fe oxyhydroxides

1. Inside the anaerobic chamber, add 40 ml Ti(III)-citrate-EDTA solution and 4 ml $NaHCO_3$ solution.

2. Tumble-shake suspension for 2 hours.

3. Centrifuge for 25 minutes at 11,000g, decant supernatant using a syringe; filter the supernant inside the syringe using 0.2 μm polycarbonate filter into a sampling vial.

4. Repeat step 1 to 3.

5. Repeat step 1 to 3 with Milli-Q water.

8. Acidify the filtrate in the sampling vials with trace metal grade HCl (final concentration 24 mM).

6. HNO_3 Step – targeting As coprecipitated with pyrite and amorphous As_2S_3

1. Inside the anaerobic chamber, add 40mL of 16N HNO_3 to the remaining residue

2. Tumble-shake suspension for 2 hours.

3. Centrifuge for 25 minutes at 11,000g, decant supernatant using a syringe; filter the supernant inside the syringe using 0.2 μm polycarbonate filter into a sampling vial.

4. Repeat step 1 to 3 twice.

5. Repeat step 1 to 3 using Milli-Q water.

7. Hot HNO_3 step – targeting orpiment and remaining recalcitrant As minerals

EPA method 3050B

1. For each digestion procedure, weigh to the nearest 0.01 g and transfer a 1-2 g sample (wet weight) or 1g sample (dry weight) to a digestion vessel. For samples with high liquid content, a larger sample size may be used as long as digestion is completed.

2. For the digestion of samples for analysis by GFAA or ICP-MS, add 10 mL of 1:1

HNO3, mix the slurry, and cover with a watch glass or vapor recovery device. Heat the sample to $95^oC \pm 5^oC$ and reflux for 10 to 15 minutes without boiling.

3. Allow the sample to cool, add 5 mL of concentrated HNO_3 , replace the cover, and reflux for 30 minutes. If brown fumes are generated, indicating oxidation of the sample by HNO_3, repeat this step (addition of 5 mL of conc. HNO_3) over and over until no brown fumes are given off by the sample indicating the complete reaction with HNO_3.

4. Using a ribbed watch glass or vapor recovery system, either allow the solution to evaporate to approximately 5 mL without boiling or heat at $95^oC \pm 5^oC$ without boiling for two hours. Maintain a covering of solution over the bottom of the vessel at all times.

5. After the sample has cooled, add 2 mL of water and 3 mL of 30% H_2O_2.

6. Cover the vessel with a watch glass or vapor recovery device and return the covered vessel to the heat source for warming and to start the peroxide reaction. Care must be taken to ensure that losses do not occur due to excessively vigorous effervescence. Heat until effervescence subsides and the vessel cools. Continue to add 30% H_2O_2 in 1-mL aliquots with warming until the effervescence is minimal or until the general sample appearance is unchanged.

7. Cover the sample with a ribbed watch glass or vapor recovery device and continue heating the acid-peroxide digestate until the volume has been reduced to

approximately 5mL or heat at 95^{o}C ± 5^{o}C without boiling for two hours. Maintain a covering of solution over the bottom of the vessel at all times.

8. After cooling, dilute to 100mL with water. Particulates in the digestate should then be removed by filtration, by centrifugation, or by allowing the sample to settle. The sample is now ready for analysis by GFAA or ICP-MS.

Analytical Procedure for Acetate Measurement using

Dionex ICS-2500 Ion Chromatograph

NOTES

The running condition for acetate measurement is:

Eluent: 0.01 N H2SO4; Flow rate: 0.3 ml / min; Column temperature: 60 °C; Detector UV wavelength: 210 nm; lamp setting: High.

The detection limit for acetate is 11 µM.

Your samples have to be filtered through 0.2 µM filter paper to remove particulate materials before analyzing with the HPLC. Unfiltered samples can damage the injection value and clog the guard column.

Screen your samples before the run. Dilution is required, once acetate concentration in your sample is greater than 500 µM.

PROCEDURE

Start Up

Before start, check the eluent reservoir and flush bottle. If necessary, fill the eluent container A with 0.01 N H2SO4 and flush bottle with Milli-Q water (18.2 mΩ) (Cascade 321). To eliminate gas bulbs in inner wall of eluent container, remove the polyethylene delivery line from the container, cap the container and tap the container several times and allow it to sit overnight. Put polyethylene delivery line back into the container. Make sure the connections between the eluent bottle and the polyethylene delivery line are tight.

Record the user information onto the EXCEL file "USER LOG" on the desktop window of the computer. Include the following information, user name, running date, sample matrix and number, dilution factor, system power up time, pump pressure before and after the run, time to start and finish, and other necessary information.

Turn on column heater with a temperature set at 60 °C. Turn on the HPLC modules in the sequence of GP50, AS50, and AD20 by pressing the on/off button on the front panels. Once turned on, the AS50, AD20 and GP50 will initialize and run through a

diagnostic self-check, and remain in LOCAL mode, with pump off and AD20 UV lamp off.

Prime the pump as described in the Manufacture's Instruction, which is located on the shelf right above the computers. We recommend priming the pump manually using a 10-ml syringe for 4 syringe volumes, followed by automatically priming with PRIME button on the front panel for 2 minutes. Before priming, reset the lower pressure limit to zero as follows:

On the front panel of GS50, press Menu and then 2.

Move the cursor up to LIMITS by pressing the upward arrow (⇧).

Set the lower pressure limit as zero by pressing 0 and then Enter. Press Menu and Enter to return to the default screen. Now the pump is ready for priming.

NOTE: DO NOTE OVER TIGHT THE PUMP VALVES, Which will break the nut inside the pump head and result in costly repair service (> $1,000).

Establish Remote Control

Turn on the computer and launch the program Chromeleon to open the Browser.

Click on the folder Dionex Templates on the left window of the Browser to open the sub-folder Panels, under the folder Dionex_IC click on the sub-folder AD20 and AD25 Absorbance Detector Panels. On the right window of the Browser, click to open the file Absorbance_Detector_Gradient_pump_AS50.pan.

On the pup-up window, click to open Control pull-down manual and select Connect to the Time Base to initiate the control panels. Establish the remote control over auto sampler, pump, and detector by checking respective box on the control panels.

Set pump speed to 0.3 ml / minute and turn on the UV lamp to HIGH. The resulting pump pressure would be around 370~400 psi. Check for leaking if the pressure is far less than 360 psi; as well, check the pump valves to make sure that they are closed.

Click to open Control pull-down manual and select Acquisition On. On the pop-up window, make sure that "UV_VIS_1" is checked and then press OK to monitor the baseline. Once the base line is stable, record the time and pump pressure. Ideal magnitude of baseline fluctuation should be less than 0.0001 μS, which usually takes 40~60 minutes to reach.

Prepare Sequence File

On the right up corner of Chromeleon program window, click File and select New. In the pop-up box, select Sequence (using Wizard) and click OK. Click Next.

Time Base. The Time base is "UOFO-30638099BE_1"; the computer is "UOFO-30638099BE"; Protocol is "My computer". Click Next.

Unknown Samples. Enter the number of samples and start position for sample vials. Set the Injection volume to 50.0 (the sample loop is 100 μL). Add 2 extra vials for analyzing repeat, 1 for column rinse, and 1 for shutdown program. Click on Apply to complete the setup. Click Next.

Standard Samples. Enter the number of standards and start position. Set Injection volume to 50.0 (the sample loop is 100 μL). Click on Apply to complete the setup. Click Next.

Methods & Reporting. Choose acetate.pgm for Program and acetate.qnt as Quantification Method. Click Next.

Saving the Sequence. Name the sequence file as "user last name followed by year month and date". Click OK.

On the Browser window, edit the sample ID, position and running programs. Scheduled a Rinse program and a Shutdown program at the end of the run. The Rinse program is to rinse the column with eluent for 60 minutes, while changing the flow rate to 0.1 ml / min and UV lamp status from HIGH to LOW. The Shutdown program runs for 1 minute and turns off the pump and UV lamp.

Loading Samples

Remove the sample tray from the auto sampler and load samples sequentially as scheduled in the Sequence file. The loading volume must be greater than 1 mL. Insufficient loading volume may cause low pump pressure and the interruption of analyzing process, which will consequently result in mandatory stop of the machine.

Note: When loading the sample tray into AS50, do not bump the sampling tray onto the sampling needle and arm! The needle and arm are very delicate and any force can cause a series of problems from adjusting needle position to major repairs.

Running the Batch

Once the baseline is stable, click to open the pull-down menu of Control, select Acquisition Off.

On the pull-down menu of Batch, click on Edit. In the pup-up dialog box, click Add to upload your sequence file. Click on Ready Check and make sure there is no error message. Start the run by clicking Start. Each sample takes about 16 minutes, including flushing and loading time.

Check occasionally to make sure that the system is operating properly.

Rinse and Shutdown

If the scheduled programs run successfully, the pump and UV lamp would be turned off at the end of the run. But you have to turn off the AS 50, AD 20, and column heater sequentially using the power switches on the front panels. Do not turn off GP50 at this point.

Bypass the column by disconnecting the tubing from the column and connect to a tubing with a union at one end.

Wash the system with Milli-Q water for one hour at flow rate of 0.3 mL/min. The systems are made of peek, which can not be stored in acid over long time.

Turn off the GP 50 using the power switches on the front panels.

Data Analysis

Click acetate.qnt within the sequence file.

Click General tab, Dimension of amount is ppm (or your desired units).

Click Peak Table tab on the bottom of the screen. Enter the retention time for acetate, which is around 9.2 minutes.

Click Amount Table tab, enter the highest concentration of your standards into the Amount column.

Adjust the baselines manually. Check the calibration curves and make sure the results of validation are correct.

NPH Derivatization Protocol of LMW Organic Acids for HPLC[2]

(Albert, D., & Martens, C., 1997)

Pre-procedure:

This protocol was based on Determination of low-molecular-weight organic acid concentrations in seawater and pore-water samples via HPLC and should be reviewed before performing.

All glassware must be acid washed, followed by a subsequent step to remove all organics: either 10% nitric acid rinse or muffling at 350-400ºC for 2hrs. Store cleaned glassware in aluminum foil.

Use only 18.2 milli-ohm DI water and Trace Grade HCl.

Need to re-crystallize NPH (see Recrystallizing NPH protocol)

All standards and reagents must be made fresh for each run.

Eluent A and Eluent B should be created and allowed to sit for 24 hrs.

See revised Protocol for preparing Eluents for the HPLC

Preparing standards:

To make **50 ml** of **stock** solutions of the individual standards:

Standard	Formula Wt. (g)	Mass (g) into 50ml	Final Conc. (M)
Sodium formate	68.02	.440	0.1
Sodium acetate	82.03	.410	0.1
Sodium propionate	96.06	.480	0.1
Butyric acid	88.11	.441	0.1
Isobutyric acid	88.11	.441	0.1
Sodium Lactate*	112.06	0.560	0.1
Valeric acid*	102.13	0.511	0.1
Isovaleric acid*	102.13	0.511	0.1

Add 20µl of 2M NaOH to all the standards except Butyric/Isobutyric acid for preservation and store at -20ºC.

From the 100 mM (0.1 M) set of stock solutions, combine to create a 1 mM standard solution. This solution will not be derivitized but it will be used to create the 8 more dilute standards.

With the 1 mM standard solution, use the HPLC Standardization Protocol Spreadsheet to create the following standard concentrations: 100µM, 10µM, 5µM, 1µM, 500nM, 100nM, and a BLANK. These should be made fresh for each dervatization.

Use the excel spreadsheet to create the standards. Use a piece of styrofoam to hold the falcon tube (without the cap) upright on the platform of the digital scale. Make sure the total volume for each standard is correctly entered in the spreadsheet (probably 14g), then accurately weigh out (via aliquoting into a tube on the balance) the calculated amount. Write this amount into the box provided on the sheet. Then fill the tube with milli-Q DI H_2O to a total weight of 14g (or whatever the volume has been decided for the standards). Write the exact amount of the total weight in the spreadsheet. It is okay if the values are not exactly what you tried to aliquot, the spreadsheet will calculate the molarity of the standard and the subsequent dilution factor that will be entered into the HPLC software.

Preparing Derivatization Reagents:

*All solutions should be made fresh for each derivatization, mixed in the fumehood in 10ml, acid-washed glass vials, and should be made to a total volume of 5ml using milli-Q DI H_2O unless stated otherwise.

For the Pyridine:HCl solution:

Instead of using a 1:1 ratio of pyridine:HCl, a 4:3 ratio has been determined to work better with our specific chemicals. If the solution is too acidic, derivitization will be retarded.

aliquot 3 ml of the molecular biology grade (>99%) pyridine into the vial first

then slowly aliquot in 2.25ml of concentrated HCl (~12N)

this reaction is very exothermic and will off-gas chlorine, refrigerate between HCl aliquots if necessary. Do this step under the fume hood.

Confirm the pH is between 4 and 5. Small amounts of additional pyridine may have to be added to adjust the pH.

For the NPH solution:

aliquot 4.895ml of H2O into the vial

aliquot 105µl of concentrated HCl (~12N)

add 76.7mg of the freeze-dried NPH; be sure to add this in small quantities and swirl until dissolved before adding more….this may take patience

For the EDC solution:

aliquot 5ml of H2O into the vial

add 287.55mg of EDC (stored at -20ºC) and swirl until dissolved

Performing the Derivatization:

Aliquot 2ml of sample/standard into a 4ml glass vial with a Teflon cap.

Aliquot 200µl of the Pyridine:HCl solution into the vials and mix.

Then bubble N2 into vials for 4min to remove CO2

Either

Use ethanol/flamed gas syringes at the gas bench.

Use a Precision Glide 23 Gauge 1 inch disposal needle for each vial

Aliquot 200µl of the NPH solution to the vials.

Aliquot 200µl of the EDC solution to the vials, mix well, and let sit at room temperature for 1.5hrs.

Aliquot 175µl of 45% KOH into the vials, mix, and place the vials in 70ºC heat bath 10min

The heat bath takes about 4 hours to heat up to 70ºC. The bath should also be calibrated with a thermometer every few derivitizations.

After heating remove the samples from the bath and let them cool to room temperature.

The samples can now be run in the HPLC (see Running HPLC protocol) or can be stored at 4ºC in the dark for 1 week.

Sulfide Spectrophotometer Procedure

Reagents: Hach Sulfide 1 Reagent and Sulfide 2 Reagent

Sulfide Standards

1. Weight about one gram Na2S·9H2O (M.W. 240.18 g·mol−1), dry using a piece of ChemWipe paper.

2. Stock Solution A (100 mM S2-). Weight 0.60045 g Na2S·9H2O and add into a 25 ml volumetric flask. Bring the final volume to 25 ml using Milli-Q water (18.2 mΩ). (25ml×100mM×240.18g·mol−1 = 0.60045 g).

3. Prepare the standards according to the following table:

Standard	mM	Mixing	
		ml of Standard	mL of water
B	10	10 / A	90
C	1	1 / A	99
D	0.5	5 / B	95
E	0.1	1/ B	99
F	0.05	5/ C	95
G	0.01	1/ C	99
H	0.005	1 / D	99
I	0.001	1 / E	99
J	0.0005	1 / F	99

Procedure

1. Turn on Beckman Coulter DU 530 Spectrophotometer by pressing ON/OFF button on the back left side; let warm up for at least five minutes before analysis.

2. Inside 1.5 ml Eppendorf tubes, add 1 ml of filtered samples or standards, 100µl of reagent 1, and 100 µl of reagent 2. Mix the solution by inverting the tubes on a rack three times.

3. Incubate the mixture at room temperature for 3 minutes.

4. Need more details on the spectrophotometer steps.

5-3 user program

665 wavelength

Blank – DI water

Read – samples

Sulfide concentration (μM)) is the following equation:

$$[HS^-] = a\ A_{665}^2 + b\ A_{665} + c$$

where a = 11.555, b = 28.841, and c = 0.9906.

don't need to reblank between samples

Ferrous Iron Spectrophotometer Procedure

Reagents[3]

A. Ferrozine (FW 492.47, 97%, Aldrich #16,060-1): 10−2 mol·l−1 repared in an ammonium acetate (CH3COONH4, Aldrich #37,233-1, 99.999%) solution of 10−1 mol·l−1.

B. Reducing agent — hydroxylamine hydrochloride (H2NOH.HCl, 99.9999%, Aldrich #37, 992-1): 1.4 mol·l−1 prepared in a solution of analytical grade hydrochloric acid 2 mol·l−1.

C. Buffer — ammonium acetate: a 10 mol·l−1 solution adjusted to pH 9.5 with a solution of ammonium hydroxide (28–30%, NH4OH, JT Baker #9721-02).

Ferrous Iron Standards

1. Weight about one gram FeSO4·7H2O (M.W. 278.02 g·mol–1), dry in the oven at 105oC for two hours, and cool the chemical in a desiccator to room temperature.

2. Stock Solution A (100 mM Fe2+). Weight 0.69505 g FeSO4·7H2O and add into a 25 ml volumetric flask. Bring the final volume to 25 ml using Milli-Q water (18.2 mΩ). (25ml×100mM×278.02g·mol–1 = 0.69505 g).

3. Prepare the standard solution according to the following table:

Standard	mM	Mixing	
		ml of Standard	mL of water
B	50	5 / A	5
C	25	2.5 / A	7.5
D	10	1 / A	9
E	5	1/ B	9
F	2.5	1/ C	9
G	1	1/ D	9
H	0.5	1 / E	9
I	0.25	1 / F	9
J	0.1	1 / G	9

Ferrous Iron Analysis

Add 1 ml of filtered samples or standards to 100 μl of reagent A.

Total Iron Analysis

Add 800 μl filtered samples to 150 μl of reagent B; incubate the mixture at room temperature for 10 minutes. Add 50 μl of reagent C.

Iron Chemical Extraction Procedure

A. Total "reactive" Fe (amorphous+crystalline Fe(III) oxides and surface-associated Fe(II))

Add 0.1-1 g (we normally target approximately 0.5 g, depending on the Fe content of the material) of wet sediment to 10 mL of a solution of 0.2M sodium citrate plus 0.35M acetic acid adjusted (e.g. with 6N HCl) to a pH of 4.8. The citrate/acetic acid solution DOES NOT need to be anoxic. We typically use serum vials (nominal volume 10 mL, actual volume 15 mL) capped with thick black rubber stoppers (i.e. the kind used for anaerobic culturing) for this procedure; some other kind of gas-tight tube or bottle would be fine as well. Note that you can start this extraction procedure in the anaerobic chamber if you want to (e.g. in parallel with the other Fe and U extractions), but strictly speaking it's not necessary since the dithionite reduces all the Fe in the sample.

Working in a fume hood, immediately add approximately 0.5 g of sodium dithionite (also called sodium hydrosulfite) to the vial and cap tightly (this is important as the dithionite smells terrible).

Place vial on a rotary (or some other kind of) shaker for 1 hour.

Remove vial from shaker to fume hood, uncap vial to allow air to enter, and let sit overnight. This allows the residual dithionite to oxidize, which is important because in its reduced form the dithionite interferes with the colorimetric ferrozine assay of the Fe content of the extract.

Next day, add a small volume (hopefully something on the order of 0.1 mL or less) of extract to 5 or 10 mL of ferrozine (1 g/L in 50 mM of Hepes buffer, pH 4) plus 0.25 mL of 10% (wt/vol, i.e. 10 g in 100 mL of H_2O) of hydroxylamine hydrochloride (HA).

Let the reaction mixture sit overnight, during which time the Fe(III) in the extract will be reduced by the HA to Fe(II), which in turn reacts with the ferrozine.

Next day, read the A_{562} of the ferrozine+extract mixture.

B. Poorly-crystalline Fe(III) and surface-associated Fe(II)

Working inside the anaerobic chamber, add 0.1-1 g of wet sediment to 10 mL of 0.5M HCl, cap, and place on shaker for 1 hour. The 0.5M HCl DOES NOT need to be

anoxic. We typically use scintillation vials (approximately 20 mL total volume) with foil-lined caps for this procedure

Remove vial from shaker and let sit for 1-2 hours to allow solids to settle. If you want to analyze these immediately after extraction, transfer 1 mL of the slurry to a microcentrifuge tube, spin, and then analyze the supernatant as described below.

Add ≤ 0.5 mL of the extract to 5 mL of ferrozine, and then immediately withdraw 1 mL (using a pipettor) to measure the A_{562}; this measurement gives you the Fe(II) content of the extract.

Next, add 0.25 mL of 10% HA to the remaining ferrozine+extract mixture, and wait 10-15 minutes, during which time the HA reduces any Fe(III) in the extract to Fe(II), which in turn reacts with the ferrozine.

Read the A_{562} again; this measurement gives you the total (Fe(II) plus Fe(III)) content of the extract. The poorly-crystalline Fe(III) content of your sample is then calculated from the difference between total Fe and Fe(II).

Sulfide mineral sequential extraction procedure

The purpose of this procedure is to examine the concentration of two groups of sulfide minerals in sediment samples. The sample is first treated with acid to measure acid volatile sulfide (AVS), which can be assumed to be primarily associated with amorphous and crystalline FeS (mackinawite), pyrrhotite, and greigite. Next, the samples are treated with Cr(II) solution, to measure chromium reducible sulfur (CRS), which can be assumed to be largely associated with pyrite and marcasite. Some greigite may come out in the CRS extraction (Cornwell and Morse, 1987). The sulfide (S(-II)) that is evolved in each step is transported by a flow of nitrogen gas to another bottle where it is trapped in solution and may later be quantified using a method such as the methylene blue method (Eaton et al., 1995).

The overall extraction approach is taken from Canfield et al. (1986) and Tuttle et al. (1986). Cornwell and Morse (1987) and Rice (1993) provide a nice analysis of the procedure. Benning et al. (2000), Lowers et al. (2007), Morse and Cornwell (1987), and Spadini et al. (2003) are example studies in which this procedure was implemented. This protocol is designed for samples collected from cultures. For recently formed sediments such as these, the extraction can be carried out at room temperature (Cornwell and Morse, 1987). To apply this to ancient sediments, the extractions should be heated (Rice et al., 1993).

Extraction set-up

Extractions can be carried out using septum bottles sealed with butyl rubber stoppers as shown in the picture below. The bottle that the sample will be injected into (bottles on the right in the picture) should contain a needle for N_2 inflow that is long enough that the N_2 bubbles through the solution. The tubes coming in from the right side of the image are supplying N_2. An outflow needle also needs to be present to allow N_2 and H_2S to travel to the trap solution. It should be a short needle that does not extend into

the solution otherwise solution will flow out instead of H_2S and N_2. Each of these needles needs to have a syringe valve attached so they can be sealed from the atmosphere between extractions. The outflow needle needs to have a short tube extending to another long inflow needle in a bottle containing a sulfide trap solution (bottles on the left in the picture). This trap also needs an outflow needle. The entire set up needs to be free of O_2, so once it is assembled, flush it with N_2 for at least a half an hour. The bottles and solutions they contain, furthermore, should be purged of O_2 prior to assembling the extraction set up. This is critical to preventing oxidation of sulfide by O_2 during the extraction. During the extraction, the rate of N_2 flow should be very slow; only a few bubbles per second. Adjust this flow rate prior to injecting samples. Be sure to use needles that do not core the septum. If N_2 flow is restricted in one needle more than other needles, the flow rate will be uneven among extractions carried out simultaneously.

Reagents

7.5 mM zinc acetate [$Zn(CH_3COO)_2 \cdot 2H_2O$; FW 219.51] with a pH of about 9. You will need 40 mL/bottle and 2 bottles per sample (one for AVS and one for CRS). Make the solution and accurately add 40 mL to serum bottles and then purge with N_2 to remove O_2. This bottle serves to trap sulfide liberated during each extraction. The zinc reacts with the sulfide and precipitates as ZnS. The solution is basic to ensure that the sulfide exists as HS^- rather than H_2S. This favors formation of ZnS and also serves to ensure that the sulfide remains largely in solution. The solution is based upon that recommended by Eaton et al. (1995). Because this solution is used, wait at least 10 minutes for color development when measuring sulfide with the methylene blue method.

I used 7.5 mM zinc acetate. You may need to adjust the concentration of zinc so that at least an order of magnitude more zinc is present than AVS or CRS. I used sequential traps the first time I tried this procedure to ensure the traps were effective at retaining sulfide. I was unable to detect sulfide in any of the traps beyond the first, demonstrating that one trap was suitable. This might not be the case if the flow rate of N_2 is too high.

6 N HCl with 5% $SnCl_2$. You will need 30 mL/sample. Make the acid solution and accurately add 30 mL aliquots to bottles containing 1.5 g of $SnCl_2$. Purge the bottle with N_2 to remove O_2. The $SnCl_2$ is present because it prevents oxidation of sulfide by ferric iron that may be present; it reduces the ferric iron. If a lot of ferric iron is present in the sample, you may consider adding more $SnCl_2$. Don't add too much $SnCl_2$ though because this could overwhelm the Cr(II) solution that is added later during the CRS extraction. The Cr(II) quickly reduces the Sn(II) to Sn metal, thereby consuming Cr(II).

1 M Cr(II) solution. You will need 30 mL/sample. Purchasing a Cr(II) salt is fairly costly and they are unstable. Cr(III) salts, in contrast, are quite inexpensive and more stable. As described by Tuttle (1986), to make 1M Cr(II) solution from a Cr(III) salt, dissolve 133 g of reagent-grade $CrCl_3 \cdot 6H_2O$ in 500 mL of 0.1 M HCl. Pass the solution through a Jones reductor (described below). The color changes from bright green to bright blue as the Cr(III) is reduced to Cr(II). The solution is unstable in air and should be prepared within a day or two of use and stored in a sealed septum bottle that has been purged of O_2. It does not matter how much volume you add to the storage bottle because you will have to remove the appropriate aliquot from this bottle to add it to the sample with a syringe.

Concentrated HCl: 15 mL/sample.

Ethanol: 10 mL/sample.

Procedure

Mix reactor solution and sediment thoroughly and remove 5 mL using a syringe.

Dissolution of AVS: Inject the sample slowly into a serum bottle containing 30 mL of 6 M HCl solution with 1% stannous chloride ($SnCl_2$) and flowing N_2. If you inject the sample too rapidly, you might disrupt the flow of N_2 and even cause solution to back up into the gas manifold supplying the N_2.

Incubate the sediments in the acid for 1 hour. N_2 should be flowing through the bottles slowly the whole time.

Dissolution of CRS: Once the AVS extraction is complete, seal the valves on each sampling bottle and install fresh sulfide traps. Add 10 mL of ethanol to the extraction bottle and flush for a few minutes with N_2. Next, inject 30 mL of 1 M Cr(II) solution and 15 mL of concentrated HCl.

Incubate the extraction at room temperature for 1 hour and then seal valves.

Quantify the sulfide content of each trap. Use this to determine how much AVS and CRS sulfide was present in the original sample. If the sample pore solution contained significant sulfide content, you will need to factor this out of your result.

Jones reductor

Amalgamated granular zinc is used as a reducing agent in a Jones reductor. You amalgamate the zinc by treating it with a mercuric (Hg^{2+}) solution. An amalgam is defined as any compound containing mercury. The procedure I used to amalgamate zinc is taken from Kolthoff et al. (1969). I modified the procedure only slightly by changing the amounts of reagents to suit my needs. The proportions of each reagent are not changed:

Add 200 mL of 2 % (by weight) mercuric chloride (or nitrate) to 1 mL of concentrated nitric acid to 200 g of pure 20 – 30 mesh zinc in a beaker.

Stir the mixture thoroughly for 10 minutes.

Decant the solution and wash the zinc 3 times with distilled water.

The amalgamated zinc should have a bright silvery luster. Fill the reductor tube with water and then slowly add the zinc until the column is packed.

Wash the column with 500 mL of distilled water. Store the column full of deionized water after washing to prevent formation of salts.

Ideally, the reductor should be about 25 to 35 cm in height and should have an internal diameter of about 2 cm (KOLTHOFF et al., 1969). I used an old 100 mL burret with a small plug of glass wool to prevent the zinc from reaching the stopcock.

Appendix A References Cited

Albert, D., & Martens, C. (1997). Determination of low-molecular-weight organic acid concentrations in seawater and pore-water samples via HPLC. *Marine Chemistry*, *56*(1-2), 27–37. doi:10.1016/S0304-4203(96)00083-7

Benning, L.G., Wilkin, R.T., and Barnes, H.L., 2000, Reaction pathways in the Fe-S system below 100 degrees C: Chemical Geology, v. 167, p. 25-51.

Canfield, D.E., Raiswell, R., Westrich, J.T., Reaves, C.M., and Berner, R.A., 1986, The Use of Chromium Reduction in the Analysis of Reduced Inorganic Sulfur in Sediments and Shales: Chemical Geology, v. 54, p. 149-155.

Cornwell, J.C., and Morse, J.W., 1987, The characterization of iron sulfide minerals in anoxic marine sediments: Marine Chemistry, v. 22, p. 193-206.

Eaton, A.D., Clesceri, L.S., and Greenberg, A.E., 1995, Standard Methods for the Examination of Water and Wastewater: Washington, DC, American Public Health Association, American Water Works Association, and Water Environmental Federation.

Keon, N. E.; Swartz, C. H.; Brabander, D. J.; Harvey, C.; Hemond, H. F. 2001. Validation of an Arsenic Sequential Extraction Method for Evaluating Mobility in Sediments. *Environ. Sci. Technol.* 35:2778-2784.

Kolthoff, I.M., Sandell, E.B., Meehan, E.J., and Bruckenstein, S., 1969, Quantitative Chemical Analysis: London, Macmillan Company, 1199 p.

Lowers, H.A., Breit, G.N., Foster, A.L., Whitney, J., Yount, J., Uddin, N., and Muneem, A., 2007, Arsenic incorporation into authigenic pyrite, bengal basin sediment, Bangladesh: Geochimica Et Cosmochimica Acta, v. 71, p. 2699-2717.

Morse, J.W., and Cornwell, J.C., 1987, Analysis and Distribution of Iron Sulfide Minerals in Recent Anoxic Marine-Sediments: Marine Chemistry, v. 22, p. 55-69.

Rice, C.A., Tuttle, M.L., and Reynolds, R.L., 1993, The Analysis of Forms of Sulfur in Ancient Sediments and Sedimentary-Rocks - Comments and Cautions: Chemical Geology, v. 107, p. 83-95.

Spadini, L., Bott, M., Wehrli, B., and Manceau, A., 2003, Analysis of the major Fe bearing mineral phases in recent lake sediments by EXAFS spectroscopy: Aquatic Geochemistry, v. 9, p. 1-17.

Tuttle, M.L., Goldhaber, M.B., and Williamson, D.L., 1986, An Analytical Scheme for Determining Forms of Sulfur in Oil Shales and Associated Rocks: Talanta, v. 33, p. 953-961.

Viollier, et al. 2000. The ferrozine method revisited: Fe(II)/Fe(III) determination in natural waters. *Applied Geochemistry* 15:785-790.

APPENDIX B

CHAPTER II SUPPLEMENTARY MATERIAL

APPENDIX B

CHAPTER II SUPPLEMENTARY MATERIAL

Table B1. Synthetic groundwater composition

Ca	mmolal	0.6
Mg	mmolal	0.3
K	mmolal	0.2
Na	mmolal	16.7
HCO_3^-	mmolal	12.8
Cl	mmolal	1.5
$SO_4^=$	mmolal	2.5
As(V)	(ppb)	2000

Table B2. Ferrous iron data from laboratory experiments

Fe^{2+} (mM)								
time (d)	Reactor A	Stdevpa	Reactor N	Stdevpa	Reactor E	Stdevpa	Reactor ES	Stdevpa
1	0.00	0.00	0.00	0.00	0.00	0.00	0.00	0.00
3	-	0.02	0.13	0.01	0.13	0.02	0.13	0.00
7	0.00	0.00	0.00	0.00	0.05	0.06	0.00	0.00
10	0.00	0.00	0.00	0.00	0.09	0.02	0.18	0.03
13	0.00	0.00	0.00	0.00	0.24	0.00	0.24	0.00
16	0.01	0.00	0.01	0.00	0.49	0.05	0.39	0.02
20	0.00	0.00	0.00	0.00	0.57	0.05	0.39	0.02
23	0.00	0.00	0.00	0.00	0.47	0.07	0.28	0.09
29	0.00	0.00	0.00	0.00	0.47	0.06	0.30	0.03
31	0.01	0.01	0.05	0.03	0.18	0.01	0.16	0.01
34	0.00	0.00	0.00	0.00	0.39	0.04	0.25	0.01
37	0.00	0.00	0.00	0.00	0.11	0.08	0.22	0.05
42	0.00	0.00	0.00	0.00	0.24	0.09	0.22	0.04
45	0.02	0.00	0.02	0.01	0.23	0.05	0.23	0.04
49	0.02	0.00	0.02	0.00	0.11	0.03	0.17	0.00
52	0.02	0.01	0.02	0.00	0.08	0.05	0.10	0.02

Table B3. Sulfide data from laboratory experiments

Sulfide (mM)								
time (d)	Reactor A	Stdevpa	Reactor N	Stdevpa	Reactor E	Stdevpa	Reactor ES	Stdevpa
1	0.000	0.000	0.000	0.000	0.000	0.000	0.000	0.000
3	0.008	0.001	0.001	0.001	0.003	0.001	0.007	0.005
7	0.169	0.015	0.036	0.018	0.181	0.051	0.131	0.026
10	0.164	0.022	0.030	0.014	0.081	0.020	0.290	0.097
13	0.132	0.021	0.178	0.051	0.109	0.017	0.343	0.065
16	0.353	0.146	0.544	0.035	0.161	0.012	0.150	0.030
20	0.100	0.018	0.174	0.045	0.059	0.013	0.063	0.042
23	0.019	0.014	0.018	0.021	0.000	0.000	0.002	0.003
29	0.000	0.000	0.000	0.000	0.000	0.000	0.000	0.000
31	0.000	0.000	0.000	0.000	0.000	0.000	0.000	0.000
34	0.000	0.000	0.000	0.000	0.000	0.000	0.000	0.000
37	0.000	0.000	0.000	0.000	0.000	0.000	0.000	0.000
42	0.000	0.000	0.000	0.000	0.000	0.000	0.000	0.000
45	0.000	0.000	0.000	0.000	0.000	0.000	0.000	0.000
49	0.000	0.000	0.000	0.000	0.000	0.000	0.000	0.000
52	0.052	0.002	0.000	0.000	0.000	0.000	0.000	0.000

Table B4. Sulfate data from laboratory experiments

Sulfate (mM)								
time (d)	Reactor A	Stdevpa	Reactor N	Stdevpa	Reactor E	Stdevpa	Reactor ES	Stdevpa
1	2.433	0.228	2.293	0.282	0.075	0.028	2.504	0.416
3	3.130	0.129	2.901	0.614	0.107	0.028	2.949	0.182
7	2.780	0.372	2.400	0.349	0.194	0.013	2.138	0.422
9	2.319	0.189	2.506	0.579	0.225	0.013	1.778	0.353
13	2.084	0.038	2.778	1.075			1.353	0.212
15	2.070	0.612	2.793	0.370	0.586	0.067	1.079	0.114
20	4.453	0.104	3.567	0.281	0.082	0.022	1.670	0.218
23	3.009	0.674	5.473	0.708	0.057	0.022	0.932	0.218
29	2.859	1.153	4.492	0.583	0.051	0.002	0.420	0.103
31	3.071	0.316	4.170	0.334	0.058	0.016	0.072	0.036
34	3.300	0.113	4.824	0.763	0.053	0.017	-	-
37	2.811	0.000	4.716	0.405	0.069	0.010	0.027	0.074
42							0.033	0.014
45	3.028	0.554	4.429	0.779	0.091	0.011	0.071	0.006
49	4.041	1.397	4.774	1.151	0.055	0.036	0.041	0.018

Table B5. Methane results from laboratory experiments

Methane (mmol L-1)								
time (d)	Reactor A	Stdevpa	Reactor N	Stdevpa	Reactor E	Stdevpa	Reactor ES	Stdevpa
1	0.00	0.00	0.00	0.00	0.00	0.00	0.00	0.00
3	0.00	0.00	0.00	0.00	0.00	0.00	0.00	0.00
7	0.00	0.00	0.00	0.00	0.00	0.00	0.00	0.00
13	0.00	0.00	0.00	0.00	0.02	0.00	0.03	0.00
16	0.00	0.00	0.00	0.00	0.28	0.03	0.17	0.03
20	0.00	0.00	0.00	0.00	0.60	0.09	0.48	0.03
29	0.00	0.00	0.00	0.00	3.44	0.41	2.10	0.38
31	0.00	0.00	0.00	0.00	4.78	0.62	2.73	0.37
34	0.00	0.00	0.00	0.00	5.58	0.81	3.58	0.96
37	0.00	0.00	0.00	0.00	4.82	0.76	2.03	0.31
42	0.00	0.00	0.00	0.00	7.12	1.05	2.74	0.52
45	0.00	0.00	0.00	0.00	8.29	0.49	4.20	0.88
49	0.00	0.00	0.00	0.00	10.16	0.85	3.10	0.29
52	0.00	0.00	0.00	0.00	24.08	4.21	12.66	3.41

Table B6. Total Dissolved inorganic carbon data from laboratory experiments

Total Dissolved Inorganic Carbon (mmol/L)								
Days	Reactor A	std	Reactor N	Std	Reactor E	std	Reactor ES	std
1	18.5	2.3	36.6	11.5	45.6	18.3	39.8	4.9
7	27.4	7.6	25.3	9.0	86.0	27.4	84.0	17.1
10	14.4	1.1	24.9	2.7	4.8	0.7	3.3	0.3
13	14.3	6.9	34.3	5.3	1.6	0.2	2.5	0.2
20	21.3	3.2	25.2	2.6	2.2	0.1	3.3	0.5
23	9.7	3.0	14.5	1.9	2.7	0.3	5.0	0.5
31	19.6	11.2	30.7	11.2	4.7	0.5	7.4	0.4
34	33.9	3.6	32.0	4.4	9.2	0.7	10.9	0.7
37	17.4	1.6	19.7	0.8	5.9	0.7	7.5	1.2
42	17.7	2.9	23.9	6.8	5.7	1.5	6.7	0.8
45	15.3	0.5	18.8	2.5	6.1	0.5	8.2	1.5
49	15.3	2.9	17.5	4.5	9.4	0.6	8.1	0.9
52	9.7	13.7	48.1	7.4	25.3	1.7	29.4	7.5

Table B7. Anion data from laboratory experiments

Reactor A						
Time (d)	Fluoride (mM)	stdev	Chloride (mM)	stdev	Nitrate (mM)	stdev
1	0.265	0.060	6.346	0.405	0.000	0.000
3	0.511	0.063	6.376	0.065	0.000	0.000
7	0.434	0.096	5.889	0.802	1.276	0.616
9	2.373	0.000	6.351	0.132	0.442	0.019
13	3.104	2.029	6.375	0.155	0.504	0.081
15	2.220	0.592	6.124	0.420	0.000	0.000
20	1.081	0.219	6.494	0.202	0.000	0.000
23	0.388	0.102	5.542	0.715	0.000	0.000
29	0.269	0.242	5.403	1.230	0.000	0.000
31	0.376	0.045	6.435	0.040	0.000	0.000
34	0.323	0.034	6.225	0.200	0.017	0.014
37	0.330	0.000	5.797	0.000	0.000	0.000
42	0.233	0.207	-	-	0.025	0.025
45	0.392	0.165	6.024	0.384	0.012	0.012
49	0.334	0.093	5.001	0.913	0.005	0.005
Reactor N						
	Fluoride (mM)	stdev	Chloride (mM)	stdev	Nitrate (mM)	stdev
1	0.182	0.166	5.332	0.644	0.005	0.029
3	0.285	0.066	5.336	0.675	0.037	0.031
7	0.429	0.069	5.119	0.551	0.000	0.000
9	2.337	0.157	5.747	2.686	0.379	0.178
13	2.923	1.021	6.326	0.788	0.398	0.191
15	2.823	1.476	5.806	1.343	0.258	0.029
20	0.573	0.398	5.856	1.193	0.000	0.000
23	0.409	0.126	5.193	0.994	0.000	0.000
29	0.397	0.140	6.057	0.324	0.000	0.000
31	0.428	0.094	6.104	1.114	0.007	0.012
34	0.313	0.072	5.791	1.367	0.013	0.022
37	0.316	0.066	6.013	1.121	0.000	0.000
42	0.407	0.166	5.620	0.317	0.017	0.016
45	0.574	0.135	5.777	1.097	0.118	0.016
49	0.288	0.066	5.035	1.670	0.033	0.024

Table B7. (continued)

Reactor E						
	Fluoride (mM)	stdev	Chloride (mM)	stdev	Nitrate (mM)	stdev
1	0.176	0.092	6.451	1.239	0.018	0.026
3	0.482	0.148	6.776	0.689	0.084	0.034
7	1.760	0.784	7.734	1.097	0.163	0.134
9	5.884	1.182	7.013	0.694	0.588	0.237
13	9.309	1.789	7.581	0.897	1.149	0.141
15	10.771	1.184	7.797	0.788	0.695	0.030
20	7.613	1.397	7.136	1.139	0.000	0.000
23	7.788	1.399	7.009	0.576	0.000	0.000
29	8.278	0.235	7.459	0.833	0.000	0.000
31	7.462	0.674	7.567	0.822	0.000	0.000
34	8.366	0.142	7.577	0.456	0.000	0.000
37	8.881	0.865	7.654	1.096	0.000	0.000
42	-	-	-	-	-	-
45	7.878	0.736	7.414	0.722	0.000	0.000
49	6.852	0.172	7.257	0.523	0.000	0.000
Reactor ES						
	Fluoride (mM)	stdev	Chloride (mM)	stdev	Nitrate (mM)	stdev
1	0.378	0.195	6.501	0.458	0.000	0.000
3	0.696	0.023	6.718	0.420	0.090	0.008
7	5.043	1.156	6.685	0.830	0.404	0.091
9	5.534	1.101	6.282	1.685	0.198	0.052
13	8.865	2.365	6.827	0.549	0.531	0.130
15	8.411	2.182	5.714	0.930	0.080	0.113
20	7.413	0.869	6.712	0.678	0.000	0.000
23	5.822	0.806	6.048	1.796	0.000	0.000
29	6.459	2.001	6.081	1.606	0.000	0.000
31	5.334	2.431	3.622	2.807	0.000	0.000
34	-	-	-	-	0.000	0.000
37	7.036	2.495	2.234	6.374	0.000	0.000
42	-	-	-	-		
45	7.552	0.776	6.652	0.386	0.091	0.037
49	7.225	0.395	6.675	0.505	0.000	0.000

APPENDIX C

CHAPTER III SUPPLEMENTARY MATERIAL

Table C1. Field observation data

		Well Arsenic speciation								
Well ID		Arsenic as As^{+5},	Arsenic as MMA,	Arsenic as As^{+3},	Arsenic as DMA,	Sum of Arsenic Species,	Arsenic as As^{+5},	Arsenic as MMA,	Arsenic as As^{+3},	Arsenic as DMA,
		µg/L	µg/L	µg/L	µg/L	µg/L	µg/L	µg/L	µg/L	µg/L
3		< 0.4	< 0.2	< 0.4	< 1	< 1	0	0	0	0
6		0.574	< 0.2	< 0.4	< 1	0.574	0.574	0	0	0
7		5.688	< 0.2	< 0.4	< 1	5.688	5.688	0	0	0
8		0.598	< 0.2	25.32	< 1	25.918	0.598	0	25.32	0
10		250	1.528	4.572	< 1	256.1	250	1.528	4.572	0
11		62.28	< 0.2	1800	8.196	1870.476	62.28	0	1800	8.196
13		44.8	< 0.2	2300	13.366	2358.166	44.8	0	2300	13.366
14		2.15	< 0.2	26.12	< 1	28.27	2.15	0	26.12	0
15		73.44	< 0.2	3300	16.504	3389.944	73.44	0	3300	16.504
16		< 0.4	< 0.2	240	< 1	240	0	0	240	0
17		8.972	< 0.2	150	< 1	158.972	8.972	0	150	0
18		40.2	0.314	8.62	< 1	49.134	40.2	0.314	8.62	0
19		< 0.4	< 0.2	110	< 1	110	0	0	110	0
21		36.24	< 0.2	30.62	< 1	66.86	36.24	0	30.62	0
22		24.06	< 0.2	100	< 1	124.06	24.06	0	100	0
23		330	< 1	750	2.51	1082.51	330	0	750	2.51
24		150	< 1	860	2.645	1012.645	150	0	860	2.645
25		110	< 1	83.12	0.551	193.671	110	0	83.12	0.551
26		17.094	< 1	1800	5.578	1822.672	17.094	0	1800	5.578
27		7.23	< 1	19.342	< 1	26.572	7.23	0	19.342	0
28		61.66	< 1	310	1.218	372.878	61.66	0	310	1.218
29		320	< 1	350	1.581	671.581	320	0	350	1.581
30		28.4	< 1	3100	8.974	3137.374	28.4	0	3100	8.974

Table C2. Field observation data

Well ID		pH	T	TDS	DO	H_2S	Fe^{++}	SO_4^{--}	Alkanility	DOC
			oC	microS	ppm	ppm	ppm	ppm	meq/L	ppm
3		8.17	14.1	189.5	1.22	0.005	0.06	7	2.36	4.488
6		7.93	13.5	197	1.89	0.044	0.1	28	2.4	5.654
7		7.95	14	191	0.39	0	0	11	2.8	4.841
8		8.18	14.4	360	0.05	0.002	0	11	3.56	5.342
10		7.01	13.3	2210	0.71	0.052	0.12	40	2.8	4.478
11		7.07	13.7	2320	0.07	0.028	0.36	21	4	5.233
13		7.47	15.7	2090	0.21	0	0.39	>>	12.8	5.809
14		7.43	15.7	808	0.11	0.01	0.04	22	8.89	5.496
15		7.36	16.2	2220	0.09	0.031	0	38	4.56	5.874
16		8.36	14.5	492	0.03	0	0	7	2.56	4.453
17		7.62	16.1	331	0.95	0.016	0.54	0	2.6	3.702
18		7.89	15	731	?	0.075	0	>>	7.8	10.03
19		8.67	14.6	335	?	0.013	0	21	3.36	4.957
21		7.69	13.1	340	0.05	0	0	9	4.32	4.416
22		7.9	12.4	1416	?	0	0.02	>>	7.2	5.561
23		8.34	12.4	863	0.09	0.03	0	40	6.88	18.61
24		7.65	13.3	1349	0.07	0	0.06	>>	8.16	2.174
25		7.01	13.7	281	0.49	0.006	0	0	5.92	1.18
26		7.64	15.1	633	0.06	0.004	0.16	>>	8.4	1.003
27		8.19	14.6	2550	0.13	0.008	>>	42	8.08	1.918
28		7	12.8	1138	0.09	0.006	0.93	8	4.44	1.173
29		7.9	14.8	1131	0.32	0.003	0.01	>>	12.32	1.167
30		8.16	16.9	2380	0.09	0.004	0.18	>>	9.36	1.39
31									8.8	

Table C3. Field observation data from ICP-AES analyses

ID	Fluoride	Chloride	Sulfate	Na	Ca	Mg	K	Si	Al
	ppm	ppm	ppm	ppm	ppm	ppm	ppm	ppm	ppm
3	0.4	7.3	5.9	12.8	20.3	-0.2	1.4	7.8	0.0
6	1.0	2.7	3.4	7.5	19.7	3.9	1.4	13.8	0.0
7	0.7	4.8	3.4	15.9	18.6	1.5	1.4	15.0	0.1
8	1.4	10.2	7.1	38.3	1.2	-0.5	1.6	5.6	0.0
10	0.6	958.3	41.3	211.6	128.1	76.2	11.2	15.2	0.1
11	n.a.	1026.1	18.5	196.8	195.3	68.5	12.1	15.4	0.0
13	0.7	245.4	87.6	188.9	23.7	7.9	8.3	5.1	0.0
14	1.4	210.6	5.6	133.1	8.3	1.8	4.8	3.8	0.0
15	0.9	1599.5	54.6	588.3	32.0	7.2	14.0	4.5	0.0
16	1.3	74.1	6.5	50.8	3.2	0.0	2.3	5.0	0.1
17	0.7	20.0	1.7	28.2	5.9	2.0	2.0	10.8	0.1
18	0.7	26.6	131.6	98.6	14.1	2.6	4.0	18.2	0.1
19	0.5	5.5	20.5	34.2	0.8	-0.6	1.4	7.9	0.1
21	1.0	3.8	1.2	10.1	25.3	13.8	2.9	13.6	0.1
22	1.5	239.7	147.0	152.3	20.3	6.7	4.3	8.3	0.0
23	1.1	60.1	33.6	82.3	4.3	1.1	4.1	5.9	0.3
24	0.6	154.3	56.9	128.4	18.9	6.4	6.7	5.9	0.2
25	0.5	5.4	2.7	22.8	37.7	13.2	3.8	10.3	
26	0.8	179.0	55.3	134.8	17.3	5.5	6.7	8.7	0.2
27	n.a.	4600.5	38.2	1405.7	47.1	77.6	49.5	5.0	
28	1.0	244.4	4.8	50.2	81.9	31.4	3.5	13.6	0.3
29	2.2	99.7	60.8	154.0	16.7	4.8	6.2	7.9	0.3
30	0.2	550.4	84.5	245.6	26.0	8.3	11.3	7.3	0.3
31				82.8	17.5	7.5	4.2	8.7	0.3

REFERENCES CITED

Chapter I

(1) ATSDR. Agency for Toxic Substances and Disease Registry.

(2) WHO. WHO Guidelines for Drinking-water Quality. IARC Monogr. Eval. Carcinog. Risks to Humans 2004, 84, 41–267.

(3) Fendorf, S.; Michael, H. a; van Geen, A. Spatial and temporal variations of groundwater arsenic in South and Southeast Asia. Science 2010, 328, 1123–1127.

(4) Sen, P.; Biswas, T.; Journal, B. M. Arsenic: the largest mass poisoning of a population in history. Br. Med. J. 2013, 346, 3625–3625.

(5) Smith, A. H.; Lingas, E. O.; Rahman, M. Contamination of drinking-water by arsenic in Bangladesh: A public health emergency. Bull. World Health Organ. 2000, 78, 1093–1103.

(6) Hinkle, S. R.; Polette, D. J. Arsenic in Ground Water of the Willamette Basin , Oregon Arsenic in Ground Water of the Willamette Basin , Oregon. US Geol. Surv. 1999.

(7) Braman, R. S.; Foreback, C. C. Methylated foms of arsenic in the environment. Science (80-.). 1973, 182, 1247–1249.

(8) Serfes, M. E.; Spayd, S. E.; Herman, G. C. Arsenic occurrence, sources, mobilization, and transport in groundwater in the Newark Basin of New Jersey. ACS Symp. Ser. 2006, 915, p. 175–190.

(9) Bentley, R.; Chasteen, T. G. Microbial Methylation of Metalloids : Arsenic , Antimony , and Bismuth. Microbiol. Mol. Biol. … 2002, 66, 250–271.

(10) Kent, D.; Niedan, V.; Isenbeck-Schröter, M.; Stadler, S.; Jann, S.; Höhn, R.; Davis, J. The influence of oxidation-reduction and adsorption reactions on arsenic transport in the oxic, suboxic, and anoxic zones of a mildly acidic sand and gravel aquifer. URL http//wwwbrr. cr. usgs. gov/Arsenic/FinalAbsPDF/kent. pdf (accessed 2003-04-29) 2003, 2–5.

(11) Wilkie, J. a.; Hering, J. G. Adsorption of arsenic onto hydrous ferric oxide: Effects of adsorbate/adsorbent ratios and co-occurring solutes. Colloids Surfaces A Physicochem. Eng. Asp. 1996, 107, 97–110.

(12) Kirk, M. F.; Roden, E. E.; Crossey, L. J.; Brealey, A. J.; Spilde, M. N. Experimental analysis of arsenic precipitation during microbial sulfate and iron reduction in model aquifer sediment reactors. Geochim. Cosmochim. Acta 2010, 74, 2538–2555.

(13) Kirk, M. F.; Holm, T. R.; Park, J.; Jin, Q.; Sanford, R. a.; Fouke, B. W.; Bethke, C. M. Bacterial sulfate reduction limits natural arsenic contamination in groundwater. Geology 2004, 32, 953–956.

(14) Qin, J.; Rosen, B. P.; Zhang, Y.; Wang, G.; Franke, S.; Rensing, C. Arsenic detoxification and evolution of trimethylarsine gas by a microbial arsenite S-adenosylmethionine methyltransferase. Proc. Natl. Acad. Sci. 2006, 103, 2075–2080.

(15) Zhu, Y.-G.; Yoshinaga, M.; Zhao, F.-J.; Rosen, B. P. Earth Abides Arsenic Biotransformations. Annu. Rev. Earth Planet. Sci. 2014, 42, 443–467.

(16) Zhang, J.; Cao, T.; Tang, Z.; Shen, Q.; Rosen, B. P.; Zhao, F.-J. Arsenic Methylation and Volatilization by Arsenite S -Adenosylmethionine Methyltransferase in Pseudomonas alcaligenes NBRC14159. Appl. Environ. Microbiol. 2015, 81, 2852–2860.

(17) Zhao, F. J.; Zhu, Y. G.; Meharg, A. a. Methylated arsenic species in rice: Geographical variation, origin, and uptake mechanisms. Environ. Sci. Technol. 2013, 47, 3957–3966.

(18) Maguffin, S. C.; Kirk, M. F.; Daigle, A. R.; Hinkle, S. R.; Jin, Q. Substantial contribution of biomethylation to aquifer arsenic cycling http://www.nature.com/doifinder/10.1038/ngeo2383.

(19) Zhao, F.-J.; McGrath, S. P.; Meharg, A. A. Arsenic as a Food Chain Contaminant: Mechanisms of Plant Uptake and Metabolism and Mitigation Strategies. Annu. Rev. Plant Biol. 2010, 61, 535–559.

(20) Wang, S.; Mulligan, C. N. Natural attenuation processes for remediation of arsenic contaminated soils and groundwater. J. Hazard. Mater. 2006, 138, 459–470.

(21) Mestrot, A.; Feldmann, J.; Krupp, E. M.; Hossain, M. S.; Roman-Ross, G.; Meharg, A. a. Field fluxes and speciation of arsines emanating from soils. Environ. Sci. Technol. 2011, 45, 1798–1804.

(22) Mestrot, A.; Planer-Friedrich, B.; Feldmann, J. Biovolatilisation: a poorly studied pathway of the arsenic biogeochemical cycle. Environ. Sci. Process. Impacts 2013, 15, 1639–1651.

(23) Mestrot, A.; Uroic, M. K.; Plantevin, T.; Islam, M. R.; Krupp, E. M.; Feldmann, J.; Meharg, A. a. Quantitative and qualitative trapping of arsines deployed to assess loss of volatile arsenic from paddy soil. Environ. Sci. Technol. 2009, 43, 8270–8275.

Chapter II

(1) Kinniburgh, D. .; Smedley, P. . Arsenic contamination of groundwater in Bangladesh. *Br. Geol. Surv. Rep. WC/00/19* **2001**, *1:Summary*.

(2) WHO. Exposure to Arsenic: A Major Public Health Concern. *Agriculture* **2010**, 5.

(3) Bundschuh, J.; Litter, M. I.; Parvez, F.; Román-Ross, G.; Nicolli, H. B.; Jean, J.-S.; Liu, C.-W.; López, D.; Armienta, M. A.; Guilherme, L. R. G.; et al. One century of arsenic exposure in Latin America: A review of history and occurrence from 14 countries. *Sci. Total Environ.* **2012**, *429*, 2–35.

(4) Stollenwerk, K. Geochemical Processes Controlling Transport of Arsenic in Groundwater: A Review of Adsorption http://resources.metapress.com/pdf-preview.axd?code=p2k65mu74l311520&size=largest (accessed Jan 4, 2012).

(5) Harvey, C. F. Arsenic Mobility and Groundwater Extraction in Bangladesh. *Science (80-.).* **2002**, *298*, 1602–1606.

(6) Stollenwerk, K. G.; Breit, G. N.; Welch, A. H.; Yount, J. C.; Whitney, J. W.; Foster, A. L.; Uddin, M. N.; Majumder, R. K.; Ahmed, N. Arsenic attenuation by oxidized aquifer sediments in Bangladesh. *Sci. Total Environ.* **2007**, *379*, 133–150.

(7) Ahmann, D.; Krumholz, L. R.; Hemond, H. F.; Lovley, D. R.; Morel, F. M. M. Microbial mobilization of arsenic from sediments of the Aberjona watershed. *Environ. Sci. Technol.* **1997**, *31*, 2923–2930.

(8) Islam, F. S.; Gault, A. G.; Boothman, C.; Polya, D. A.; Charnock, J. M.; Chatterjee, D.; Lloyd, J. R. Role of metal-reducing bacteria in arsenic release from Bengal delta sediments. *Nature* **2004**, *430*, 68–71.

(9) Rowland, H. a L.; Pederick, R. L.; Polya, D. a.; Pancost, R. D.; Van Dongen, B. E.; Gault, a. G.; Vaughan, D. J.; Bryant, C.; Anderson, B.; Lloyd, J. R. The control of organic matter on microbially mediated iron reduction and arsenic release in shallow alluvial aquifers, Cambodia. *Geobiology* **2007**, *5*, 281–292.

(10) Corsini, A.; Cavalca, L.; Crippa, L.; Zaccheo, P.; Andreoni, V. Impact of glucose on microbial community of a soil containing pyrite cinders: Role of bacteria in arsenic mobilization under submerged condition. *Soil Biol. Biochem.* **2010**, *42*, 699–707.

(11) Cummings, D. E.; Caccavo, F.; Fendorf, S.; Rosenzweig, R. F. Arsenic mobilization by the dissimilatory Fe(III)-reducing bacterium Shewanella alga BrY. *Environ. Sci. Technol.* **1999**, *33*, 723–729.

(12) Huang, J. H.; Matzner, E. Dynamics of organic and inorganic arsenic in the solution phase of an acidic fen in Germany. *Geochim. Cosmochim. Acta* **2006**, *70*, 2023–2033.

(13) Tadanier, C. J.; Schreiber, M. E.; Roller, J. W. Arsenic mobilization through microbially mediated deflocculation of ferrihydrite. *Environ. Sci. Technol.* **2005**, *39*, 3061–3068.

(14) Fendorf, S.; Michael, H. a; van Geen, A. Spatial and temporal variations of groundwater arsenic in South and Southeast Asia. *Science* **2010**, *328*, 1123–1127.

(15) Lowers, H. a.; Breit, G. N.; Foster, A. L.; Whitney, J.; Yount, J.; Uddin, M. N.; Muneem, A. A. Arsenic incorporation into authigenic pyrite, Bengal Basin sediment, Bangladesh>. *Geochim. Cosmochim. Acta* **2007**, *71*, 2699–2717.

(16) Buschmann, J.; Berg, M. Impact of sulfate reduction on the scale of arsenic contamination in groundwater of the Mekong, Bengal and Red River deltas. *Appl. Geochemistry* **2009**, *24*, 1278–1286.

(17) O'Day, P. a; Vlassopoulos, D.; Root, R.; Rivera, N. The influence of sulfur and iron on dissolved arsenic concentrations in the shallow subsurface under changing redox conditions. *Proc. Natl. Acad. Sci. U. S. A.* **2004**, *101*, 13703–13708.

(18) Kirk, M. F.; Holm, T. R.; Park, J.; Jin, Q.; Sanford, R. a.; Fouke, B. W.; Bethke, C. M. Bacterial sulfate reduction limits natural arsenic contamination in groundwater. *Geology* **2004**, *32*, 953–956.

(19) Omoregie, E. O.; Couture, R. M.; Van Cappellen, P.; Corkhill, C. L.; Charnock, J. M.; Polya, D. a.; Vaughan, D.; Vanbroekhoven, K.; Lloyd, J. R. Arsenic bioremediation by biogenic iron oxides and sulfides. *Appl. Environ. Microbiol.* **2013**, *79*, 4325–4335.

(20) Smith, J. G. *Geologic map of upper Eocene to Holocene volcanic and related rocks in the Cascade Range, Washington*; 1993.

(21) Gannett, M.; Caldwell, R. *Geologic framework of the Willamette Lowland aquifer system, Oregon and Washington*; 1998.

(22) Kirk, M. F.; Roden, E. E.; Crossey, L. J.; Brealey, A. J.; Spilde, M. N. Experimental analysis of arsenic precipitation during microbial sulfate and iron reduction in model aquifer sediment reactors. *Geochim. Cosmochim. Acta* **2010**, *74*, 2538–2555.

(23) Seitz, H. J.; Schink, B.; Pfennig, N.; Conrad, R. Energetics of syntrophic ethanol oxidation in defined chemostat cocultures - 1. Energy requirement for H2 production and H2 oxidation. *Arch. Microbiol.* **1990**, *155*, 82–88.

(24) Dey, S.; Goswami, S.; Ghosh, U. C. Hydrous Ferric Oxide (HFO)—a Scavenger for Fluoride from Contaminated Water. *Water, Air, Soil Pollut.* **2004**, *158*, 311–323.

(25) Huang, J. H.; Voegelin, A.; Pombo, S. a.; Lazzaro, A.; Zeyer, J.; Kretzschmar, R. Influence of arsenate adsorption to ferrihydrite, goethite, and boehmite on the kinetics of arsenate reduction by Shewanella putrefaciens strain CN-32. *Environ. Sci. Technol.* **2011**, *45*, 7701–7709.

(26) Goldberg, S.; Johnston, C. T. Mechanisms of Arsenic Adsorption on Amorphous Oxides Evaluated Using Macroscopic Measurements, Vibrational Spectroscopy, and Surface Complexation Modeling. *J. Colloid Interface Sci.* **2001**, *234*, 204–216.

(27) Goldberg, S. Competitive Adsorption of Arsenate and Arsenite on Oxides and Clay Minerals. *Soil Sci. Soc. Am. J.* **2002**, *66*, 413.

(28) Jessen, S.; Larsen, F.; Koch, C. B.; Arvin, E. Sorption and desorption of arsenic to ferrihydrite in a sand filter. *Environ. Sci. Technol.* **2005**, *39*, 8045–8051.

(29) Raven, K. P.; Jain, A.; Loeppert, R. H. Arsenite and Arsenate Adsorption on Ferrihydrite: Kinetics, Equilibrium, and Adsorption Envelopes. *Environ. Sci. Technol.* **1998**, *32*, 344–349.

Chapter III

(1) Smith, A. H.; Arroyo, A. P.; Guha Mazumder, D. N.; Kosnett, M. J.; Hernandez, A. L.; Beeris, M.; Smith, M. M.; Moore, L. E. Arsenic-induced skin lesions among Atacameno people in Northern Chile despite good nutrition and centuries of exposure. *Environ. Health Perspect.* **2000**, *108*, 617–620.

(2) WHO. Exposure to Arsenic: A Major Public Health Concern. *Agriculture* **2010**, 5.

(3) Stýblo, M.; Drobná, Z.; Jaspers, I.; Lin, S.; Thomas, D. J. The role of biomethylation in toxicity and carcinogenicity of arsenic: A research update. *Environ. Health Perspect.* **2002**, *110*, 767–771.

(4) Hinkle, S. R.; Polette, D. J. Arsenic in Ground Water of the Willamette Basin , Oregon Arsenic in Ground Water of the Willamette Basin , Oregon. *US Geol. Surv.* **1999**.

(5) Braman, R. S.; Foreback, C. C. Methylated foms of arsenic in the environment. *Science (80-.).* **1973**, *182*, 1247–1249.

(6) Serfes, M. E.; Spayd, S. E.; Herman, G. C. Arsenic occurrence, sources, mobilization, and transport in groundwater in the Newark Basin of New Jersey. *ACS Symp. Ser.* **2006**, *915*, p. 175–190.

(7) Bentley, R.; Chasteen, T. G. Microbial Methylation of Metalloids : Arsenic , Antimony , and Bismuth. *Microbiol. Mol. Biol. …* **2002**, *66*, 250–271.

(8) O'Day, P. a. Chemistry and mineralogy of arsenic. *Elements* **2006**, *2*, 77–83.

(9) Tabelin, C. B.; Igarashi, T.; Yoneda, T.; Tamamura, S. Utilization of natural and artificial adsorbents in the mitigation of arsenic leached from hydrothermally altered rock. *Eng. Geol.* **2013**, *156*, 58–67.

(10) Polizzotto, M. L.; Harvey, C. F.; Li, G.; Badruzzman, B.; Ali, A.; Newville, M.; Sutton, S.; Fendorf, S. Solid-phases and desorption processes of arsenic within Bangladesh sediments. *Chem. Geol.* **2006**, *228*, 97–111.

(11) Kirk, M. F.; Holm, T. R.; Park, J.; Jin, Q.; Sanford, R. a.; Fouke, B. W.; Bethke, C. M. Bacterial sulfate reduction limits natural arsenic contamination in groundwater. *Geology* **2004**, *32*, 953–956.

(12) Bauer, M.; Blodau, C. Mobilization of arsenic by dissolved organic matter from iron oxides, soils and sediments. *Sci. Total Environ.* **2006**, *354*, 179–190.

(13) Rowland, H. a L.; Pederick, R. L.; Polya, D. a.; Pancost, R. D.; Van Dongen, B. E.; Gault, a. G.; Vaughan, D. J.; Bryant, C.; Anderson, B.; Lloyd, J. R. The control of organic matter on microbially mediated iron reduction and arsenic release in shallow alluvial aquifers, Cambodia. *Geobiology* **2007**, *5*, 281–292.

(14) Nickson, R.; McArthur, J.; Burgess, W.; Ahmed, K. M.; Ravenscroft, P.; Rahman, M. Arsenic poisoning of Bangladesh groundwater. *Nature*, 1998, *395*, 338.

(15) Burnol, A.; Garrido, F.; Baranger, P.; Joulian, C.; Dictor, M.-C.; Bodénan, F.; Morin, G.; Charlet, L. Decoupling of arsenic and iron release from ferrihydrite suspension under reducing conditions: a biogeochemical model. *Geochem. Trans.* **2007**, *8*, 12.

(16) Harvey, C. F. Arsenic Mobility and Groundwater Extraction in Bangladesh. *Science (80-.).* **2002**, *298*, 1602–1606.

(17) Manning and Goldberg, S., B. A. Arsenic(III) and arsenic (V) adsorption on three california soils. *Soil Sci.* **1997**, *162*, 886–895.

(18) Smedley, P. .; Kinniburgh, D. . A review of the source, behaviour and distribution of arsenic in natural waters. *Appl. Geochemistry* **2002**, *17*, 517–568.

(19) He, Y. T.; Fitzmaurice, A. G.; Bilgin, A.; Choi, S.; O'Day, P.; Horst, J.; Harrington, J.; James Reisinger, H.; Burris, D. R.; Hering, J. G. Geochemical processes controlling arsenic mobility in groundwater: A case study of arsenic mobilization and natural attenuation. *Appl. Geochemistry* **2010**, *25*, 69–80.

(20) Burton, E. D.; Johnston, S. G.; Planer-Friedrich, B. Coupling of arsenic mobility to sulfur transformations during microbial sulfate reduction in the presence and absence of humic acid. *Chem. Geol.* **2013**, *343*, 12–24.

(21) Du Laing, G.; Chapagain, S. K.; Dewispelaere, M.; Meers, E.; Kazama, F.; Tack, F. M. G.; Rinklebe, J.; Verloo, M. G. Presence and mobility of arsenic in estuarine wetland soils of the Scheldt estuary (Belgium). *J. Environ. Monit.* **2009**, *11*, 873–881.

(22) Omoregie, E. O.; Couture, R. M.; Van Cappellen, P.; Corkhill, C. L.; Charnock, J. M.; Polya, D. a.; Vaughan, D.; Vanbroekhoven, K.; Lloyd, J. R. Arsenic bioremediation by biogenic iron oxides and sulfides. *Appl. Environ. Microbiol.* **2013**, *79*, 4325–4335.

(23) Saalfield, S. L.; Bostick, B. C. Changes in iron, sulfur, and arsenic speciation associated with bacterial sulfate reduction in ferrihydrite-rich systems. *Environ. Sci. Technol.* **2009**, *43*, 8787–8793.

(24) Keimowitz, a. R.; Mailloux, B. J.; Cole, P.; Stute, M.; Simpson, H. J.; Chillrud, S. N. Laboratory investigations of enhanced sulfate reduction as a groundwater arsenic remediation strategy. *Environ. Sci. Technol.* **2007**, *41*, 6718–6724.

(25) Holm, T. R.; Kelly, W. R.; Wilson, S. D.; Roadcap, G. S.; Talbott, J. L.; Scott, J. S. Arsenic distribution and speciation in the Mahomet and Glasford aquifers, Illinois. In *ACS Symposium Series*; O'Day, P. A.; Vlassopoulos, D.; Meng, X. G.; Benning, L. G., Eds.; ACS Symposium Series; American Chemical Society, 2005; Vol. 915, pp. 148–160.

(26) Counties, T.; Holm, T. R. Ground-Water Quality in the Mahomet Aquifer ,. **1995**.

(27) Kirk, M. F.; Roden, E. E.; Crossey, L. J.; Brealey, A. J.; Spilde, M. N. Experimental analysis of arsenic precipitation during microbial sulfate and iron reduction in model aquifer sediment reactors. *Geochim. Cosmochim. Acta* **2010**, *74*, 2538–2555.

(28) Smith, J. G. *Geologic map of upper Eocene to Holocene volcanic and related rocks in the Cascade Range, Washington*; 1993.

(29) Gannett, M.; Caldwell, R. *Geologic framework of the Willamette Lowland aquifer system, Oregon and Washington*; 1998.

(30) Albert, D. B.; Martens, C. S. Determination of low-molecular-weight organic acid concentrations in seawater and pore-water samples via HPLC. *Mar. Chem.* **1997**, *56*, 27–37.

(31) Blute, N. K.; Jay, J. a.; Swartz, C. H.; Brabander, D. J.; Hemond, H. F. Aqueous and solid phase arsenic speciation in the sediments of a contaminated wetland and riverbed. *Appl. Geochemistry* **2009**, *24*, 346–358.

(32) Wilkin, R. T.; Ford, R. G. Arsenic solid-phase partitioning in reducing sediments of a contaminated wetland. *Chem. Geol.* **2006**, *228*, 156–174.

Chapter IV

(1) Cummings, D. E.; Caccavo, F.; Fendorf, S.; Rosenzweig, R. F. Arsenic mobilization by the dissimilatory Fe(III)-reducing bacterium Shewanella alga BrY. *Environ. Sci. Technol.* **1999**, *33*, 723–729.

(2) Cutting, R. S.; Coker, V. S.; Telling, N. D.; Kimber, R. L.; Van Der Laan, G.; Pattrick, R. a D.; Vaughan, D. J.; Arenholz, E.; Lloyd, J. R. Microbial reduction of arsenic-doped schwertmannite by geobacter sulfurreducens. *Environ. Sci. Technol.* **2012**, *46*, 12591–12599.

(3) Bhowmick, S.; Nath, B.; Halder, D.; Biswas, A.; Majumder, S.; Mondal, P.; Chakraborty, S.; Nriagu, J.; Bhattacharya, P.; Iglesias, M.; et al. Arsenic mobilization in the aquifers of three physiographic settings of West Bengal, India: understanding geogenic and anthropogenic influences. *J. Hazard. Mater.* **2013**, *262*, 915–923.

(4) Tareq, S. M.; Safiullah, S.; Anawar, H. M.; Rahman, M. M.; Ishizuka, T. Arsenic pollution in groundwater: a self-organizing complex geochemical process in the deltaic sedimentary environment, Bangladesh. *Sci. Total Environ.* **2003**, *313*, 213–226.

(5) Chow, S. S.; Taillefert, M. Effect of arsenic concentration on microbial iron reduction and arsenic speciation in an iron-rich freshwater sediment. *Geochim. Cosmochim. Acta* **2009**, *73*, 6008–6021.

(6) Dhar, R. K.; Zheng, Y.; Saltikov, C. W.; Radloff, K. a.; Mailloux, B. J.; Ahmed, K. M.; Van Geen, A. Microbes enhance mobility of arsenic in pleistocene aquifer sand from Bangladesh. *Environ. Sci. Technol.* **2011**, *45*, 2648–2654.

(7) Kirk, M. F.; Holm, T. R.; Park, J.; Jin, Q.; Sanford, R. a.; Fouke, B. W.; Bethke, C. M. Bacterial sulfate reduction limits natural arsenic contamination in groundwater. *Geology* **2004**, *32*, 953–956.

(8) Zhao, F.-J.; McGrath, S. P.; Meharg, A. A. Arsenic as a Food Chain Contaminant: Mechanisms of Plant Uptake and Metabolism and Mitigation Strategies. *Annu. Rev. Plant Biol.* **2010**, *61*, 535–559.

(9) Maguffin, S. C.; Kirk, M. F.; Daigle, A. R.; Hinkle, S. R.; Jin, Q. Substantial contribution of biomethylation to aquifer arsenic cycling http://www.nature.com/doifinder/10.1038/ngeo2383.

(10) Challenger, F. Biological methylation. *Sci. Prog.* **1945**, *35*, 315–361.

(11) Thomas, D. J.; Styblo, M.; Lin, S. The Cellular Metabolism and Systemic Toxicity of Arsenic. *Toxicol. Appl. Pharmacol.* **2001**, *176*, 127–144.

(12) Sierra-Alvarez, R.; Yenal, U.; Field, J. a; Kopplin, M.; Gandolfi, a J.; Garbarino, J. R. Anaerobic biotransformation of organo-arsenical pesticides monomethylarsonic acid and dimethylarsinic acid. *J. Agric. Food Chem.* **2006**, *54*, 3959–3966.

(13) Rosen, B.; Marapakala, K.; Abdul Salam, A.A. Packianathan, C.; Yoshinaga, M. *:Pathways of arsenic biotransformations: the arsenic methylation cycle. Understanding the Geological and Medical Interface of Arsenic*; 2012.

(14) Wang, S.; Mulligan, C. N. Natural attenuation processes for remediation of arsenic contaminated soils and groundwater. *J. Hazard. Mater.* **2006**, *138*, 459–470.

(15) Mestrot, A.; Feldmann, J.; Krupp, E. M.; Hossain, M. S.; Roman-Ross, G.; Meharg, A. a. Field fluxes and speciation of arsines emanating from soils. *Environ. Sci. Technol.* **2011**, *45*, 1798–1804.

(16) Mestrot, A.; Planer-Friedrich, B.; Feldmann, J. Biovolatilisation: a poorly studied pathway of the arsenic biogeochemical cycle. *Environ. Sci. Process. Impacts* **2013**, *15*, 1639–1651.

(17) Mestrot, A.; Uroic, M. K.; Plantevin, T.; Islam, M. R.; Krupp, E. M.; Feldmann, J.; Meharg, A. a. Quantitative and qualitative trapping of arsines deployed to assess loss of volatile arsenic from paddy soil. *Environ. Sci. Technol.* **2009**, *43*, 8270–8275.

(18) Styblo, M.; Del Razo, L. M.; Vega, L.; Germolec, D. R.; LeCluyse, E. L.; Hamilton, G. A.; Reed, W.; Wang, C.; Cullen, W. R.; Thomas, D. J. Comparative toxicity of trivalent and pentavalent inorganic and methylated arsenicals in rat and human cells. *Arch. Toxicol.* **2000**, *74*, 289–299.

(19) Shraim, A.; Sekaran, N. C.; Anuradha, C. D.; Hirano, S. Speciation of arsenic in tube-well water samples collected from West Bengal, India, by high-performance liquid chromatography-inductively coupled plasma mass spectrometry. *Appl. Organomet. Chem.* **2002**, *16*, 202–209.

(20) Xie, X.; Ellis, A.; Wang, Y.; Xie, Z.; Duan, M.; Su, C. Geochemistry of redox-sensitive elements and sulfur isotopes in the high arsenic groundwater system of Datong Basin, China. *Sci. Total Environ.* **2009**, *407*, 3823–3835.

(21) Lin, N. F.; Tang, J.; Bian, J. M. Characteristics of Environmental Geochemistry in the Arseniasis Area of the Inner Mongolia of China. *Environ. Geochem. Health* **2002**, *24*, 249–259.

(22) Lin, T. H.; Huang, Y. L.; Wang, M. Y. Arsenic species in drinking water, hair, fingernails, and urine of patients with blackfoot disease. *J. Toxicol. Environ. Health. A* **1998**, *53*, 85–93.

(23) Christodoulidou, M.; Charalambous, C.; Aletrari, M.; Nicolaidou Kanari, P.; Petronda, a.; Ward, N. I. Arsenic concentrations in groundwaters of Cyprus. *J. Hydrol.* **2012**, *468-469*, 94–100.

(24) Watts, M. J.; O'Reilly, J.; Marcilla, a L.; Shaw, R. a; Ward, N. I. Field based speciation of arsenic in UK and Argentinean water samples. *Environ. Geochem. Health* **2010**, *32*, 479–490.

(25) Razo, L. M. Del. The Oxidation States of Arsenic in Well-Water from a Chronic Arsenicism Area of Northern Mexico. *Environ. Pollut.* **1990**, *64*, 143–153.

(26) Maguffin, S. C. Redox controls on arsenic speciation and concentration in a volcanoclastic aquifer, 2016.

(27) (in prep) Maguffin, S. C. Attenuation of groundwater arsenic through stimulation of aquifer microorganisms, 2016.

(28) Braman, R. S.; Foreback, C. C. Methylated foms of arsenic in the environment. *Science (80-.).* **1973**, *182*, 1247–1249.

(29) Holland, G.; Tanner, S. D.; Royal Society of Chemistry (Great Britain). *Plasma source mass spectrometry : applications and emerging technologies*; Holland, G.; Tanner, S., Eds.; Royal Society of Chemistry, 2003.

(30) Huang, J. H.; Voegelin, A.; Pombo, S. a.; Lazzaro, A.; Zeyer, J.; Kretzschmar, R. Influence of arsenate adsorption to ferrihydrite, goethite, and boehmite on the kinetics of arsenate reduction by Shewanella putrefaciens strain CN-32. *Environ. Sci. Technol.* **2011**, *45*, 7701–7709.

(31) Fuller, C. C.; Davis, J. a.; Waychunas, G. a. Surface chemistry of ferrihydrite: Part 2. Kinetics of arsenate adsorption and coprecipitation. *Geochim. Cosmochim. Acta* **1993**, *57*, 2271–2282.

(32) Raven, K. P.; Jain, A.; Loeppert, R. H. Arsenite and arsenate adsorption on ferrihydrite: Kinetics, equilibrium, and adsorption envelopes. *Environ. Sci. Technol.* **1998**, *32*, 344–349.

(33) Keimowitz, a. R.; Mailloux, B. J.; Cole, P.; Stute, M.; Simpson, H. J.; Chillrud, S. N. Laboratory investigations of enhanced sulfate reduction as a groundwater arsenic remediation strategy. *Environ. Sci. Technol.* **2007**, *41*, 6718–6724.

(34) Stollenwerk, K. Geochemical Processes Controlling Transport of Arsenic in Groundwater: A Review of Adsorption http://resources.metapress.com/pdf-preview.axd?code=p2k65mu74l311520&size=largest (accessed Jan 4, 2012).